CHARACTERIZATION AND ANTI-HIV ACTIVITY OF THE PROPROTEIN CONVERTASE-DIRECTED SERINE PROTEASE INHIBITOR, Spn4A

by

VESNA POSARAC

A THESIS SUBMITTED IN PARTIAL FULFILLMENT
OF THE REQUIREMENTS FOR THE DEGREE OF

MASTER OF SCIENCE

in

THE FACULTY OF GRADUATE STUDIES

(Microbiology)

THE UNIVERSITY OF BRITISH COLUMBIA

(Vancouver)

December 2008

Abstract

HIV/AIDS is a global health problem of immense magnitude, with 33 million people living with HIV and 2 million AIDS-related deaths per year. As the development of drug resistance undermines treatment efficacy, the long-term success of anti-retroviral therapy depends upon the introduction of novel drugs aimed at additional targets essential for the viral life cycle. With a critical role in many viral diseases including the proteolytic maturation of the HIV-1 envelope glycoprotein gp160, the secretory pathway proprotein convertases (PCs) represent a potential anti-viral target.

Our laboratory has reported the identification of Spn4A, a potent naturally occurring secretory pathway serine protease inhibitor directed at the prototype PC member, furin. Because of the requirement for the PCs in the production of infectious HIV-1, we hypothesized that strategic manipulation of PC activity by Spn4A and Spn4A-engineered variants would provide a means of effectively limiting HIV-1 infection.

This thesis details the investigation of the anti-proteolytic activities and anti-HIV-1 properties of recombinant adenoviruses expressing Spn4A and Spn4A bio-engineered variants, including a secreted recombinant Spn4A (Spn4A S). Our data shows that the expression of Spn4A S in MAGI-CCR5 cells and furin-deficient LoVo cells inhibited the PC-dependent processing of the HIV-1 envelope precursor gp160. Furthermore, inhibition of processing resulted in a nearly complete reduction of productive HIV-1 infection as determined by HIV-1 Tat-driven β-galactosidase activity and multinuclear activation of a galactosidase indicator (MAGI) assays. Complementing the previously described anti-furin activity of Spn4A, our studies indicate that Spn4A S inhibits additional PCs involved in gp160 maturation, and that PC inhibition can serve as an effective means of limiting HIV-1 infection.

With the central role of the PCs in the replication and pathogenesis of numerous infectious agents, the identification of Spn4A S as an efficacious HIV inhibitor establishes Spn4A as a prospective broad-based agent for the inhibition of PC-related diseases.

Table of Contents

List of Tables

List of Figures

List of Abbreviations

α_1-AT	α_1-antitrypsin
α_1-PDX	α_1-antitrypsin Portland
Ad	adenovirus
Ala; A	alanine
AP	adaptor protein
Arg; R	arginine
Asn; N	asparagine
Asp; D	aspartic acid
AZT	azidothymidine
BMPs	bone morphogenetic proteins
dPC2	Drosophila PC2
E	endoprotease
EI*	SDS-stable complex
EI′	serpin/protease acyl intermediate
ER	endoplasmic reticulum
ERGIC	ER-Golgi intermediate compartments
FPLC	fast protein liquid chromatography
Gly; G	glycine
HA	avian influenza virus haemagglutinin
HAART	highly active antiretroviral therapy
HCMV	human cytomegalovirus
HEK	human embryonic kidney
His; H	histidine
hr(s)	hour(s)
Hsp	heat shock protein
I	inhibitor
I*	proteolysed inhibitor
Ile; I	isoleucine
IMC	intramolecular chaperone

K_i	constant of inhibition
Leu; L	leucine
LTR	long terminal repeat
Lys; K	lysine
Met; M	methionine
min	minute(s)
MAGI	multinuclear activation of a galactosidase indicator
MCA	7-amino-4-methylcoumarin
MOI	multiplicity of infection
MT1-MMP	membrane type I matrix metalloproteinase
ONPG	O-nitrophenyl β-d-galactopyranoside
PA	protective antigen
PACS-1	phosphofurin acidic cluster sorting protein-1
PC	proprotein convertase
PI8	human proteinase inhibitor 8
PP2A	protein phosphatase 2A
Pro; P	proline
RSL	reactive site loop
RT	room temperature
Ser; S	serine
serpin	serine protease inhibitor
SI	stoichiometry of inhibition
SP	signal peptide
Spn4A ER	His-FLAG-Spn4A-HDEL RRKR
Spn4A RRLL ER	His-FLAG-Spn4A-HDEL RRLL
Spn4A RRLL S	His-FLAG-Spn4A-ΔHDEL RRLL
Spn4A S	His-FLAG-Spn4A-ΔHDEL RRKR
TGN	*trans*-Golgi network
Thr; T	threonine
Val; V	valine

VSV	vesicular stomatitis virus
WT	wildtype

Acknowledgements

I would like to acknowledge my supervisor, Dr. François Jean. Thank you for your support and effort. I benefited greatly from your mentorship and knowledge.

I would like to thank all the lab members for creating a helpful, exciting and friendly work environment.

I would like to acknowledge Dr. Peter Cheung who greatly contributed to this work. Thank you for your dedication, enthusiasm, and energetic discussion.

I would like to express my gratitude to committee members Dr. Marc Horwitz and Dr. Ed Pryzdial for advice and constructive criticism throughout this thesis work.

I would like to thank my family for all their encouragement and all the friends who made my time as a Master's student so enjoyable. Andrea, for all the good times in the office, Jerome, for your kindness and support, and Lea – the many nights spent thesis writing were fun, I can't wait for the next chapter.

Dr. Richard Leduc (University of Sherbrooke) kindly provided the human embryonic kidney 293A wildtype and furin overexpressing C4 cells. The recombinant vaccinia expression vector encoding gp160 was a gift from Dr. Gary Thomas (Oregon Health & Science University). MAGI-CCR5 cells were kindly provided by Dr. J. Overbaugh through the AIDS Research and Reference Reagents Program, Division of AIDS, NIAID, NIH. The laboratory-adapted strains HIV-1_{BaL} from S. Gartner and HIV-1_{IIIB} from R. Gallo, were obtained from the AIDS Research and Reference Reagents Program, Division of AIDS, NIAID, NIH.

Salary and research support was provided by the Canadian Institutes of Health Research (CIHR MOP-77674 to F. Jean).

Co-Authorship Statement

The thesis project was performed in collaboration with Dr. Peter Cheung, Research Associate, B.C. Centre for Excellence in HIV/AIDS, St. Paul's Hospital, Vancouver, B.C. Dr. P. Cheung performed all biocontainment level 3 work at the BC Centre for Disease Control including HIV infections, β-galactosidase activity and MAGI assays, and construction of envelope expression vectors. Experimental design and data analysis of the HIV infection experiments was carried out by Vesna Posarac and Dr. P. Cheung. All other work was performed by Vesna Posarac.

CHAPTER I Introduction

1.1 The proprotein convertases

The proprotein convertases (PCs) are a group of serine endoproteases catalyzing the proteolytic maturation of a wide range of proproteins and prohormones, in turn affecting a number of processes ranging from homeostasis to disease. The group comprises nine members, seven of which cleave substrates after basic amino acids: PC1/3, PC2, furin, PC4, PC5/6, PACE4, and PC7/LPC; and two more distantly related proteases, SKI-1/S1P and PCSK9, which carry out cleavage at non-basic residues (1, 2). This section will focus on the structure, activation, and function of the PCs with multi-basic recognition sites, with particular emphasis on furin, the first identified and most extensively characterized human PC member.

Structure and substrate specificity

Each PC is composed of several domains, most of which are conserved between all members of the group (Fig. 1.1). All PCs are synthesized with a signal peptide at their N-terminus which directs translocation into the endoplasmic reticulum (ER). Immediately downstream of the signal peptide is the prodomain, which is flanked by an N-terminal signal peptidase cleavage site and a C-terminal autoproteolytic site composed of basic residues (3). The prodomain is critical in all components of PC function including folding, activation, transport, and regulation of activity (3-6). The site of greatest sequence similarity between the PCs lies within the catalytic domain, which includes the catalytic triad (aspartate, histidine, and serine residues) and the oxyanion hole characteristic of the subtilisin family of serine endoproteases (1). Additionally, according to the crystal structure of furin, the catalytic domain houses two calcium ions, as all PC members including furin are calcium-dependent (7). The P domain (also called the homoB or middle domain) is the final region that is conserved in all PCs, and acts in the stabilization of the catalytic domain and the regulation of calcium and pH dependence (7-9). Furin, PC7, and PC5/6B (one of the two isoforms of PC5/6 that is generated by alternative splicing) are type I transmembrane proteins, and contain at their C-terminal end, a transmembrane domain and a cytoplasmic tail which controls the localization and sorting of the proteases (10). Finally, furin, PC5/6, and PACE4 contain a cysteine-rich region, which is

important in the generation of the truncated or extracellularly 'shed' form of these proteases and in cell surface tethering of PC5/6A and PACE4 (11, 12).

The PCs cleave protein substrates C-terminal to paired basic residues, however, many have additional cleavage sequence criteria usually entailing additional basic residues upstream of the cleavage site. Furin has the most stringent basic residue requirements as studies with two furin substrates, the anthrax toxin protective antigen (PA) and avian influenza virus haemagglutinin (HA), identified the sequence -Arg-X-Lys/Arg-Arg↓- (where X is any amino acid and ↓ denotes the cleavage site) as the furin consensus cleavage sequence (13, 14). In addition, furin also favours basic residues at the P3, P5, and P6 sites (3, 5, and 6 positions N-terminal to the cleavage site) (15-17). In cases where a basic residue is present in the P4 position or beyond, a basic residue at the P2 site is not required, and furin-mediated processing can occur, albeit at reduced efficiency (13, 14, 16, 17). Thus, -Arg-X-X-Arg↓- makes up the minimal furin cleavage sequence. Finally, in some cases under acidic conditions, furin can cleave substrates that contain an Arg at the P6 position in place of the P4 Arg (9, 17, 18).

The crystal structure of the mouse furin ectodomain inhibited with decanoyl-Arg-Val-Lys-Arg-chloromethylketone has elucidated the molecular interactions involved in furin and PC substrate specificity (7). The substrate binding region was shown to contain a large cluster of negative residues, including an active-site cleft which forms highly favourable contacts with Arg at the P1 and P4 positions. Modelled PC structures based on the furin and the yeast orthologue kexin crystal structures have revealed similarities in that the substrate binding region is occupied by mostly negative residues. However, the number and distribution of these residues differ slightly between the PCs (19). Furin contains the largest number of acidic residues in the vicinity of the active site cleft with 16, followed by PACE4, PC5/6, and PC4, with 15 acidic residues each, and PC7, PC1, and PC2 with 13 acidic residues each. The observation that furin has the most extensive demands for basic residues near the cleavage site and the largest number of acidic residues in its active site, implies a positive correlation between the overall negative charge of the active site and the basic cleavage sequence requirements for a given PC. Therefore, PACE4, PC5/6, and PC4 are predicted to be similar to furin in their preference for basic residues, while PC7, PC1, and PC2 cleavage would be less dependent on positive charges at the substrate

cleavage site. These modelling studies should aid in distinguishing between the PCs potentially involved in the cleavage of a given substrate.

Activation, trafficking, and tissue distribution

The PCs are synthesized in the ER as zymogens that require proteolytic removal of the prodomain to generate the mature active form of the protease. The N-terminal 83-residue prodomain of furin functions as an intramolecular chaperone (IMC), guiding the folding, transport, and activation of the protease in the secretory pathway (20). The generation of active furin requires a pair of ordered, compartment-specific autoproteolytic cleavages (Fig. 1.2). The first cleavage event ($t_{1/2}$ = 10 min) occurs in the neutral pH of the ER at the furin consensus sequence -Arg-Thr-Lys-Arg^{107}↓-, where Arg^{107} borders the catalytic domain (3, 6, 21). This excision site cleavage is required for transport out of the ER (5, 21), and although no longer covalently bound, the propeptide of furin remains associated to the catalytic domain acting as a potent autoinhibitor (22). Propeptide release and the generation of active furin is dependent on a second cleavage event ($t_{1/2}$ = 105 min) that occurs in the mildly acidic environment of the *trans*-Golgi network (TGN)/endosomal system at the internal pH-sensitive cleavage site, -Arg-Gly-Val-Thr-Lys -Arg^{75}↓- (9). In experiments using fluorogenic peptide substrates containing the excision and internal cleavage sites, Anderson *et al.* showed that while both sites are cleaved by furin, the internal cleavage site containing the P1/P6 Arg was processed under mildly acidic conditions akin to those of the TGN/endosomal system and not at neutral pH. Additionally, a mutation at the P4 position (Val^{72}→Arg) of the internal cleavage site which abrogated its pH-sensitivity, led to an accumulation of the inactive furin mutant in the ER, indicating that the integrity of this site, and thus, the ordered cleavage of the propeptide, is necessary in guiding the proper folding and activation of furin (20). All PCs are synthesized with an N-terminal propeptide containing basic residues at putative excision and internal cleavage sites (23). This, together with findings that several PCs undergo pH-dependent autoactivation processes (24, 25) and that their propeptide acts as an autoinhibitor (25-27), suggests that the furin activation model may be generally conserved in all PCs.

Once activated, the PCs follow distinct sorting routes through various subcellular compartments where they encounter and process their substrates. PC5/6A, PC1/3, and PC2 sort

to the secretory granules (28-31), while PACE4 and the type-I membrane PCs – PC5/6B, PC7, and furin – are localized to the TGN/endosomal compartments (5, 28, 32-34). The trafficking of type-I membrane PCs is governed by the sorting signals encoded within the cytoplasmic domain. Although furin has a steady-state localization to the TGN, its sorting itinerary is more complex, as its 56 amino acid cytoplasmic domain directs furin trafficking through two cycling loops: 1) at the TGN and 2) the plasma membrane and early endosomes (Fig. 1.3) (10). Through interactions with the phosphofurin acidic cluster sorting protein-1 (PACS-1), protein phosphatase 2A (PP2A), and various adaptor proteins (AP1, 2, 4), two motifs within furin's cytoplasmic domain – the casein kinase 2 (CK2)-phosphorylated acidic cluster and a membrane-proximal segment containing two hydrophobic motifs – guide the trafficking of furin through and between the two cycling loops (5, 33, 35-37). In the TGN cycling loop, the membrane-proximal segment/AP1,4 and the CK2-phosphorylated acidic cluster/PACS1 are required for the budding of furin from the TGN to the endosomes and for its retrieval from the endosomes to the TGN, respectively (38). In the second cycling loop, furin traffics from the early endosomes to the cell surface, where it is endocytosed as a result of the binding of the hydrophobic motif with AP2 (38, 39). The direction of furin trafficking between the two loops is determined by the phosphorylation state of the CK2-phosphorylated acidic cluster. In the early endosomes, furin with a phosphorylated acidic cluster will recycle to the cell surface, while an acidic cluster dephosphorylated by PP2A will direct furin back to the TGN (40).

Owing to its dynamic and highly regulated localization, furin is able to cleave its substrates at various sites of the secretory pathway. In line with the activation and trafficking models for furin, substrate processing has been shown to occur in the TGN/biosynthetic pathway (41-43), at the cell surface (44-46), and in the endocytic pathway (47). Intriguingly, there is evidence for furin-mediated processing at two sites outside of the confines of the accepted active furin trafficking model. Numerous studies in cancer cell lines have reported the extracellular release of a soluble "shed" form of furin that is proteolytically active, raising questions of a physiological role for secreted furin (6, 48-50). Although such a role has not been fully elucidated, studies with extracellular proteins fibrillin (51) and TGF-β1,2 (52) have suggested that secreted furin may act in the extracellular processing of the precursor forms of the proteins.

There is also mounting evidence for furin-mediated processing in the early secretory pathway. Studies of a mutant insulin proreceptor that is misfolded and retained in the ER demonstrated that the proreceptor undergoes furin-dependent cleavage (53). Similarly, a construct consisting of the PC1 prosegment and a C-terminal secretory granule sorting domain was found to be cleaved in the ER or the *cis*-Golgi at the furin consensus sequence (54). Finally, it has been demonstrated that constructed mutants of profurin that remain in their zymogen form, and are presumably retained in the ER, retain the capacity to process pro-von Willebrand factor, a furin substrate (55). Two hypotheses have been put forth to explain observations of furin-mediated processing in the early secretory pathway. The first is that active furin may recycle back from the TGN to the ER (53), as there is a precedent for retrograde transport of TGN localized proteins (56). A second possible explanation is that a subset of substrates are able to competitively displace the inhibitory prosegment of furin in the ER, thus liberating furin activity in this compartment (54). Although it remains that furin activity occurs predominantly at the TGN or downstream compartments, the model for furin activation and trafficking may require refinement in light of evidence of furin activity beyond the late secretory pathway.

The tissue distribution of the PCs ranges from highly constricted to broad. PC1/3 and PC2 expression is confined to the neuroendocrine system (57-59), while the expression of PC4 is further restricted to the testicular and ovarian germ cells (60, 61). In contrast, PC5/6 (62, 63) and PACE4 (57, 63) are widely expressed in a broad range of tissues, and furin (58, 59, 64, 65) and PC7 (66-68) are ubiquitous.

Physiological role of the PCs and knockout phenotypes

The PCs process a broad and diverse range of endogenous substrates that are unified by the presence of the multi-basic PC recognition sequence at the cleavage site. Substrates that are cleaved at PC recognition sites include neuropeptides, hormones, cell surface receptors, growth factors, enzymes, adhesion molecules, and blood coagulation factors (42, 69, 70). More specifically, the precursor forms of well-known proteins such as insulin, insulin receptor, growth factors, matrix metalloproteinases, and albumin are included in the repertoire of PC substrates that numbers in the dozens (10) (Table 1.1). Given that the PC members share similar cleavage sequence criteria, a built-in redundancy in the processing of PC substrates is predicted to exist.

While this is the case in some instances, the varied tissue distribution, cell expression, subcellular localization, and cleavage sequence requirements between the PCs implicates certain members in the processing of a given substrate. However, even within these criteria, some redundancy might be expected – for example, with furin and PC7. Knockout mouse models of PCs have been useful in delineating the unique and obligatory roles of some PCs, while suggesting the redundancy of others.

The mouse PC knockout studies have yielded varied results. PC1/3 (71) and PC2 (72) null mice are viable with developmental abnormalities, and PC4 knockouts (73) are viable with reduced fertility. A knockout in PACE4 (74) is embryonic lethal in one quarter of mice, while the absence of PC5/6 (75) or furin (76) is more severe, with all mice dying in the early stages of embryogenesis. Embryonic lethality in furin null mice is attributed to hemodynamic insufficiency and cardiac ventral closure defects (76) and may be associated with the failure to process bone morphogenetic proteins (BMPs) and TGFβ (38, 42, 77, 78). In contrast, PC7 knockout mice exhibit no apparent abnormal phenotype, suggesting redundancy in vital physiological activity of the protease (79). Although these studies indicate that with the exception of PC7, all PCs have unique roles, a conditional furin knockout mouse model revealed a different scenario beyond the developmental stage. Mice with a knockout of furin in the liver exhibit no adverse effects and retain their ability to process "furin" substrates, although some with reduced efficiency (80). Therefore, the role of furin, and potentially other PCs whose knockout leads to embryonic lethality, may not be obligatory beyond development in all tissues in which they are expressed.

The PCs in microbial disease

Although the PCs play an important role in homeostasis, they are perhaps best known for their involvement in disease. The PCs are linked to a number of cancers (81), neurodegenerative disease (82, 83), and infectious diseases. Many pathogenic bacteria and viruses are dependent on furin-like processing for the generation of biologically active components. Bacterial toxins including *Pseudomonas aeruginosa* exotoxin A, diptheria toxin, and Anthrax toxin protective antigen are cleaved at furin sites. The processing of these toxins occurs at the cell surface or the endocytic pathway and allows for the entry of the toxic subunit(s) into the cell cytoplasm. A

critical process in the life cycles of many viruses is the cleavage of the precursor envelope protein, generating a functional protein capable of membrane fusion. For viruses such as measles, H5N1 influenza A, and HIV-1, furin-like PCs have been implicated in this process (1). Furin has also been associated with pathogen virulence as exemplified by the processing of HA in influenza A virus. An increase in virulence of influenza A is often associated with a shift from a mono-basic cleavage site of HA that is processed by trypsin-like proteases whose expression is limited to a few cell types, to a multi-basic cleavage sequence that is recognized by the ubiquitously-expressed furin (84). In the case of HIV-1, furin-like cleavage of its envelope precursor glycoprotein is an absolute requirement in the viral life cycle, and will be further discussed in the following section.

1.2 HIV-1 gp160 processing

HIV-1 epidemiology and current therapy

HIV-1, the causative agent of AIDS, is a virus of immense global importance, infecting CD4+ cells leading to their depletion, and eventually, death if left untreated. It is estimated that in 2007, 33 million people were living with HIV-1, 2.7 million were newly infected, and 2 million people died due to AIDS (85). While HIV-1 is most prevalent in Sub-Saharan Africa, it is also of considerable importance in Canada where an estimated 58,000 people are infected with the virus (86). Although, it has been 25 years since the Nobel Prize-winning discovery of HIV-1, efforts towards vaccine development have been largely unsuccessful (87).

Current anti-viral treatment strategies target viral gene products, however, their toxicity and the emergence of drug resistance limit their usefulness. The current treatment for HIV, highly active antiretroviral therapy (HAART), uses a combination of inhibitors targeted at the HIV reverse transcriptase, protease, integrase, and viral fusion (88). Although widely used, the efficacy of HAART is limited due to a lack of patient compliance, toxicity, and the development of drug-resistant variants (89). New therapeutics aimed at additional targets that are essential for the viral life cycle need to be explored. As drugs directed at viral proteins select for drug-resistant HIV strains, cellular proteins that mediate important events in the viral life cycle are potential targets for new antiretroviral drugs.

HIV-1 life cycle

HIV-1 belongs to the *Retroviridae* family of viruses, characterized by a positive-sense RNA genome that is translated into double stranded DNA and incorporated into the host genome. The virus infects CD4+ cells including T cells and macrophages, gaining entry via direct fusion following the binding of its mature envelope protein gp120/41 to the CD4 receptor and the chemokine co-receptor CXCR4 or CCR5. The RNA genome is reverse transcribed in the cytoplasm and the resulting double stranded DNA is incorporated into the host genome. From this point, the cell's machinery replicates and transcribes the HIV-1 genome, producing viral gene products including structural, regulatory, and replication proteins. The viral components assemble in the cytoplasm and exit the cell by budding, resulting in an enveloped virus containing mature envelope glycoproteins and requiring a final maturation step that is mediated by the viral protease shortly after exit from the cell (Fig. 1.4) (90).

A critical event required for HIV infection is the cleavage of the HIV-1 envelope precursor gp160, yielding fusion competent products gp120/gp41 (91). The mature envelope glycoprotein is present in the viral envelope as a trimer of heterodimers, with three molecules each of gp120 and gp41 associated through non-covalent interactions (92). The surface subunit of the envelope glycoprotein, gp120, contains a CD4 binding domain and mediates initial docking of the virus to the target cell via its interaction with CD4 and the chemokine co-receptor. The transmembrane subunit, gp41, contains an N-terminal fusion peptide which, following a conformational change induced by gp120 and CD4/co-receptor interaction, acts to destabilize the cellular membrane resulting in fusion and viral entry (93). Inhibition of gp160 processing, either through a mutation in the highly conserved cleavage site -Arg-Glu-Lys-Arg↓ (94), or by inhibition of gp160 endoproteolysis (95), results in the incorporation of gp160 into the viral envelope, and the production of non-infectious HIV-1 particles incapable of cell fusion and entry.

The HIV-1 envelope precursor protein is synthesized on the rough ER and inserted into the lumen of the ER where it undergoes oligomerization and extensive glycosylation (96-98). The oligomerized gp160 exits the ER and as it travels through the secretory pathway en route to the cell surface, its oligosaccharide side chains are modified and it is endoproteolytically cleaved

into gp120 and gp41 (96, 99). Although it is accepted that gp160 processing occurs late in the secretory pathway, the exact site is under some contention. Glycosylation studies point to the *trans*-Golgi or the TGN as the site of processing (99-101), while experiments with drugs disrupting intracellular trafficking suggest that the event may occur later along the secretory pathway (100, 102).

The PCs in gp160 maturation

Several members of the PCs have been suggested to process HIV-1 gp160 at the PC-recognized cleavage sequence -Arg-Glu-Lys-Arg↓ (103). A seminal study by Hallenberger *et al.* implicated furin in this process, as inhibition of the protease resulted in a dramatic reduction in gp160 processing and HIV-1 replication (104). However, the retention of gp160 processing in furin-deficient cells suggests that other PC members are also involved (105). As an endoprotease involved in envelope processing needs to co-localize with its substrate, furin, PC7, PC5/6B, and PACE4 represent potential candidates as gp160 processing proteases. Vaccinia virus co-expression studies have indicated that furin, PC7, and to a much lesser extent, PC5/6B and PACE4, increase the processing of gp160 above background levels (102, 106, 107). Furin and PC7 are constitutively expressed, while PC5/6B is only weakly expressed in HIV host cells (106, 108). Furthermore, the activation of CD4+ T cells, which is favourable for HIV-1 replication, leads to a 5- to 10-fold upregulation in the expression of furin and PC7, but not of PC5/6B (109). This suggests that *in vivo*, HIV-1 gp160 is primarily cleaved by furin and PC7 whereas in non-host cell systems, PC5/6B and PACE4 may also participate.

Despite the host cell endoprotease redundancy in gp160 processing, the proteolytic maturation of the envelope glycoprotein is inefficient, with only a fraction of gp160 being cleaved into gp120/41. The inefficiency of this processing event is attributed to the presence of the highly conserved acidic residue glutamate in the P3 position of the gp160 cleavage site (103). Both furin and PC7 contain an acidic residue at the site predicted to interact with the P3 position of the substrate, and therefore, a P3 basic residue is highly favoured for substrate recognition and processing by these proteases (7, 19). In a study where a perfect furin cleavage site was introduced to gp160 by mutation of the P3 position, it was shown that while processing efficiency had increased, the infectivity of mutant envelope viruses was attenuated. This was not

due to a functional constriction, as the mutant envelope proteins were able to induce syncytia formation. Therefore, HIV-1 may maintain the sub-optimal furin cleavage site 1) as a mechanism of immune evasion whereby the production of non-neutralizing antibodies is induced by gp160 that is represented on the cell surface, 2) to prevent premature destruction of the host cell as a result of syncytia formation mediated by cell surface gp120/41 and CD4 on neighbouring cells (110).

The central role of the PCs in many diseases including the activation of pathogens such as HIV-1, has pointed to the PCs as a strategic therapeutic target. Accordingly, there is considerable interest in the development and identification of PC inhibitors.

1.3 PC inhibitors: peptide and protein-based strategies

Given the prominence of furin in a variety of disease processes, particularly in the activation of pathogen precursor proteins, efforts in the development of PC inhibitors have focused largely on furin as the main target of interest. The majority of identified furin inhibitors fall within two classes – peptide-based inhibitors and protein-based inhibitors, with the exception of several cases in which non-peptide, non-protein small molecule furin inhibitors have been reported.

Peptide-based inhibitors

A family of decanoyl-peptidyl-chloromethylketones exploiting the PC-cleavage sequence requirements have been widely used in inhibition studies of PC-dependent processing. The inhibitors contain the furin consensus sequence -Arg-X-Arg/Lys-Arg-, and when added to cell growth medium have been shown to block the cleavage of viral precursor proteins including HIV-1 gp160, influenza virus HA, and human cytomegalovirus (HCMV) pro-gB (104, 111, 112). Although they have been instrumental in implicating furin in the cleavage of a number of pathogen proproteins, the relative cytotoxicity, lack of specificity, instability of the methyl chloride group, and low efficiency of intracellular uptake have impeded the therapeutic potential of this group of inhibitors (1, 113, 114).

Polyarginines comprise a group of peptide inhibitors composed of six arginines or more. They are relatively potent competitive inhibitors of furin with a constant of inhibition (K_i) in the

nanomolar range (115). Inhibitory activity against other PCs including PC7, PACE4, and PC1 has also been demonstrated (115, 116). Polyarginines have been shown to significantly improve survival rate in mice treated with *Pseudomonas* exotoxin A, demonstrating the application of a broad based PC inhibitor without the generation of toxic effects (117). In cell culture, polyarginines prevent productive HIV-1 infection through the inhibition of gp160 processing. The lack of reported toxic effects at the concentrations required to inhibit PC-dependent processing suggests that polyarginines may warrant further study as potential therapeutic agents (116, 117).

Small-molecule furin inhibitors

Screens for small molecule furin inhibitors have resulted in the identification of compound B3 and a class of inhibitors derived from 2,5-dideoxystreptamine (GADDs) with K_i's for furin of 12 μM and ≥6 nM, respectively (118, 119). When added to cell growth medium below the cytotoxic concentration (15 μM), B3 has been demonstrated to partially inhibit furin-mediated processing of pro-membrane type I matrix metalloproteinase (MT1-MMP) (120). MT1-MMP is involved in cancer metastasis as its activation promotes an increase in cell motility and invasiveness (121). Accordingly, the B3-induced inhibition of MT1-MMP in cell culture results in a decrease in these metastatic processes (120). The potent group of furin inhibitors, GADDs, were demonstrated to block furin-mediated cleavage of the anthrax protoxin, however, a concentration considerably higher than the K_i (4.2–12.9 μM) was required to achieve complete inhibition (119). In addition to B3 and GADDs, natural products of the andrographolide family and copper complexes have been identified as less potent non-peptide/non-protein furin inhibitors with K_i values in the high micromolar to low millimolar range (122, 123).

While moderate progress has been made in identifying effective small molecule furin inhibitors, the serpin family of protein-based inhibitors remain as the most potent furin-directed agents identified to date, and have been invaluable in studies of PC-associated physiological and pathological processes.

Serpins

Serpins are a family of proteins with a highly conserved structure that are found in all branches of life. Their functions are as varied as the species in which they are found, and include control of the Toll pathway during an immune response in *Drosophila* and the regulation of a number of proteolytic pathways in humans such as blood coagulation (124). The prime determinant of the inhibitory specificity of a serpin is found within the sequence and structure of its reactive site loop (RSL), as this sequence contains the substrate recognition site of the protease which it inhibits. Serpins have a unique slow-binding mechanism of inhibition in which the active serine of the protease cleaves the RSL of the serpin, causing the protease-bound RSL to move to the opposite pole. This repositioning results in a disruption of the protease's catalytic site, preventing the release of the protease from the complex, ultimately leading to its degradation (Fig. 1.5) (125). A serpin's efficiency as an inhibitor (I) for a given endoprotease (E) is determined by the stoichiometry of inhibition (SI). The SI is the relative flux of a serpin, following the formation of a serpin/protease acyl intermediate (EI´), through the substrate pathway (proteolysis) (I*) or the inhibitor pathway (formation of a kinetically stable SDS-stable complex) (EI*), and can be described by the equation (126):

$$\begin{array}{lll} I + E \leftrightarrow EI \rightarrow EI' \rightarrow E + I^* & \text{(substrate pathway)} \\ \qquad\qquad\quad \downarrow & \\ \qquad\qquad\quad EI^* & \text{(inhibitor pathway)} \end{array}$$

As potent suicide substrate inhibitors with the capacity for tissue- and subcellular compartment-specific targeting, serpins represent attractive agents in the inhibition of the PCs. Efforts in the development and identification of such inhibitors have yielded a widely used bioengineered serpin and several naturally occurring serpins of furin.

A furin-selective serpin, α_1-PDX

A potent and selective inhibitor of furin, α_1-antitrypsin Portland (α_1-PDX), is a bioengineered variant of the human serum serpin, α_1-antitrypsin (α_1-AT) (127). α_1-AT is a physiological inhibitor of elastase with the reactive site -Ala-Ile-Pro-Met-, and an N-terminal secretion signal (128, 129). α_1-PDX was generated by a two residue Arg substitution in the P1

and P4 positions of α_1-AT (Met→Arg; Ala→Arg), forming the minimal furin consensus sequence, and resulting in a shift in the inhibitory specificity from elastase to furin (127). Biochemical analyses indicated that α_1-PDX acts as a serpin of furin with a K_i of 0.6 nM and SI of 2, partitioning with equal probability through the substrate pathway or the inhibitor pathway. With the exception of PC5/6B, which is inhibited less potently than furin (K_i = 2.3 nM; SI = 8), α_1-PDX has no *in vitro* activity directed at other PC members (114). However, using vaccinia virus co-expression systems, it was reported that overexpression of furin, PC7, and to a lesser extent, PACE4 and PC5/6B, led to an accumulation of a cleaved α_1-PDX product, likely corresponding to I* (130). Therefore, although *in vitro* analyses indicate α_1-PDX is a furin-, and to a lesser extent, PC5/6B-specific inhibitor, in the context of the cellular environment the serpin may be recognized as a substrate by PC7 and PACE4.

α_1-PDX has been widely used in the inhibition of numerous furin-dependent processing events including the cleavage of bacterial pro-toxins, viral glycoproteins, and cellular substrates associated with cancer. Consequently, the serpin has been demonstrated to prevent bacterial toxin-induced cell lysis, productive viral infection, and tumour metastasis (114, 127, 131, 132). With respect to the anti-viral properties of α_1-PDX, the contrasting results reported on the effect of the α_1-PDX on HCMV and HIV-1 replication are of particular interest.

The proteolytic maturation of the precursor form of the HCMV envelope glycoprotein gB is furin-dependent, as demonstrated by a lack of pro-gB processing in furin-deficient cell lines. In studies by Jean *et al.*, α_1-PDX was demonstrated to be a highly effective anti-HCMV agent, generating a full block in pro-gB processing and a 3-log reduction in viral production. This inhibitory effect was generated by extracellularly applied α_1-PDX (8 μM and 20 μM for gB processing and viral production, respectively), suggesting a mechanism for the internalization of the inhibitor. It was shown that intracellular furin levels were indeed depleted in the presence of α_1-PDX in the cellular medium, and that α_1-PDX was internalized into cells by a furin-dependent mechanism. It was proposed that furin trafficking to the cell surface mediates the uptake of α_1-PDX from the media (131).

In contrast to its efficacy in limiting infectious HCMV production, α_1-PDX is a moderately effective inhibitor of HIV-1 infection. Several studies have reported the inhibition of gp160 processing in the presence of intracellularly expressed α_1-PDX, however, the degree of inhibition appears to vary with cell type, potentially due to different PC expression profiles of the cells (102, 127, 133, 134). The replication of HIV-1 in T-cells stably expressing α_1-PDX has been extensively studied by Bahbouhi *et al.* While α_1-PDX was initially successful at limiting HIV-1 replication, the virus recovered infectivity 13 days post initial infection, indicating that α_1-PDX cannot be used to stably inhibit HIV-1. Coinciding with the recovered HIV-1 infectivity, was an accumulation of the cleaved form (I*) of α_1-PDX. Ruling out mutations in the envelope protein, the authors hypothesized that another convertase such as PC7, with which α_1-PDX does not form a stable EI* complex, cleaves the serpin through the substrate pathway (134). This modulation of α_1-PDX levels would lead to a decrease of anti-furin activity, and the recovery of HIV-1 infection. These findings suggest that broad-based PC inhibitors that act predominantly through the inhibitor pathway may be required for sustained inhibition of HIV-1 infection.

Naturally occurring serpins of PCs

Recent studies have identified several naturally occurring serpins containing an N-terminal signal peptide and multiple basic residues in their RSL. These include serpins from the fruit fly, lancelet, mosquito, honey bee, and sea urchin (135-137). Some have demonstrated anti-PC activities, others are predicted PC inhibitors, suggesting that some species have evolved mechanisms to regulate PC activity. Interestingly, although the PCs are active within the late secretory compartments, the identified and predicted PC-directed secretory pathway serpins contain at their C-terminus, a variant of an ER-retrieval signal (136). Additionally, a human serpin, human proteinase inhibitor 8 (PI8), has been shown to be a potent serpin of furin (K_i = 53.8 pM), however it is unlikely that the PCs are physiological targets of PI8 as it lacks a secretion signal (138). While little is known about the physiological roles of these naturally occurring serpins, their interest extends to their therapeutic potential, particularly in the case of the most potent furin inhibitor identified to date – the *Drosophila*-encoded serpin, Spn4A (137).

The *spn4* gene from Drosophila encodes eight isoforms of the neuroserpin Spn4 (A-H), differing in their localization (presence or absence of signal peptide) and inhibitory profiles (RSL

sequence) (139). One of these isoforms, Spn4A, contains an N-terminal signal peptide and a C-terminal HDEL sequence – a functional variant of the well-known KDEL motif that directs proteins to the ER. Our laboratory has shown previously that Spn4A inhibits human furin (K_i: 13 pM; SI: 1) (50-fold more potent than α_1-PDX) and *Drosophila* PC2 (dPC2) (K_i: 3.5 nM; SI: 1) by a slow-binding mechanism characteristic of serpin molecules. The cleavage site was found to be immediately downstream of the furin consensus sequence -Arg-Arg-Lys-Arg-↓ of the RSL (137). The ability of Spn4A to inhibit furin and dPC2, two of the most evolutionarily divergent PCs, suggests that Spn4A could act as a broad-based PC inhibitor. This is further supported by recent studies demonstrating serpin activity of Spn4E (the non-secreted isoform of Spn4A) directed at *Drosophila* furin 1 and 2 (140). The inhibitory plasticity of Spn4A may be attributed to the unusual length of the RSL, one residue longer than the 17 residue RSL typically found in inhibitory serpins, as a deletion in the P6 alanine results in the loss of dPC2 inhibition without an effect on anti-furin activity (137).

When expressed in COS cells, Spn4A co-localizes with the ER marker PDI. While the wildtype serpin is intracellularly retained, a deletion in the C-terminal sequence (ΔHDEL) results in the extracellular secretion of the Spn4A mutant (141). This suggests that the HDEL sequence acts as a bona fide ER-retention motif. The localization of Spn4A within the secretory pathway, and the observation that its overexpression in a subset of cells of *Drosophila* larvae leads to a disruption in neuropeptide processing (142), points to a physiological role for Spn4A in PC regulation. Further investigation will be required to uncover a potential PC regulatory mechanism.

Despite the broad role of the PCs in the proteolytic activation of numerous viral proteins, the efficacy of Spn4A as an anti-viral agent has not been studied. Given its potential as a broad-based PC inhibitor, it is of particular interest to investigate processes with PC redundancy such as HIV-1 gp160 processing.

1.4 Research hypothesis

We hypothesize that strategic manipulation of PC activity by Spn4A or its soluble variant will effectively inhibit HIV-1 production.

1.5 Objectives

The objective of my thesis project is to determine if the naturally occurring Spn4A and the engineered Spn4A secreted variant can block PC-dependent processing of HIV-1 gp160 and inhibit productive HIV-1 infection.

Figure 1.1. Schematic diagram of PC structure. PC5/6 is expressed as either the A or B isoform generated by alternative splicing. The diagonal dashed line links the two halves of PC5/6B. The bold labels D, H and S highlight the active-site residues; the non-bold labels N and D highlight the oxyanion-hole residues. Adapted by permission from Macmillan Publishers Ltd: Nature Reviews Molecular Cell Biology (1), copyright (2002).

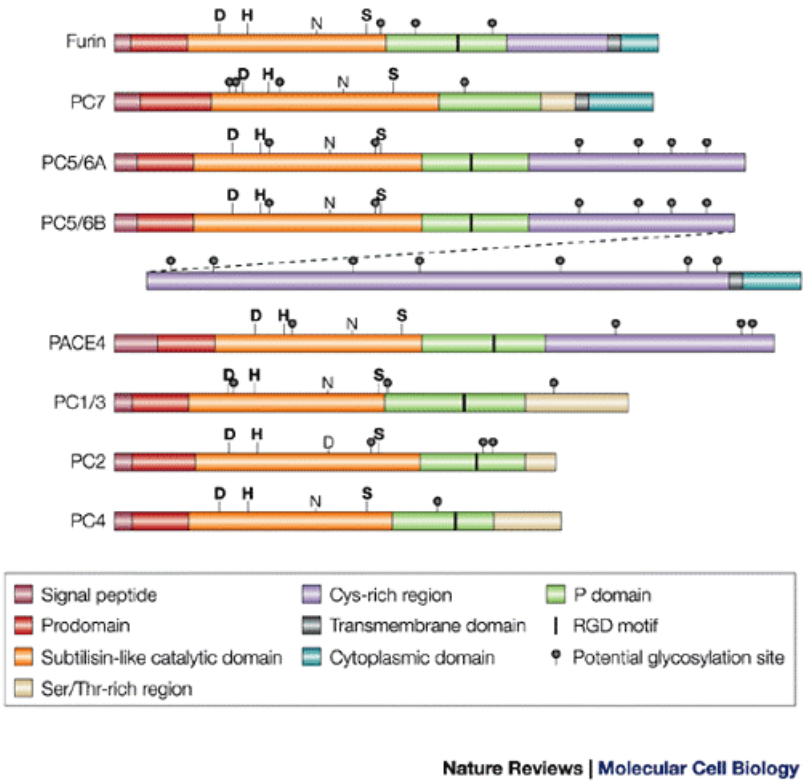

Figure 1.2. The furin autoactivation pathway. The furin prodomain acts as an IMC, guiding the folding of the unstructured, inactive catalytic domain (pink circle) into the active conformation (red oval). Following the initial folding steps, the first cleavage event occurs in the neutral pH of the ER at the Arg^{107} bordering the catalytic domain. The propeptide of furin remains associated with the catalytic domain as a potent autoinhibitor and is released following a second cleavage event at Arg^{75} in the mildly acidic environment of the *trans*-Golgi network (TGN)/endosomal system. Adapted with permission from (20), copyright (2002) American Society for Biochemistry and Molecular Biology. Reprinted by permission from Macmillan Publishers Ltd: Nature Reviews Molecular Cell Biology (1), copyright (2002).

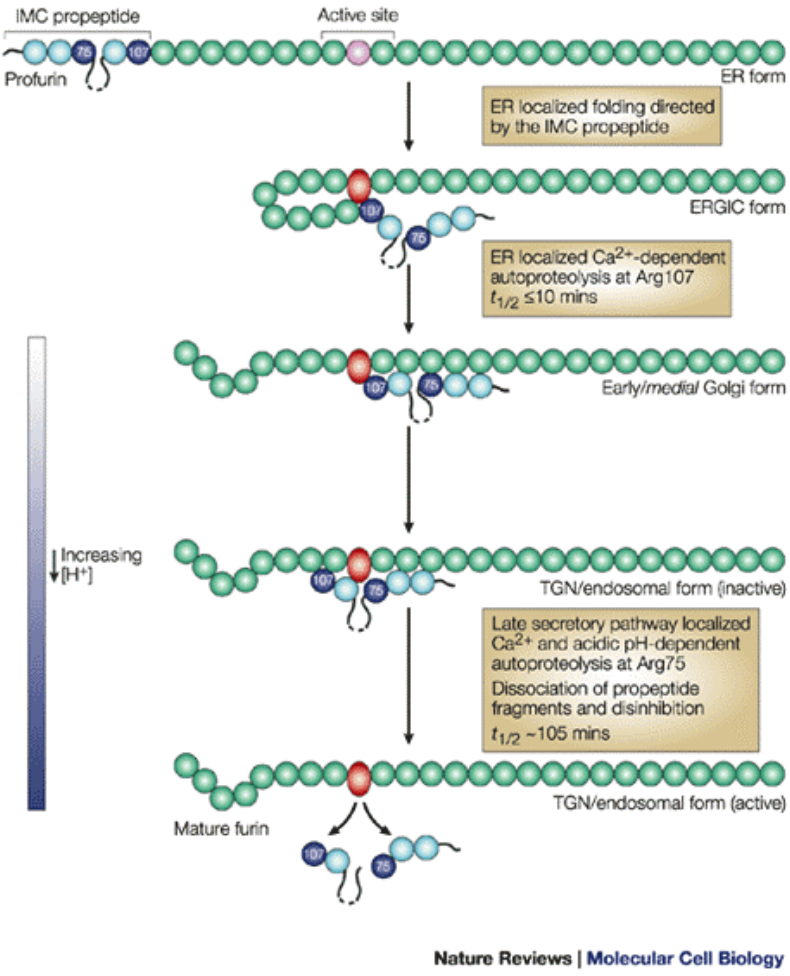

Figure 1.3. A model for furin trafficking. The TGN is the site of furin prodomain release and steady state localization. Through interactions with various adaptor proteins, the cytoplasmic domain directs furin trafficking through two cycling loops (1) at the TGN/endosomal compartments and (2) the plasma membrane and early endosomes. Furin trafficking between the two loops is determined by the phosphorylation state of the acidic cluster motif in the cytoplasmic tail. In the early endosomes, furin with a phosphorylated acidic cluster will recycle to the cell surface, while a dephosphorylated acidic cluster will direct furin back to the TGN (P) (1).

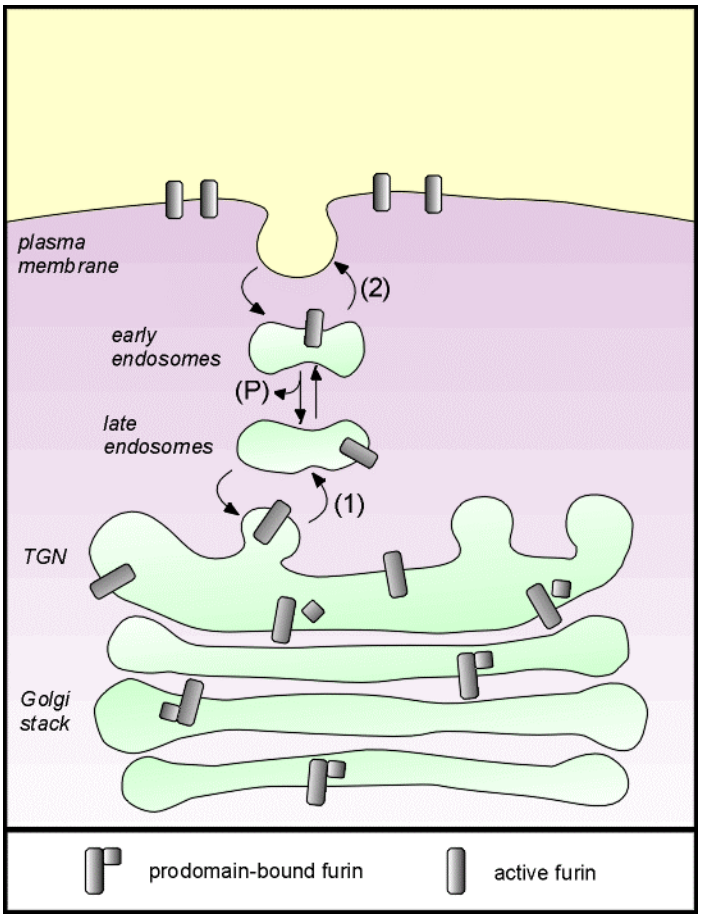

Table 1.1. A list of proproteins cleaved at proposed furin sites. Basic residues at the P1 and P4 positions form the minimal furin cleavage site, while basic residues at the P1, P2, and P4 sites constitute the consensus furin cleavage site. An alternative furin cleavage site is formed by P1, P2, and P6 basic sites. Mauve: basic P1/P4 basic residues constituting the minimal furin cleavage site; cyan: P2 basic residue; olive: P6 basic residue. For a list of references, refer to (10).[1]

	P6		P4		P2	P1	↓ P1'	P2'
Serum proteins								
Proalbumin	R	G	V	F	R	R	D	A
Pro-factor IX	L	N	R	P	K	R	Y	N
Pro-protein C	R	S	H	L	K	R	D	T
Pro-von Willebrand factor	S	H	R	S	K	R	S	L
Hormones and growth factors								
Pro-β-nerve growth factor	T	H	R	S	K	R	S	S
BMP-4 precursor	R	R	R	A	K	R	S	P
Pro-BNP	T	L	R	A	P	R	S	P
Pro-parathyroid hormone	K	S	V	K	K	R	S	V
Pro-semaphorin D (PCS 1)	K	R	R	T	R	R	Q	D
Pro-TGF β1	S	S	R	H	R	R	A	L
Cell-surface receptors								
Insulin pro-receptor	P	S	R	K	R	R	S	L
Notch1 receptor	G	G	R	Q	R	R	E	L
Scatter factor receptor	E	K	R	K	K	R	S	T
Vitamin B_{12} pro-receptor	L	Q	R	Q	K	R	S	I
'Helper' protein/chaperone								
Pro-7B2	Q	R	R	K	R	R	S	V
Extracellular matrix proteins								
BMP-1	R	S	R	S	R	R	A	A
C. elegans rol-6	S	N	R	V	R	R	Q	Q
C. elegans sqt-1	S	K	R	V	R	R	Q	Y
Human MT-MMP1	N	V	R	R	K	R	Y	A
Integrin α3-chain	P	Q	R	R	R	R	Q	L
Profibrillin	R	G	R	K	R	R	S	T
Stromelysin-3	R	N	R	Q	K	R	F	V
Xenopus laevis XMMP	K	I	R	R	K	R	F	L
ZP1	I	A	R	R	R	R	S	S
ZP2	S	L	R	S	K	R	E	A
ZP3α	A	A	R	R	R	R	S	S
Bacterial toxins								
Anthrax toxin PA	N	S	R	K	K	R	S	T
Clostridium septicum α-toxin	K	R	R	G	K	R	S	V
Diphtheria toxin	G	N	R	V	R	R	S	V
Proaerolysin	K	V	R	R	A	R	S	V
Pseudomonas exotoxin A	R	H	R	Q	P	R	G	W
Shiga toxin	A	S	R	V	A	R	M	A
Viral coat proteins								
Avian influenza HA (H5N1)	R	R	R	K	K	R	G	L
Borna disease virus	L	K	R	R	R	R	D	T
Cytomegalovirus gB	T	H	R	T	R	R	S	T
Ebola Zaire GP	G	R	R	T	R	R	E	A
Epstein–Barr virus gB	L	R	R	R	R	R	D	A
HIV-1 gp160	V	Q	R	E	K	R	A	V
Infectious bronchitis virus E2	T	R	R	F	R	R	S	I
Japan B encephalitis M	S	K	R	S	R	R	S	V
Measles virus F_O	S	R	R	H	K	R	F	A
Respiratory-syncitial virus F	K	K	R	K	R	R	F	L
Rous sarcoma virus env	G	I	R	R	K	R	S	V
Yellow fever virus M	S	G	R	S	R	R	S	V

[1] Reprinted from *trends in* Cell Biology, Vol. 9, S.S. Molloy, E.D. Anderson, F. Jean and G. Thomas, Bi-cycling the furin pathway: from TGN localization to pathogen activation and embryogenesis, 28-35, copyright (1999).

Figure 1.4. An illustration of the HIV-1 life cycle. HIV-1 enters the cell via direct fusion following the binding of the envelope proteins gp120/gp41 to the CD4 receptor and the chemokine co-receptor CXCR4 or CCR5. The RNA genome is reverse transcribed in the cytoplasm and the resulting double stranded DNA is incorporated into the host genome. Newly synthesized viral gene products include the envelope precursor protein gp160. The precursor protein travels through the secretory pathway en route to the cell surface and undergoes proteolytic maturation mediated by the PCs at the TGN or later compartments. The cleaved products gp120/gp41 are incorporated into the viral envelope upon viral assembly and budding. Illustration is based on (90).

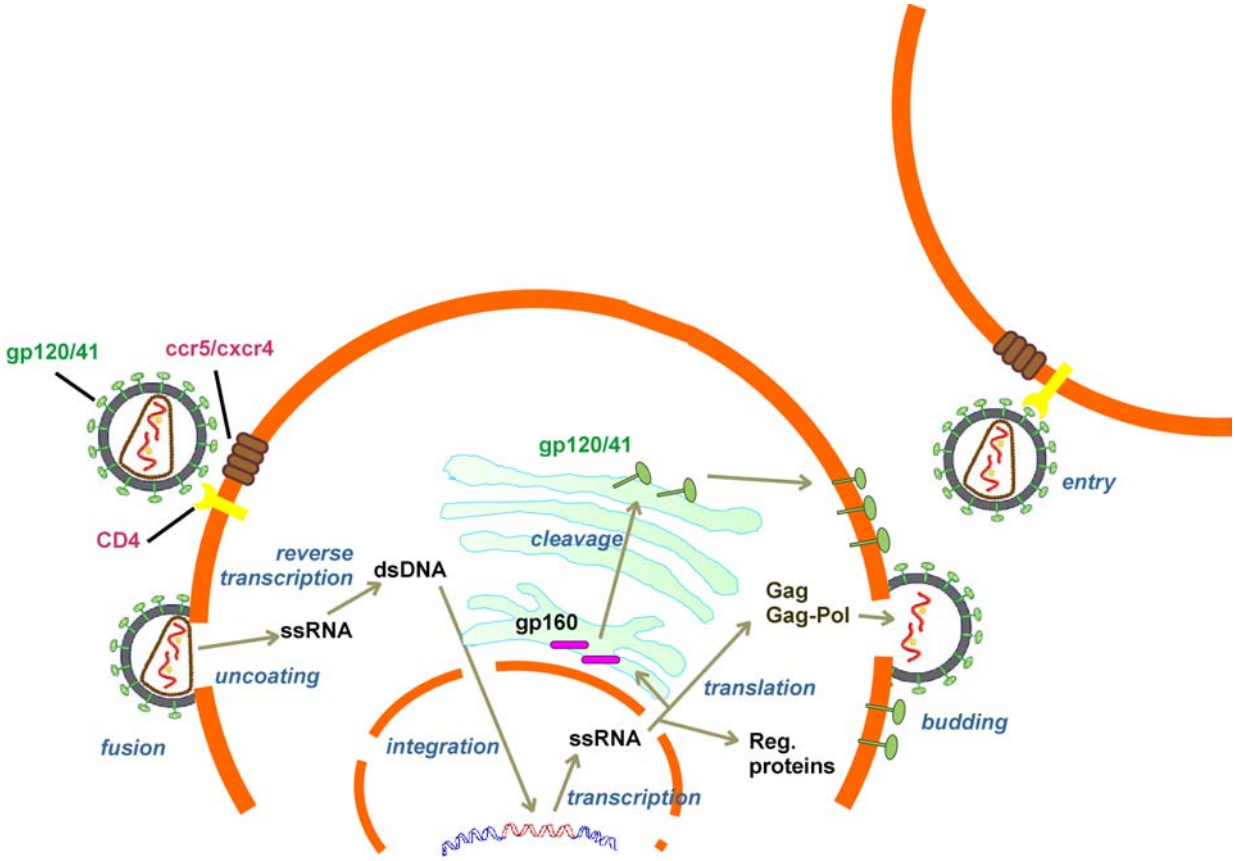

Figure 1.5. Crystal structure of a serpin protease complex. Ribbon depictions of native α_1-antitrypsin with trypsin aligned above it in the docking orientation (left), and of the complex showing the 71 Å shift of the P1 methionine of α_1-antitrypsin, with full insertion of the cleaved reactive-centre loop into the A-sheet (right). Regions of disordered structure in the complexed trypsin are shown as interrupted coils projected from the native structure of trypsin. Red, α_1-antitrypsin β-sheet A; yellow, RSL; green ball-and-stick, P1 Met; cyan, trypsin (with helices in magenta for orientation); red ball-and-stick, active serine 195. Reprinted by permission from Macmillan Publishers Ltd: Nature (125), copyright (2000).

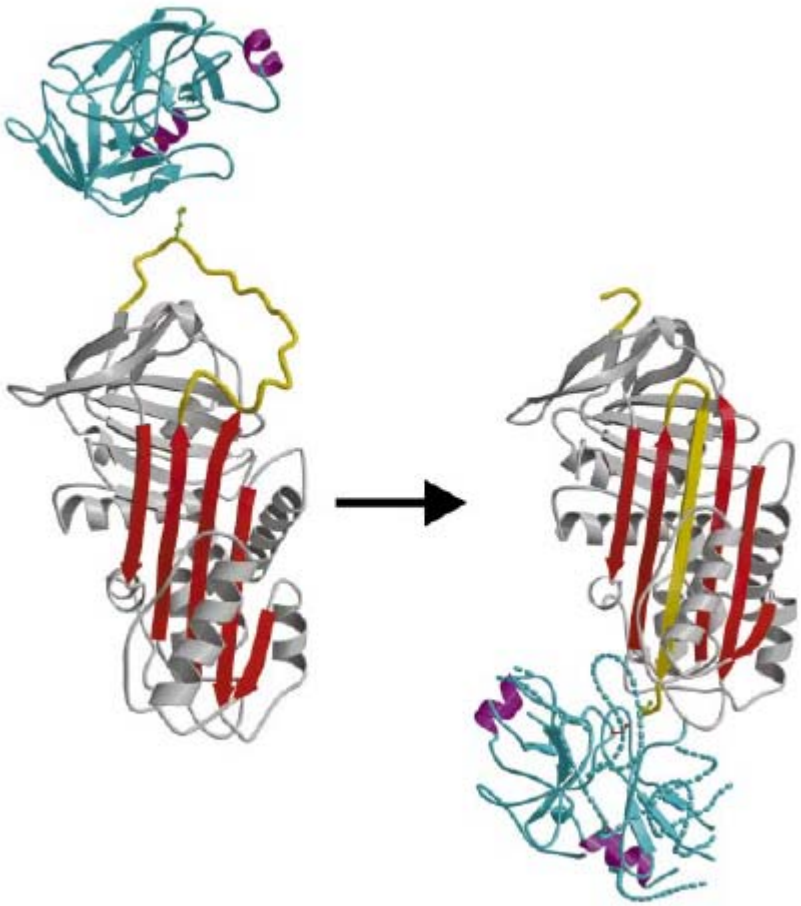

CHAPTER II Materials and methods

2.1 Cell lines and culture conditions

Wildtype (WT) and furin overexpressing (C4) 293A cells, derived from human embryonic kidney 293 (HEK 293) cells, were kindly provided by Dr. Richard Leduc (U. Sherbrooke) and were maintained in complete DMEM supplemented with 10% heat-inactivated fetal bovine serum, 100 U of penicillin, and 100 μg of streptomycin per ml. MAGI-CCR5, a HeLa-CD4 cell line that expresses CXCR4, CCR5, and an HIV-1 long terminal repeat (LTR)-driven β-D-galactosidase reporter gene, was kindly provided by Dr. J. Overbaugh through AIDS Research and Reference Reagents Program, Division of AIDS, NIAID, NIH (143). MAGI-CCR5 cells were cultured in complete DMEM supplemented with 10% heat-inactivated fetal bovine serum, 100 U of penicillin and 100 μg of streptomycin per ml, 0.2 mg of G418 per ml, 0.2 mg of hygromycin B per ml, and 1 μg of puromycin per ml. LoVo cells (144) were maintained in F12 Kaighn's Modification Nutrient Mix (Invitrogen 21127) supplemented with 10% heat-inactivated fetal bovine serum, 100 U of penicillin, and 100 μg of streptomycin per ml. Incubation conditions for all cell lines were 37°C and 5% CO_2.

2.2 Viruses, plasmids, and recombinant proteins

Recombinant His/FLAG-tagged adenovirus Spn4A variants – Spn4A WT ER, AdSpn4A S (ΔHDEL), and Spn4A RSL mutants (RRKR → RRLL), AdSpn4A RRLL ER and AdSpn4A RRLL S (Fig. 3.1) – were generated using the AdEasy^{TM} XL Adenoviral Vector System (Stratagene) by Martine Boutin (Laboratory Technician, Jean lab). CCR5-tropic laboratory-adapted strain HIV-1_{BaL} from S. Gartner and CXCR4-tropic laboratory-adapted strain HIV-1_{IIIB} from R. Gallo (both subtype B), were obtained from AIDS Research and Reference Reagents Program, Division of AIDS, NIAID, NIH. The recombinant vaccinia expression vector encoding gp160 was a gift from Dr. Gary Thomas (Oregon Health & Science University).

The envelope glycoprotein expression vectors of HIV-1_{BaL} and HIV-1_{IIIB} were constructed by amplification by PCR of the *env* fragment of each viral strain, using forward primer SC04F 5' CCC TGGAAGCATC CAGGAAGTCA GCCTA 3' and reverse primer 3LTRi 5' TTAAGCCT CAATAAAGCT TGCCTTGA 3'. The subsequent 3.8kb fragments were re-

amplified with the primer pair PC160ST 5' (forward) GAGCAGAATTCAGTGGCAATGAGAG 3' and PC160REV (reverse) 5' GACCACTTGCATGCCATCTTATAGC 3' which contain EcoR1 and Sph1 sites, respectively. These amplicons were cloned into the pCAGGS/MCS virus envelope expression vector, kindly provided by Dr. Nigel Templeton (University College London).

The *E. coli*-expressed recombinant His/FLAG-Spn4A ER was purified as previously reported (137) by Steven McArthur (Research Assistant, Jean lab) using the AKTApurifier FPLC system (Amersham Biosciences). The *E. coli*-expressed recombinant His/FLAG-Spn4A S was purified using the MagneHis^{TM} Protein Purification System (Promega) according to manufacturer's directions. To produce MAGI-CCR5 cell-expressed recombinant soluble serpins, 1.2×10^6 MAGI-CCR5 cells were seeded in 10 cm diameter plates and incubated for 24 hrs prior to infection. The cells were incubated with 50 µl AdSpn4A S or RRLL S (MOI 3) in 5 ml medium for 2 hrs, washed with PBS, and incubated in 8 ml medium containing 2% FBS for 48 hrs. The medium was collected, 0.22 µm-filtered, filtered again with Viresolve^{R} NFR (Millipore) virus exclusion filter, and concentrated 10X using Amicon Ultra-15 30,000 kDa MW Cut-Off Centrifugal Filter Devices (Millipore) centrifuged in a swinging bucket rotor at 3600 rpm for 7 min. The presence and absence of serpin was determined by Western blot analysis of the concentrate and flowthrough, respectively. Secreted recombinant human furin/His was purchased from R&D Systems (1503-SE).

2.3 In-Cell Western Analysis of cellular actin levels and expression of AdSpn4A variants

To determine relative expression levels of AdSpn4A variants and their effect on cellular actin levels, 3000 MAGI-CCR5 cells per well were seeded in 96 well plates and incubated for 24 hrs. Media was removed, and cells were treated with a series of seven two-fold dilutions of AdSpn4A ER (MOI 3 = dilution factor of 1), AdSpn4A S (MOI 40 = dilution factor of 1), AdSpn4A RRLL ER (MOI 7 = dilution factor of 1) or AdSpn4A RRLL S (MOI 40 = dilution factor of 1) in 200 µl media, and incubated for 7 days. Relative levels of Spn4A and actin were determined by In-Cell Western Analysis using the Li-Cor Odyssey Infrared Imaging System and Application Software Version 2.0 (Li-Cor Biosciences). Assays were performed according to the Li-Cor Odyssey In-Cell Western Assay protocol with the following amendments/conditions. All

steps requiring the use of Li-Cor Odyssey Blocking Buffer were performed with the blocking buffer diluted 1:1 in PBS. The cells were probed with 1:500 anti-FLAG MAb M2 (Sigma F1804) overnight, and subsequently treated for 1 hr with secondary antibody 1:800 IRDye^{TM} 800CW goat anti-mouse Ab (LI-COR 926-32210) and 1:5000 Alexa Fluor 680 phalloidin actin dye (Molecular Probes, Invitrogen A22286). Relative expression of FLAG normalized to actin intensity was determined as described in the Li-Cor In-Cell Western Assay Analysis manual.

2.4 Analysis of the secretion patterns and furin-directed activity of AdSpn4A variants

In six well plates, 1×10^5 MAGI-CCR5 cells per well or 2×10^5 HEK 293 WT or C4 cells per well were seeded 24 hrs prior to AdSpn4A infection. Media was removed and replaced with medium containing 2% FBS and AdSpn4A variants ER, S, RRLL ER, RRLL S (MOI 0.5, 8, 1, 8, respectively) to MAGI-CCR5 cells, and (MOI 0.1, 1, 0.2, 1, respectively) to HEK 293 cells. The infected HEK 293 cells and MAGI-CCR5 cells were incubated for 24 and 48 hrs, respectively, and media and whole cell lysates were prepared according to the protocol in section 2.5.

2.5 Media collection, preparation of whole cell lysates and cellular membrane fractionation

Media was collected and centrifuged at 3000 × g for 5 min to pellet the cell debris. Cells were washed with 2 ml PBS, detached by scraping, and harvested by centrifugation at 3000 × g for 5 min. To prepare whole cell lysates, cell pellets were re-suspended in 200 µl hypotonic buffer (20 mM Tris pH 7.4, 10 mM $MgCl_2$, 10 mM $CaCl_2$, and 10% protease inhibitor cocktail). Re-suspended cells were incubated on ice for 15 min and vortexed every five min. Cell extract was mixed with equal volume of 2X SDS sample buffer containing 5% β-mercaptoethanol and heated at 95°C for 10 min. For cellular membrane fractionation, cell pellets were resuspended in 300 µl ice-cold hypotonic buffer (10 mM Tris-HCl, pH 7.8; 10 mM NaCl) and subjected to three 5 min freeze thaw cycles. Nuclei were removed by centrifugation at 900 × g for 5 min at 4°C and the supernatants were subjected to further centrifugation at 15000 × g for 20 min at 4°C to pellet the cellular membranes. Membrane pellets were resuspended in 20 µl hypotonic buffer, mixed with 10 µl 2X SDS sample buffer containing 5% β-mercaptoethanol and heated at 95°C for 10 min.

2.6 Western blot analysis conditions

Samples were separated by SDS-PAGE on a 10% gel run at 100 V for 2 hrs. Western transfer onto a nitrocellulose membrane was performed using Biorad Trans-Blot SD Semi-dry Transfer Cell at 25 V for 45 min. Infrared Western blot was performed according to the Li-Cor Odyssey Western Blot protocol (145) with the following amendments/conditions. All steps requiring the use of Li-Cor Odyssey Blocking Buffer were performed with the blocking buffer diluted 1:1 in PBS. Blots were incubated in primary antibodies 1:200 anti-gp120 rabbit polyclonal Ab (ABI 13-108-100), 1:1000 anti-Hsp47 mouse monoclonal Ab (Stressgen SPA-470), 1:500 anti-His mouse monoclonal Ab (ABM G020), 1:500 anti-FLAG rabbit polyclonal Ab (ABR PA1-984B), or 1:500 anti-FLAG mouse monoclonal M2 Ab (Sigma F1804) and secondary antibodies 1:15 000 IRDye^{TM} 800CW goat anti-mouse Ab (LI-COR 926-32210) and 1:15 000 IRDye^{TM} 680CW goat anti-rabbit Ab (LI-COR 926-32221). Band intensities were quantified using the Application Software Version 2.0 (Li-Cor Biosciences) as described in the software manual, using median top/bottom as the background subtraction method.

For chemiluminescence Western blot**,** membranes were blocked at 4°C overnight in 0.05% TBS-Tween containing 5% milk powder, and incubated at RT with gentle rocking in 1:1000 anti-FLAG MAb M2 (Sigma F1804). Membranes were then washed 3 times for 10 min in 0.05% TBS-Tween, incubated for 1 hr with gentle rocking in 1:1000 antimouse horseradish peroxidase conjugate antibody (Amersham NA931V), and again washed 3 times for 10 min in 0.05% TBS-Tween and twice with TBS only. Membrane was incubated at RT for 3 min in 2 ml ECL Detecton Reagent kit (Amersham Biosciences RPN 2109) and chemiluminescence film was exposed for 10 seconds prior to development.

2.7 HIV-1 gp160 processing in the presence of Spn4A

For AdSpn4A experiments, 1×10^5 MAGI-CCR5 cells per well were seeded in six well plates and incubated overnight. Media was replaced with 2 ml media containing AdSpn4A ER (MOI 8 or 0.5), AdSpn4A S (MOI 8), AdSpn4A RRLL ER (MOI 8) or AdSpn4A RRLL S (MOI 8) and cells were incubated for 48 hrs. For recombinant Spn4A experiments, 2×10^5 MAGI-CCR5 cells per well were seeded in six well plates and incubated overnight. At time points 24 hrs pre-transfection, 18 hrs pre-transfection, at time of transfection, 12 hrs post transfection, or at

each time point, *E. coli*-expressed Spn4A ER (350 μM), *E. coli*-expressed Spn4A S (3.8 μM), or Spn4A S MAGI-CCR5 media concentrate (4.5 μM) was added to media.

Media of the serpin-treated cells was changed and cells were transfected with 2 μg pCAGGS IIIB gp160 or pCAGGS BaL gp160 plasmid per well using Mirus TransIT^{R}-LT1 Transfection reagent according to manufacturer's recommendations with the following specifications. Eight μl TransIT^{R}-LT1 Transfection reagent was mixed with 250 μl OptiMEM^{TM} reduced serum media (Invitrogen) and incubated for 15 min at RT. Plasmid DNA was added and incubated at RT for an additional 25 min, and the mixture was added to cells. One μM azidothymidine (AZT) was added to corresponding cells at time of transfection. Cells were incubated for 48 hrs and harvested according to the cellular membrane fractionation protocol in section 2.5.

For analysis of furin-independent processing, 4×10^5 LoVo cells per well were seeded in six well plates and incubated overnight. Media was replaced with 2 ml media containing AdSpn4A S or AdSpn4A RRLL S (MOI 3) and cells were incubated for 36 hrs followed by infection with the vaccinia virus expression vector encoding gp160. Twelve hrs post-vaccinia infection, cellular membrane fractions were prepared for SDS-PAGE as described in section 2.5.

2.8 Detection of productive HIV-1 infection in the presence of Spn4A

Three thousand MAGI-CCR5 cells per well were seeded in 96 well plates and incubated for 24 hrs. Media was removed and cells were inoculated with 200 μl media containing AdSpn4A ER, AdSpn4A S, AdSpn4A RRLL ER, or AdSpn4A RRLL S (MOI 8).

Forty eight hrs post-AdSpn4A infection, medium from each well was removed, and the cells were inoculated with HIV-1_{IIIB} (MOI 0.005) or HIV-1_{BaL} (MOI 0.01) in a total volume of 50 μl containing 20 μg of DEAE-dextran per ml. After 2 hrs incubation (37°C, 5% CO_2), the viral inoculum was removed and 200 μl of fresh medium was added. For AZT-treated samples, 1 μM AZT was added with the viral inoculum and reapplied with the fresh medium. Four days later, the medium was removed and reserved for secondary infection, and the monolayer was fixed for 5 min at room temperature with 100 μl of 4% paraformaldehyde solution in PBS. To generate secondary infection, 96 well-plates containing freshly plated MAGI-CCR5 cells were

inoculated with 100 µl of medium from the primary infection and incubated for 48 hrs prior to fixing with 4% paraformaldehyde solution. Levels of primary and secondary HIV-1 infections were determined by β-galactosidase activity and enumeration of blue foci by the MAGI (multinuclear activation of galactosidase indicator) assay.

To determine β-galactosidase activity, cells were incubated with the β-galactosidase substrate O-nitrophenyl β-d-galactopyranoside (ONPG) dissolved at 3 mg/ml in PBS containing 0.5% NP-40. At one and two hrs post-substrate addition, the plates were read at OD405 nm in a Spectra Max 250 ELISA reader. To visualize and quantify blue foci, cells were washed twice with PBS, stained with 4 mM potassium ferrocyanide, 4 mM potassium ferricyanide, 2 mM $MgCl_2$, and 0.4 mg/ml 5-bromo-4-chloro-3-indolyl-β-D-galactopyranoside (X-gal stain, Invitrogen) in PBS at 37°C, 5% CO_2 for 50 min. Cells were again washed twice with PBS. Blue foci were quantified using the CellProfiler cell image analysis software (Broad Institute).

2.9 Furin assays and SDS-PAGE of furin-Spn4A reactions

The furin assay data was obtained using a SpetraMax Gemini XS spectrofluorometer equipped with a temperature-controlled 96 well plate reader (Molecular Devices) at excitation and emission wavelengths of 370 and 460 nm to measure release of 7-amino-4-methylcoumarin. Assays were performed with 0.2 µg recombinant furin, 100 µM pRTKR-MCA, and 10 µl recombinant Spn4A in 100 mM Hepes, pH 7.5, containing 0.5% Triton X-100 and 1 mM $CaCl_2$ in a total volume of 100 µl. For titration of furin by Spn4A S, 8 ng recombinant furin was incubated with increasing amounts of Spn4A concentrate for 15 min. pRTKR-MCA (100 µM) was added to determine residual furin activity. For SDS-PAGE of furin–Spn4A, reactions were performed under the buffer conditions for furin assays in a total volume of 50 µl. Recombinant furin (0.5 µg) was incubated with Spn4A for 10 min, reactions were stopped with addition of 50 mM EDTA, mixed immediately with SDS-loading buffer, and heated at 95°C for 10 min. Western blot analyses were performed as described in section 2.6.

CHAPTER III Cell-based expression studies and anti-furin activity of Spn4A variants

As a potent furin inhibitor, Spn4A holds potential in the inhibition of gp160 processing and infectious HIV-1 production. In preliminary evaluation of its applicability as an anti-viral agent, we sought to validate an expression system for Spn4A and its bioengineered variants and to determine the effect of Spn4A expression on cellular actin levels. Furthermore, to expand upon the previously published properties of Spn4A *in vitro* and in non-human cell lines, we studied the trafficking and anti-furin activity of Spn4A and its variants in human cell-based systems.

3.1 Development of Spn4A variants

In our studies of PC-directed inhibition and HIV-1 gp160 processing and virus production, we employed four signal peptide-containing FLAG-Spn4A variants differing in their RSL sequence and cellular sorting motifs (Fig. 3.1). The naturally occurring *Drosophila* serpin is represented by variant *a* (Spn4A ER), containing the furin consensus cleavage sequence RRKR in the P4 to P1 positions of the RSL, and a C-terminal HDEL sequence predicted to act as an ER-retention motif. Because the trafficking and activity of type-I secretory pathway PCs is predominantly confined to the late secretory compartments (10), we constructed a ΔHDEL variant of Spn4A (variant *b*) (Spn4A S) that was predicted to encounter subcellular sites of PC activity en route to its extracellular secretion. Additionally, we engineered the ER (variant *c*) and S (variant *d*) forms of a RSL Spn4A variant, containing a two-residue substitution in the P1 and P2 positions (RRKR→RRLL) (Spn4A RRLL ER and S). The Spn4A RRLL variants were predicted to be inactive as serpins of furin, as Arg in the P1 position and a basic residue in the P2 position are critical and highly favourable for furin recognition, respectively (13, 14). The Spn4A variants were encoded within adenovirus vectors (AdSpn4A), which were used as a means of delivery and intracellular expression of the serpins.

3.2 Spn4A expression studies

To determine the expression levels of Spn4A variants in MAGI-CCR5 cells and their effect on actin levels following seven days of AdSpn4A infection, we employed a quantitative cell-based assay (Li-Cor Odyssey In-cell Western^{TM}) (146). The expression of all four variants

was successfully detected, validating the adenovirus system as a method of Spn4A delivery (Fig. 3.2). Additionally, Spn4A levels correlated with those of AdSpn4A, as higher viral titers resulted in higher Spn4A detection with an eventual plateau at the lowest AdSpn4A dilution factors (Fig. 3.2 A-D). Cellular actin levels suggested that at the tested titers, the ER Spn4A variants (Fig. 3.2 A, C) did not affect cell proliferation rate. In contrast, in the cells expressing the S Spn4A variants, actin levels were significantly lower at the highest AdSpn4A titers (Fig. 3.2 B, D, suggesting cell toxicity at high levels of adenovirus infection/Spn4A WT/RRLL S expression. Furthermore, a comparison of intracellular Spn4A variant levels indicated that there was a markedly greater accumulation of the ER forms, suggesting that Spn4A WT and RRLL ER are indeed intracellularly retained, while Spn4A WT and RRLL S are largely secreted (Fig. 3.2 E).

3.3 Localization of Spn4A variants

Immunofluorescence studies of overexpressed Spn4A localization in COS-7 cells (141) and HEK 293 cells (unpublished observations, Stephanie Condotta, Jean lab) indicate that the wildtype serpin is localized to the ER and that a deletion of the C-terminal HDEL motif results in the secretion of the serpin (140). We sought to confirm the predicted secretion patterns of the Spn4A variants by their detection in cell extracts and media of MAGI-CCR5 cells infected with AdSpn4A. Western blot analysis indicated that the serpins containing the HDEL ER-retention motif, Spn4A ER and Spn4A RRLL ER, were retained intracellularly, whereas the serpin variants with the HDEL deletion, Spn4A S and Spn4A RRLL S, were detected both intracellularly and secreted in the media (Fig. 3.3). To estimate the proportion of Spn4A that was intracellularly-retained or secreted, we quantified the relative intensities of the Spn4A variant bands. Our analysis indicated that 98 and 99% of Spn4A ER and RRLL ER, respectively, were retained within the cells, while 93 and 98% of Spn4A S and RRLL S, respectively, were estimated to be secreted (Table 3.1). The secreted Spn4A migrated to a slightly higher molecular weight than the intracellularly-retained Spn4A, which may reflect a differential glycosylation state at the single putative glycosylation site of the serpin (137). Additionally, Spn4A RRLL ER was detected in two molecular weight forms, suggesting that it is susceptible to cleavage in the ER by an endogenous protease (Fig. 3.3). A possible candidate for this cleavage is the S1P/Ski-1

serine protease, which is active in the secretory pathway and processes substrates at the RRLL sequence (147, 148).

3.4 SDS-stable complex formation in furin overexpressing mammalian cell lines

Although anti-furin activity of Spn4A has been demonstrated *in vitro* and in *Drosophila* cells (137, 141), the ability of Spn4A to inhibit furin in mammalian cells is a prerequisite for its application as an anti-HIV agent. In order to determine if Spn4A acts as a serpin of furin in mammalian cells, we expressed the four variants in human embryonic kidney (HEK)-derived 293A wildtype (WT) and FLAG-furin overexpressing (C4) cells, and detected by Western blotting, the presence of an SDS-stable complex in cell extracts and media (Fig. 3.4). FLAG-furin was present in the cell extracts as a 106/100 kDa doublet corresponding to differential glycosylation states, and in the media, in the 81 kDa shed form (41, 49). Spn4A variant expression was detected in both cell lines and was in line with the secretion patterns observed in MAGI-CCR5 cells. However, whereas in MAGI-CCR5 cells the Spn4A variants were present as a single band (with the exception of Spn4A RRLL ER) (Fig. 3.3), Spn4A variants expressed in HEK WT and C4 cells appeared to be subject to proteolytic cleavage, as a majority were detected as two bands or more (Fig. 3.4). The additional bands were likely not generated by overexpressed furin, except in the case of Spn4A S, which was detected as a single band in the media of HEK WT cells, and two bands in the media of HEK C4 cells.

High molecular weight doublet bands (~160 kDa) corresponding to EI* complexes between furin in its two glycosylation states and Spn4A were observed in C4 cells expressing Spn4A ER and S and not in WT cells (Fig. 3.4 A). An intracellular complex was not detected in cells expressing the RSL variants of Spn4A (Fig. 3.4 B), indicating that the two-residue substitution in the P1 and P2 positions abolished furin recognition. In the media of HEK C4 cells expressing Spn4A S, a single band of slightly lower molecular weight than the intracellular doublet was detected, and likely corresponds to an EI* complex between Spn4A S and shed furin (Fig. 3.4 A). Unexpectedly, a faint band of approximately the same molecular weight was detected in the media of HEK C4 cells expressing Spn4A RRLL S, suggesting that in the extracellular environment, a small proportion of the variant may complex with furin (Fig. 3.4 B).

Our results demonstrate the furin-directed serpin activity of Spn4A ER and S in a mammalian cell-based furin overexpression system. Furthermore, they suggest that the RSL variants do not complex with furin intracellularly, but may do so extracellularly to a lesser extent than the wildtype RSL variants.

3.5 *In vitro* anti-furin activity of secreted Spn4A

The processing of many furin substrates occurs at the cell surface, including those of several bacterial protoxins (1). Our SDS-stable complex analyses in 293A C4 cells suggested that Spn4A S is active extracellularly (Fig. 3.4 A) and may therefore be functional in the inhibition of furin-mediated cell surface processing events. Additionally, our analyses did not rule out the ability of Spn4A RRLL S to inhibit furin, as a high molecular weight band was detected in the media of 293A C4 cells expressing the variant (Fig. 3.4 B). To further investigate the anti-furin activity of the secreted serpin variants, we determined their ability to inhibit recombinant furin *in vitro* as measured by enzyme inhibition assays and SDS-stable complex formation.

Media from MAGI-CCR5 cells expressing the secreted Spn4A variants was collected and concentrated 10X, and the resulting serpin concentrate was used in furin activity assays. In enzyme inhibition assays, furin was incubated with the fluorogenic substrate pRTKR-MCA and serpin concentrate, and furin activity was measured by the release of fluorescent MCA. The assays indicated that in the presence of Spn4A S concentrate, furin activity was inhibited, whereas it remained unchanged compared to the control in the presence of Spn4A RRLL S concentrate (Fig. 3.5 A). Serpin titration analyses indicated that the inhibitory effect of Spn4A S was concentration-dependent as furin activity decreased in concurrence with increasing volumes of Spn4A S concentrate (Fig. 3.5 B).

To determine the ability of the Spn4A concentrates to form an EI* complex with furin *in vitro*, we co-incubated furin with Spn4A concentrates and detected the presence of an SDS-stable complex by Western blot analysis. A complex was detected in samples containing Spn4A S or *E. coli*-expressed Spn4A ER and furin (Fig. 3.5 C). In contrast to the results obtained in our 293A C4 Spn4A expression experiments (Fig. 3.4 B), Spn4A RRLL S did not form a complex with

furin *in vitro* (Fig. 3.5 C). This may signify a relaxed furin recognition specificity when high concentrations of shed furin and Spn4A RRLL S are co-incubated in 293A media, that is not observed under *in vitro* Hepes-buffered conditions. Interestingly, although an SI value of 1 of Spn4A for furin has been previously reported (137), we observed a cleavage of Spn4A in the presence of furin, suggesting that under our experimental conditions, a proportion of Spn4A ER/S is processed by furin through the substrate pathway.

3.6 Summary

By adenoviral vector-mediated Spn4A variant expression in mammalian cells, we analyzed cell actin levels in response to Spn4A expression, the differences in secretion patterns attributed to the C-terminal HDEL sequence, and the RSL sequence-determined furin specificity of the Spn4A variants. Our results indicated that cell numbers as measured by actin levels were not significantly affected except at the highest tested AdSpn4A titers, a deletion of the HDEL sequence resulted in the extracellular secretion of the otherwise intracellularly retained serpin, and that furin inhibition by Spn4A was abrogated with a substitution in the P1 and P2 positions of the RSL (RRKR → RRLL). Thus, we hypothesized that when expressed at levels below the toxic range, Spn4A ER and S may serve as effective inhibitors of gp160 processing and productive HIV-1 infection.

Figure 3.1. Schematic representation of His/FLAG-tagged Spn4A variants. The wildtype Spn4A (*a*) and the secreted variant with a deletion of the HDEL ER-retention sequence (*b*) contain the furin consensus sequence (RRKR). Variants *c* (containing the HDEL ER-retention sequence) and *d* (ΔHDEL) contain a two-residue substitution in the RSL (RRKR → RRLL). All four variants contain an N-terminal signal peptide (SP).

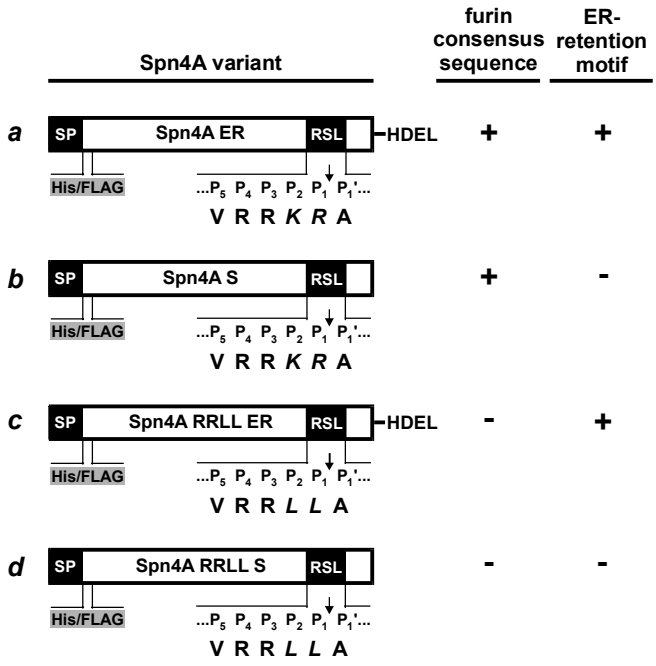

Figure 3.2. Relative intracellular accumulation of His/FLAG-Spn4A (black bars) and actin levels (grey line plot) in MAGI-CCR5 cells 7 days post-infection with AdSpn4A. Cells were infected with a 2-fold dilution series of AdSpn4A **A)** WT ER (MOI 3, 1.5, 0.75, 0.375, 0.1875, 0.0938, 0.0469, 0.0234), **B)** WT S (MOI 40, 20, 10, 5, 2.5, 1.25, 0.625, 0.3125), **C)** RRLL ER (MOI 7, 3.5, 1.75, 0.875, 0.4375, 0.2188, 0.1094, 0.0547), and **D)** RRLL S (MOI 40, 20, 10, 5, 2.5, 1.25, 0.625, 0.3125). Seven days post infection, cells were fixed, permeabilized, and probed with mouse monoclonal anti-FLAG Ab and secondary IRDye^{TM} 800CW goat anti-mouse Ab and stained with Alexa Fluor 680 phalloidin actin dye. Plates were scanned and analysed using the Li-Cor Odyssey Infrared Imaging System and Application Software Version 2.0 (Li-Cor Biosciences). Relative FLAG intensity normalized to actin integrated intensity (800/700 nm) with highest MOI as the 100% value is shown in **A-D**. Panel **E** depicts comparative Spn4A variant intracellular levels based on integrated FLAG intensity normalized to actin integrated intensity (800/700 nm). Data are averages of three independent experiments [error bars represent standard error].

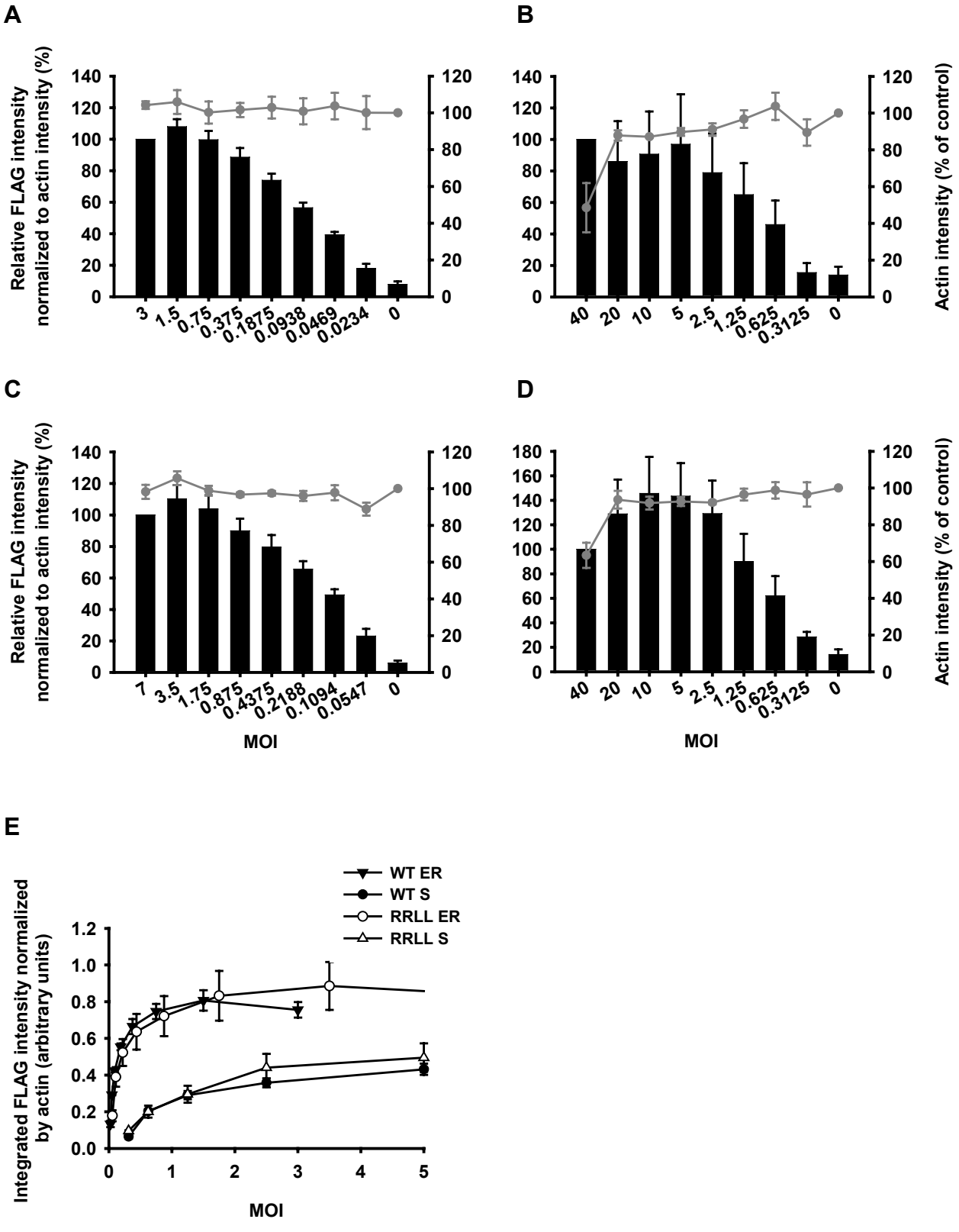
A
Relative FLAG intensity normalized to actin intensity (%)
3
1.5
0.75
0.375
0.1875
0.0938
0.0469
0.0234
0
B
Actin intensity (% of control)
40
20
10
5
2.5
1.25
0.625
0.3125
0
C
Relative FLAG intensity normalized to actin intensity (%)
7
3.5
1.75
0.875
0.4375
0.2188
0.1094
0.0547
0
MOI
D
Actin intensity (% of control)
40
20
10
5
2.5
1.25
0.625
0.3125
0
MOI
E
WT ER
WT S
RRLL ER
RRLL S
Integrated FLAG intensity normalized by actin (arbitrary units)
MOI

Figure 3.3. Secretion patterns of Spn4A variants expressed in MAGI-CCR5 cells. MAGI-CCR5 cells were infected with AdSpn4A variants ER, S, RRLL ER, RRLL S (MOI 0.5, 8, 1, 8, respectively) and incubated 48 hrs. Cell extracts (C) and media (M) were prepared for SDS-PAGE as described in section 2.5 and analyzed by Western blotting probing with mouse monoclonal anti-FLAG Ab and secondary infrared 800CW anti-mouse Ab as described in section 2.6. A representative image of two independent experiments is shown; molecular weight (kDa) is shown on the left.

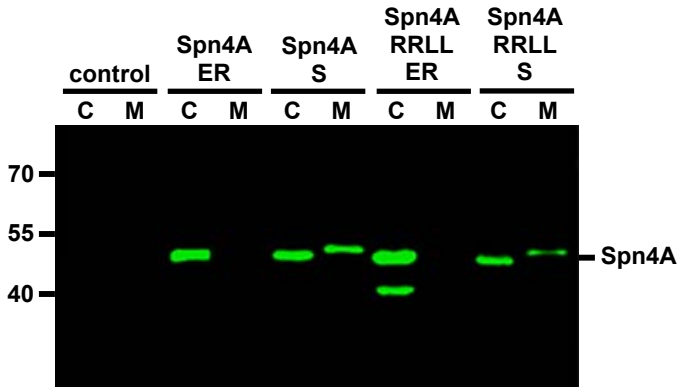

Table 3.1. Relative intracellular and extracellular levels of Spn4A variants expressed in MAGI-CCR5 cells. The percentage of intracellularly-retained and secreted Spn4A was determined by band intensity quantification of Western blot images from Fig. 3.3 as described in section 2.6. Data are averages of two independent experiments.

Variant	% Retained	% Secreted
WT ER	98	2
WT S	7	93
RRLL ER	99	1
RRLL S	2	98

Figure 3.4. SDS-stable complex formation between furin and Spn4A variants in furin overexpressing mammalian cells. 293A wildtype (WT) and FLAG-furin overexpressing (C4) cells were infected with **A)** Spn4A ER and S (MOI 0.1 and 1, respectively) and **B)** Spn4A RRLL ER and S (MOI 0.2 and 1, respectively) and incubated for 48 hrs. Cell extracts (C) and media (M) were prepared for SDS-PAGE as described in section 2.5 and analyzed by Western blotting probing with mouse monoclonal anti-FLAG Ab and secondary anti-mouse-HRP Ab as described in section 2.6. Representative images of two independent experiments are shown; molecular weight (kDa) is shown on the left.

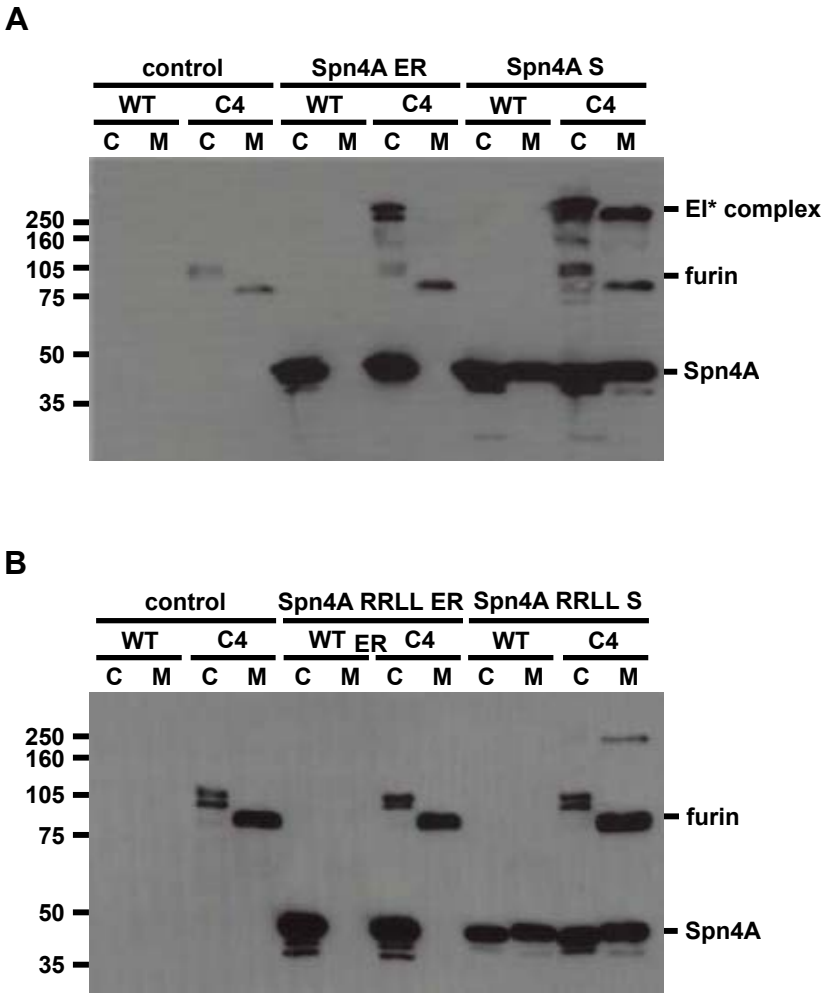

Figure 3.5. *In vitro* anti-furin activity of secreted Spn4A from concentrated media of MAGI-CCR5 cells. MAGI-CCR5 cells were infected with AdSpn4A S and RRLL S (MOI 3) and incubated for 48 hrs. Media was collected and concentrated 10X. The resulting Spn4A concentrate was used in: **A)** Enzyme inhibition assay where furin/His was incubated with pRTKR-MCA (100 μM) in the absence or presence of Spn4A S/RRLL S concentrate; **B)** Titration of furin/His by Spn4A S concentrate in which furin was incubated with increasing amounts of Spn4A concentrate for 15 min. pRTKR-MCA (100 μM) was added to determine residual furin activity as described in section 2.9. The concentration of Spn4A used in assay was estimated by Western blot band intensity titration against known Spn4A ER (*E. coli*) concentrations (Appendix 1); **C)** Complex formation by furin/His and Spn4A S. Furin was incubated with Spn4A S/RRLL S concentrates or *E. coli*-produced Spn4A ER for 10 min, reactions were stopped with addition of EDTA and processed for Western blot analyses. Blots were probed with mouse anti-His and rabbit anti-FLAG Abs, and secondary infrared 800CW anti-mouse (green) and 700CW anti-rabbit (red) Abs. Data and image are representative of two independent experiments performed in duplicate. Molecular weight (kDa) is shown on the left.

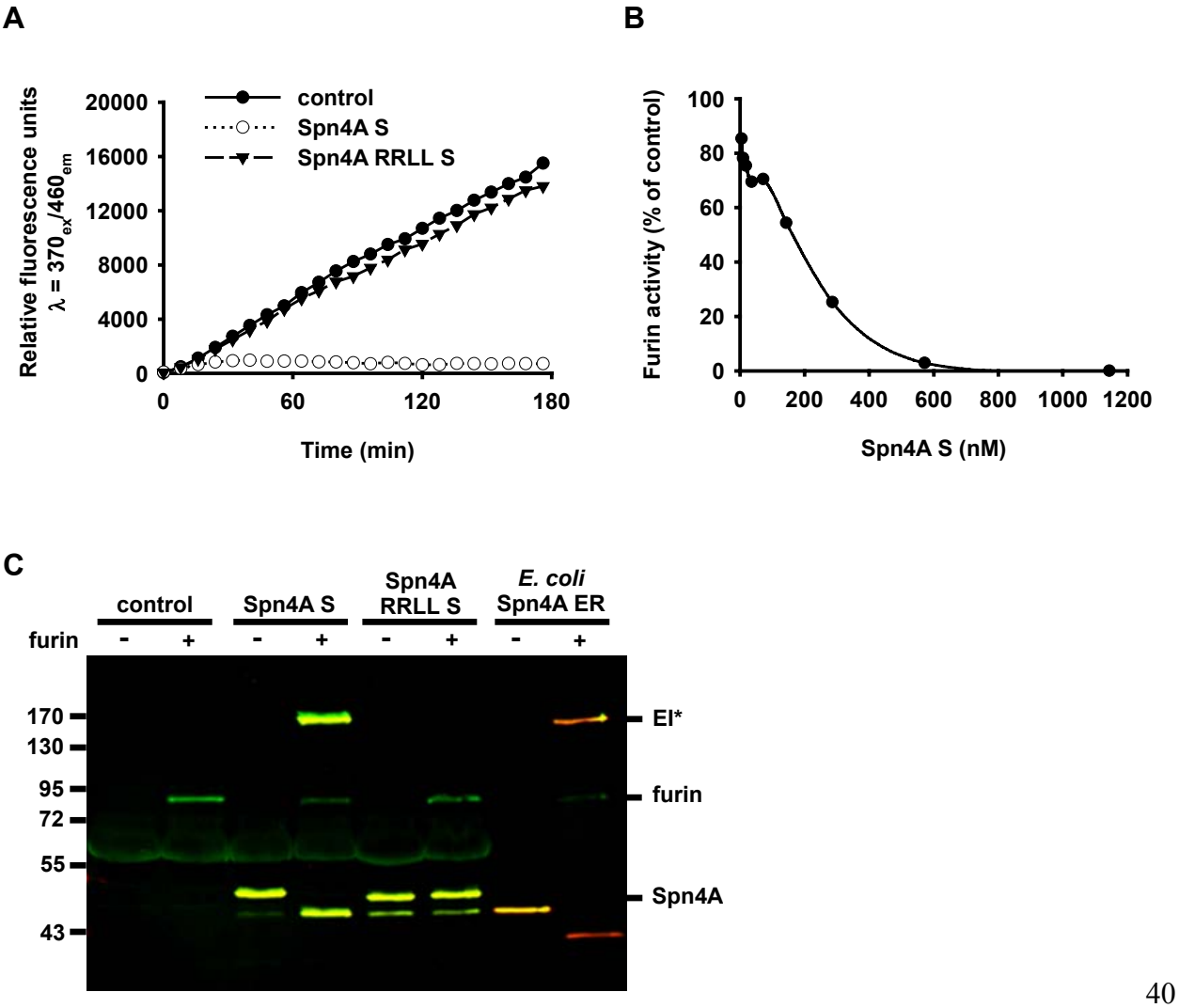

CHAPTER IV Anti-HIV-1 activity of Spn4A variants

In Chapter III we confirmed the ability of the Spn4A variants containing the furin consensus sequence in their RSL (Spn4A ER and Spn4A S) to act as serpins of furin. In addition, our cell expression studies indicated that the intracellular retention or secretion of Spn4A variants is dependent on the presence of the C-terminal HDEL ER-retention sequence. In the studies described in the present chapter, we evaluated the ability of the four Spn4A variants differing in their furin specificity and localization to inhibit HIV-1 gp160 processing and the production of infectious virions. Our studies were conducted in MAGI-CCR5 cells, a HeLa cell line expressing the HIV receptor and co-receptors (CD4 and CXCR4, CCR5) and HIV-1 Tat-induced β-galactosidase as a marker of HIV-1 replication (143). In studies of furin-independent gp160 processing, LoVo cells (144), a human adenocarcinoma cell line deficient in furin activity were used.

4.1 Anti-HIV activity of adenovirus-delivered Spn4A variants in MAGI-CCR5 cells

In order to assess if the furin-directed serpins Spn4A ER and S can act as inhibitory agents of PC-dependent HIV-1 gp160 processing, we sequentially infected and transfected MAGI-CCR5 cells with AdSpn4A and the envelope expression vector gp160 from the CCR5-tropic HIV-1 BaL strain, respectively. Two days post-transfection, cellular membrane fractions were prepared and analyzed by Western blotting probing for gp160, the cleaved product gp120, and a membrane marker, heat shock protein 47 (Hsp47) – a non-inhibitory ER-localized serpin (149). The precursor protein gp160 and the cleaved product gp120 were detected in all membrane fractions transfected with the envelope construct except in those of cells expressing Spn4A S, in which only gp160 was present (Fig. 4.1 A). Analyses of gp160 cleavage efficiency obtained by quantification of gp160 and gp120 band intensities indicated a nearly complete block in gp160 processing in cells expressing Spn4A S. Additionally, Spn4A ER appeared to partially impair gp160 processing, as the efficiency of cleavage averaged 68 of the control value ($p = 0.08$) (Fig. 4.1 B). The RSL variants of Spn4A and the reverse transcriptase inhibitor AZT did not significantly affect precursor cleavage. Hence, the furin-directed serpin variant Spn4A S

was an effective inhibitor of gp160 processing when expressed in MAGI-CCR5 cells, while Spn4A ER may have inhibited processing to a lesser extent.

In our gp160 processing analyses, we consistently observed a doublet band of Hsp47 in membrane fractions expressing the ER Spn4A variants, while only a single band was present in untreated and S Spn4A variant expressing cells (Fig. 4.1 A). Hsp47 is an ER-localized glycoprotein with a C-terminal RDEL sequence acting as an ER-retention motif (149). Like the HDEL sequence, the RDEL motif is thought to be recognized by a KDEL-like receptor, which shuttles the motif-containing protein from the *cis*-Golgi back to the ER (150). The appearance of the higher molecular weight band of Hsp47 when the ER Spn4A variants are overexpressed may correspond to differentially glycosylated, and hence, differentially localized Hsp47. This led us to hypothesize that overexpression of a protein whose localization is managed by a KDEL-like receptor, could lead to the saturation of the receptor and secretion of the otherwise ER-retained protein. We thus collected the media of the cells in our gp160 processing experiments and probed for the presence of Spn4A. Although at more moderate titers of AdSpn4A ER and RRLL ER the expressed serpin variants were retained within the cells (Fig. 3.3), the titers used in the gp160 processing experiments led to the secretion of the ER Spn4A variants (Fig. 4.1 A). However, the Spn4A ER and RRLL ER secretion patterns reported in Fig. 3 were performed in the absence of gp160 transfection, therefore, further controls are required in order to establish a direct association between AdSpn4A titers and secretion. Nevertheless, the observed secretion of Spn4A ER and RRLL ER suggests that the partial, although not statistically significant, block in gp160 processing by Spn4A ER (Fig. 4.1 B) could be mediated by Spn4A ER that had escaped the ER-Golgi intermediate compartment (ERGIC) pathway. Accordingly, a lower titer of AdSpn4A ER, which did not result in the secretion of the serpin variant (Fig. 3.3), had no impact on gp160 processing (Fig. 4.1 C). Conversely, a longer time of infection with AdSpn4A ER resulted in a greater degree of inhibition than was observed in the results presented in Fig. 4.1 A (Fig. 4.1 D).

Because gp160 processing is a critical component of the HIV-1 life cycle, we hypothesized that the expression of Spn4A S, which fully inhibited the cleavage of gp160 (Fig. 4.1), could provide a means of inhibiting productive HIV-1 infection. To examine the effect of

Spn4A variants on HIV-1 replication, we sequentially infected MAGI-CCR5 cells with AdSpn4A and HIV-1_{BaL}. Four days post infection, cells were processed for detection of primary infection and the growth media from the primary infection was transferred to otherwise untreated MAGI-CCR5 cells. These cells were fixed two days post-inoculation and processed for detection of secondary infection. The level of productive HIV-1 infection was determined by β-galactosidase activity and MAGI (enumeration of blue foci) assays (151). Due to cell overconfluence in the primary infection, blue foci could not be accurately quantified; hence, only secondary infection MAGI assay results are shown. β-galactosidase activity assays indicated that in cells expressing Spn4A S, productive infection was reduced to 19 and 7% of the control in the primary and secondary infections, respectively (Fig. 4.2 A, B). The inhibitory effect was comparable to that of 1 μM AZT which reduced productive infection to 23 and 1.6% of the control. Our MAGI assays confirmed that Spn4A S was indeed an inhibitor of productive HIV-1_{BaL} infection as its expression resulted in a 92% decrease in the number of blue foci during secondary infection (Fig. 4.2 C, D). The RSL variants Spn4A RRLL ER and S, and Spn4A ER, which partially blocked gp160 processing (Fig. 4.1), did not reduce β-galactosidase activity and blue foci counts, indicating that the variants were ineffective as anti-HIV agents (Fig. 4.2)

Our studies of HIV-1_{BaL} replication in the presence of Spn4A S indicated that the serpin variant is an effective inhibitor of HIV-1 production. The ability of Spn4A S to block furin activity and gp160 processing suggests that the anti-HIV activity of the serpin occurs through the inhibition of PC-dependent gp160 processing. The gp160 cleavage sequence -Arg-Glu-Lys-Arg- is highly conserved in all HIV-1 strains, and therefore, we predicted that Spn4A S could act as an anti-HIV agent independent of viral strain. We tested the effect of Spn4A S on gp160 processing and infectious virus production of the CXCR4-tropic virus, HIV-1_{IIIB}. As in our HIV-1_{BaL} gp160 processing analyses, cleavage of HIV-1_{IIIB} gp160 was fully inhibited by Spn4A S while the RSL variant of the secreted serpin, Spn4A RRLL S, did not have an inhibitory effect on envelope precursor cleavage compared to the control (Fig. 4.3). Similarly, β-galactosidase activity assays indicated that in primary and secondary infection Spn4A S was as effective as 1 μM AZT in reducing productive infection to nearly background levels (Fig. 4.4 A, B). In agreement with the β-galactosidase activity assays, Spn4A S expression resulted in the complete block of syncytia

formation (Fig. 4.4C, D). Interestingly, although Spn4A RRLL S did not affect gp160 processing, there was a downward trend in productive HIV-1 infection with average β-galactosidase activity values of 90 and 66% of the control in primary and secondary infection, respectively (Fig. 4.4 A, B). This trend was more pronounced in the MAGI assays, as Spn4A RRLL S expression resulted in a significant reduction in the number of blue foci (44% of the control) (Fig. 4.4 D).

4.2 Effect of Spn4A S on furin-independent gp160 processing

Despite a deficiency in furin activity, LoVo cells are able to correctly process HIV-1 gp160, indicating that other furin-like PCs can act in the proteolytic cleavage of the envelope precursor (105). The ability of Spn4A to inhibit two of the most evolutionarily divergent PCs – human furin and *Drosophila* PC2 (137) – led us to hypothesize that Spn4A may be a broad-based PC inhibitor and could therefore target other furin-like PCs involved in gp160 processing. We tested this hypothesis by determining the effect of Spn4A S expression on furin-independent gp160 processing in LoVo cells. In Western blot analysis of LoVo cells infected with AdSpn4A and a vaccinia virus expression vector encoding gp160, gp120 was detected in the control and AdSpn4A RRLL S-treated cells, but not in cells expressing Spn4A S (Fig. 4.6 A). Quantification of the cleavage efficiency indicated that processing was fully inhibited by Spn4A S, whereas 27 and 30% of gp160 was cleaved in control cell and cells expressing Spn4A RRLL S, respectively (Fig. 4.5 B). The complete block of furin-independent gp160 processing by Spn4A S suggests that the serpin variant inhibits the non-furin PC(s) involved in the cleavage event in LoVo cells (105).

4.3 Studies of gp160 processing in the presence of extracellularly applied Spn4A

One of the major challenges in the development of protein-based therapeutics is associated with the delivery of the protein drug across the cell membrane. The PCs involved in gp160 processing are active in the secretory pathway, and in the case of furin, traffic to the cell surface as a part of a complex sorting itinerary. It has been previously shown that the furin selective serpin, α_1-PDX, can be internalized by cells by a furin-dependent mechanism. Furthermore, when applied to cellular growth media, recombinant α_1-PDX inhibits furin-

mediated pro-gB processing and HCMV replication. Similarly, the extracellular introduction of recombinant Spn4A could potentially result in its internalization into cells by a PC-dependent mechanism, providing a means of inhibition of gp160 processing and HIV-1 production. To determine if extracellularly applied Spn4A could be used as an anti-viral agent, we generated three preparations of recombinant Spn4A and tested their ability to inhibit gp160 processing (summarized in Table 4.1).

In vitro analysis of the first preparation, *E. coli*-expressed Spn4A ER purified by fast protein liquid chromatography (FPLC) (generated by Martine Boutin and Steven McArthur, Jean lab) indicated that the recombinant Spn4A was active as a serpin of furin (Fig. 3.5 C). To test whether it can inhibit gp160 processing, a time course addition of recombinant Spn4A ER to the media of MAGI-CCR5 cells was performed (24 hrs, 18 hrs pre-, 12 hrs post-gp160 transfection, at the time of transfection, or at each time point). The rationale for the reapplication of Spn4A at the different time points was to avoid the potential loss of anti-PC activity as a result of Spn4A degradation. Incubation of MAGI-CCR5 cells in up to 350 μM of Spn4A ER did not affect gp160 processing, indicating that the extracellularly applied serpin failed to inhibit the PCs involved in the cleavage event. Similarly, our studies with up to 3.8 μM *E. coli*-expressed Spn4A S did not result in an inhibitory effect on gp160 processing (Table 4.1).

Spn4A contains a single putative glycosylation site, which may be important for the activity and stability of the serpin. In Chapter III, we showed that Spn4A S secreted into the media of AdSpn4A S infected MAGI-CCR5 cells retains its anti-furin activity (Fig. 3.5). To determine if the lack of inhibition in envelope protein processing by *E. coli*-expressed Spn4A can be attributed to a requirement for glycosylation, we tested the effect of MAGI-CCR5-expressed Spn4A S present in concentrated media on gp160 cleavage. As with the *E. coli-expressed* serpins, gp160 was unaffected when MAGI-CCR5 cells were incubated in the presence of up to 4.5 μM Spn4A S (Table 4.1). This suggests that Spn4A, regardless of glycosylation state, is not active as an anti-viral agent when applied to cellular media without an expression vector. Further studies of the stability of the recombinant serpins in the media will be required to determine if the lack of inhibition resulted from degradation of Spn4A.

4.4 Summary

We performed studies of gp160 processing and HIV replication in cells expressing four Spn4A variants differing in their localization and RSL sequence. Spn4A S was shown to fully inhibit gp160 processing in MAGI-CCR5 and furin-deficient LoVo cells, indicating that in addition to inhibiting furin, the serpin variant targets other PCs involved in precursor cleavage. The inhibition of gp160 processing by Spn4A S translated to a nearly complete block in productive HIV-1_{BaL} and HIV-1_{IIIB} infection. In contrast, Spn4A ER blocked only 32% of gp160 cleavage and did not impact viral production in cells infected with HIV-1_{BaL}. The anti-HIV activity of Spn4A S appears to require a means of intracellular expression, as incubation of cells in the presence of the protein failed to generate an inhibitory effect on gp160 processing.

Figure 4.1. Effect of Spn4A variant expression on HIV-1_{BaL} gp160 processing in MAGI-CCR5 cells. Cells were infected with AdSpn4A variants (MOI 8) for 48 hrs, media was changed and cells were transfected with the HIV-1 envelope expression vector $gp160_{BaL}$. Two days post-transfection, cellular membrane fractions and media were prepared for SDS-PAGE as described in section 2.5 and analyzed by Western blotting. Membrane fractions were probed with rabbit polyclonal anti-gp120 Ab, mouse monoclonal anti-Hsp47 Ab and secondary infrared 800CW anti-mouse (green) and 700CW anti-rabbit (red) Abs (top panel **A)**. Media was probed with mouse monoclonal anti-FLAG Ab and secondary infrared 800CW anti-mouse (green) Ab (bottom panel **A**). A representative image of three independent experiments is shown. **B)** gp160 cleavage efficiency determined by quantification of gp160 and gp120 band intensities using the formula gp120/(gp120 + gp160)*100. Data are averages of three independent experiments. Cleavage efficiency in MAGI-CCR5 cells infected with AdSpn4A ER (MOI 0.5) **(C)**, and (MOI 8) where media was not changed prior to transfection **(D)**. Data are averages of three and two independent experiments, respectively [error bars represent standard error; ***p < 0.001].

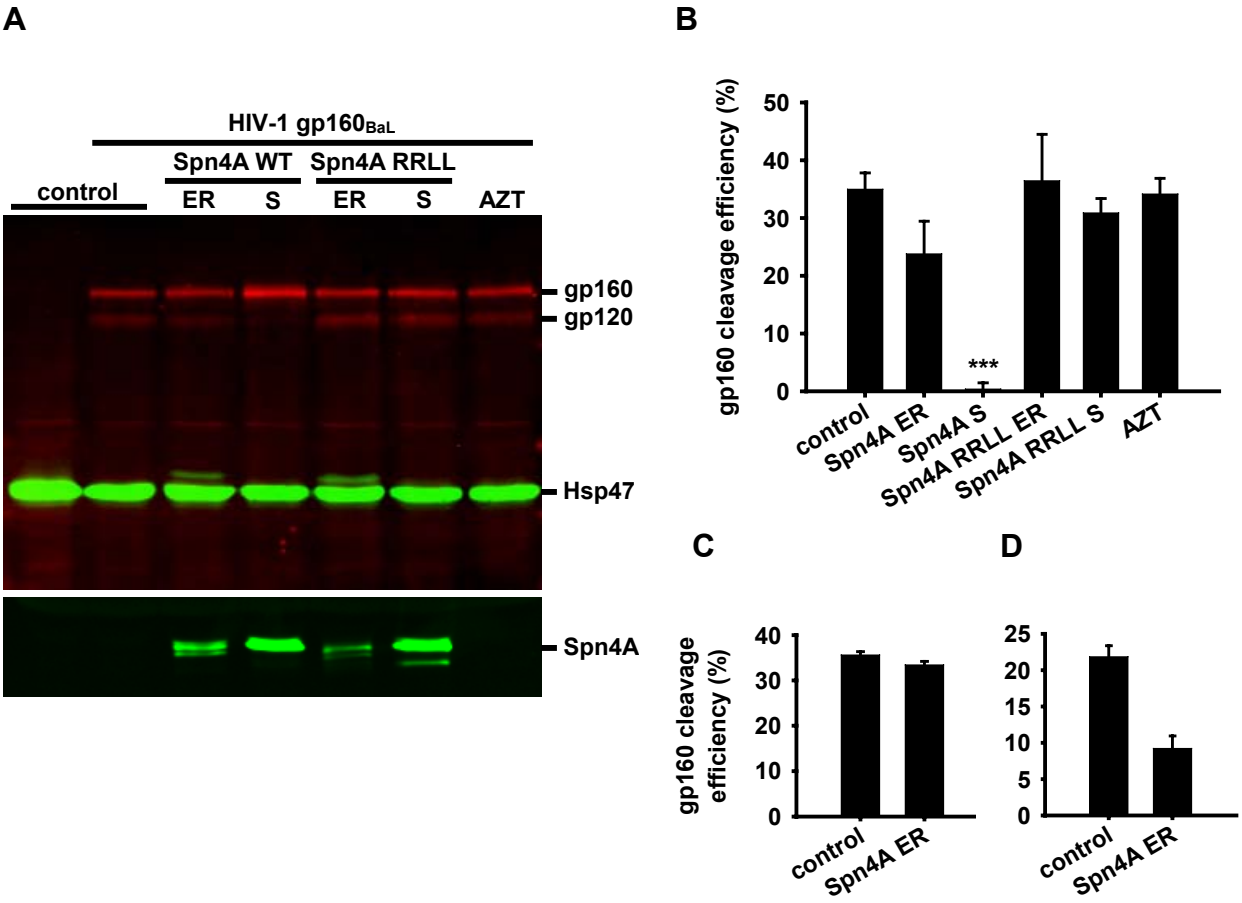

Figure 4.2. HIV-1_{BaL} production during primary and secondary infection in MAGI-CCR5 cells expressing Spn4A variants. MAGI-CCR5 cells were sequentially infected with AdSpn4A variants (MOI 8) for 48 hrs and HIV-1_{BaL} (MOI 0.01) for four days. Cells were fixed and processed for detection of primary infection by β-galactosidase activity assay **(A)** as described in section 2.8. To generate secondary infection, media from the primary infection was transferred to otherwise untreated MAGI-CCR5 cells. Two days post-inoculation, cells were fixed and processed for detection secondary infection by β-galactosidase activity assay **(B)** and MAGI assay **(C, D)** as described in section 2.8. Representative images of blue foci are shown in **(C)** and quantified in **(D)**. β-galactosidase activity and MAGI assays are averages of at least two independent experiments, respectively [error bars represent standard error; *p < 0.05, **p < 0.01, ***p < 0.001].

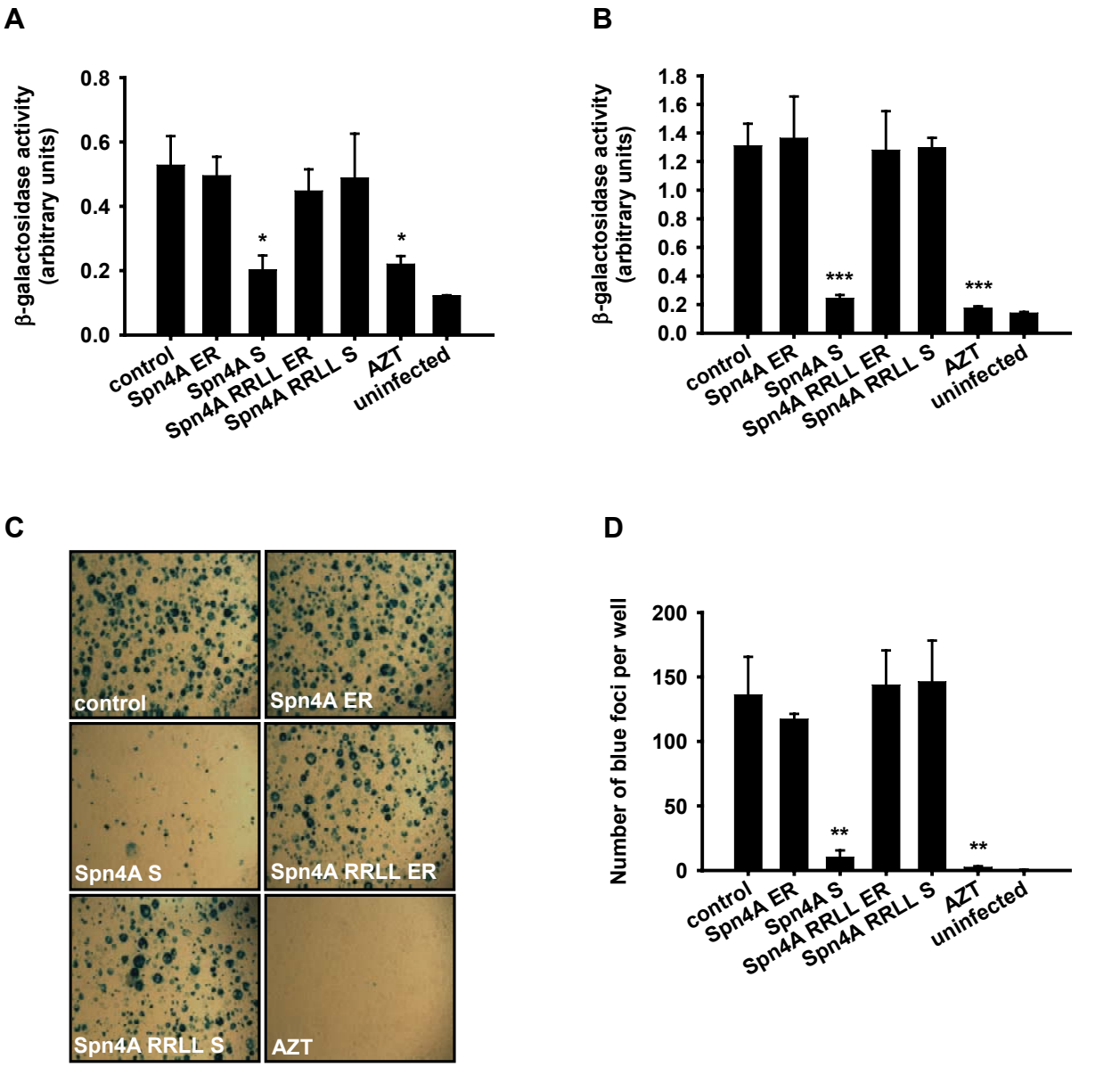

Figure 4.3. Effect of Spn4A variant expression on HIV-1_{IIIB} gp160 processing in MAGI-CCR5 cells. MAGI-CCR5 cells were infected with AdSpn4A variants (MOI 8) for 48 hrs, media was changed, and cells were transfected with the HIV-1 envelope expression vector $gp160_{IIIB}$. Two days post-transfection, cellular membrane fractions were prepared for SDS-PAGE as described in section 2.5 and analyzed by Western blotting, probing with rabbit polyclonal anti-gp120 Ab, mouse monoclonal anti-Hsp47 Ab, and secondary infrared 800CW anti-mouse (green) and 700CW anti-rabbit (red) Abs. A representative Western blot image is shown in **A**. Panel **B** depicts gp160 cleavage efficiency determined by quantification of gp160 and gp120 band intensities using the formula gp120/(gp120+gp160)*100. Data are averages of three independent experiments [error bars represent standard error; ***$p < 0.001$].

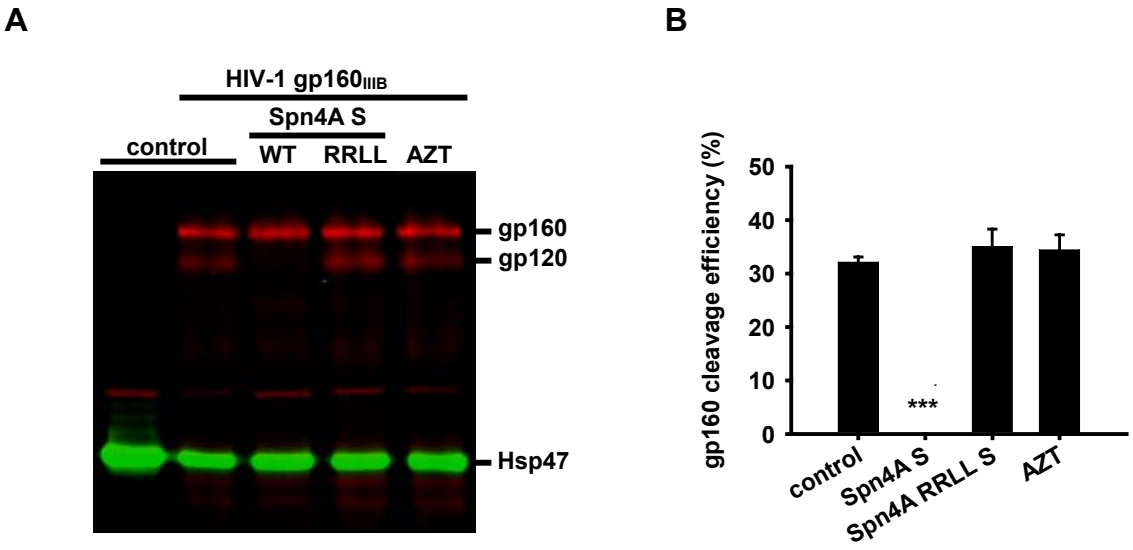

Figure 4.4. HIV-1_{IIIB} production during primary and secondary infection in MAGI-CCR5 cells expressing Spn4A variants. MAGI-CCR5 cells were sequentially infected with AdSpn4A variants (MOI 8) for 48 hrs and HIV-1_{IIIB} (MOI 0.005) for four days. Cells were fixed and processed for detection of primary infection by β-galactosidase activity assay **(A)** as described in section 2.8. To generate secondary infection, media from the primary infection was transferred to otherwise untreated MAGI-CCR5 cells. Two days post-inoculation, cells were fixed and processed for detection secondary infection by β-galactosidase activity assay **(B)** and MAGI assay **(C, D)** as described in section 2.8. Representative images of blue foci are shown in **(C)** and quantified in **(D)**. β-galactosidase activity and MAGI assays are averages of four and three independent experiments, respectively [error bars represent standard error; *p < 0.05, **p < 0.01, ***p < 0.001].

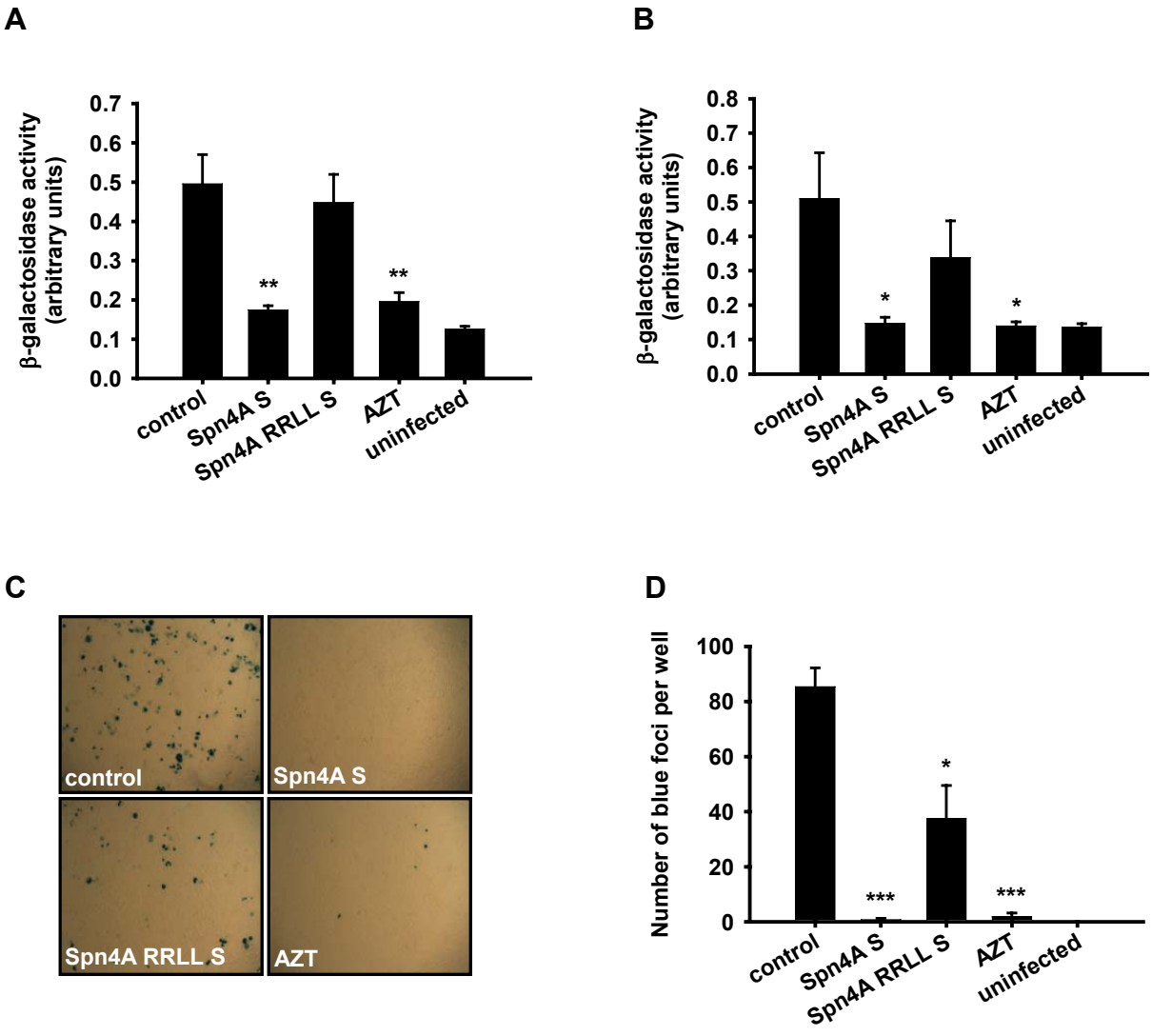

Figure 4.5. Inhibition of furin-independent gp160 processing by Spn4A S. LoVo cells were sequentially infected with AdSpn4A variants (MOI 3) for 36 hrs and with the vaccinia virus expression vector encoding gp160. Twelve hrs post-vaccinia infection, cellular membrane fractions were prepared for SDS-PAGE as described in section 2.5 and analyzed by Western blotting, probing with rabbit polyclonal anti-gp120 Ab, mouse monoclonal anti-Hsp47 Ab, and secondary infrared 800CW anti-mouse (green) and 700CW anti-rabbit (red) Abs. A representative Western blot image is shown in **A**. Panel **B** depicts gp160 cleavage efficiency determined by quantification of gp160 and gp120 band intensities using the formula gp120/(gp120+gp160)*100. Data are averages of three independent experiments [error bars represent standard error; ***$p < 0.001$].

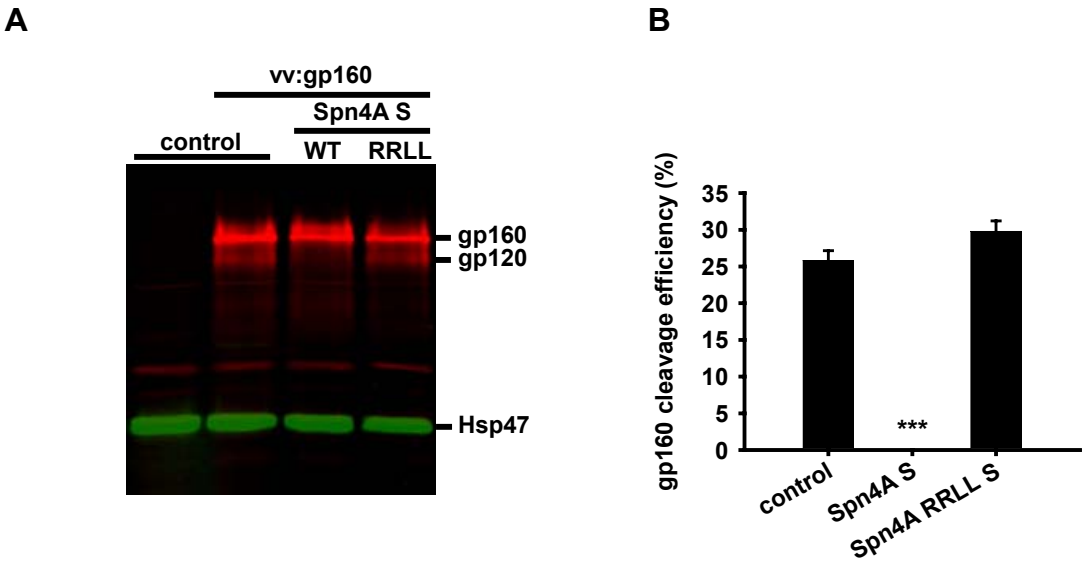

Table 4.1. Summary of extracellulary applied Spn4A studies. The ability of Spn4A secreted from MAGI-CCR5 cells (column two) and *E. coli*-expressed Spn4A ER (column three) and Spn4A S (column four) to inhibit HIV-1 gp160 processing when applied to MAGI-CCR5 growth media was determined. Source and preparation refer to the expression and concentration/purification method of recombinant Spn4A. The *in vitro* anti-furin activity was determined by enzyme inhibition assay and detection of SDS-stable complex formation (Fig 3.5). The concentration of Spn4A used in the gp160 processing experiments was estimated by Western blot band intensity titration against known Spn4A ER (*E. coli*) concentrations (Appendix 1). + and − denote a positive and negative result obtained in the corresponding analysis, respectively; not determined (ND) indicates analysis was not performed.

	Spn4A ER	**Spn4A S**	**Spn4A S**
Source	*E. coli*	*E. coli*	Media from AdSpn4A S infected MAGI-CCR5 cells
Preparation	FPLC	Magnetic nickel bead His tag protein purification kit	Virus exclusion filter Concentrated 10X
***In vitro* anti-furin activity**	+	ND	+
Inhibition of gp160 processing	–	–	–
Estimated concentration tested	350 μM	3.8 μM	4.6 μM
Comments	Importance of glycosylation HDEL impacts trafficking	Importance of glycosylation May require a higher concentration	May require a higher concentration

CHAPTER V Discussion

In the present study we evaluated the ability of the potent furin inhibitor, Spn4A, targeted to three different sites to inhibit PC-directed HIV-1 gp160 processing and viral production. By adenoviral vector delivery, we expressed Spn4A ER – the naturally occurring serpin with a C-terminal ER-retention motif (HDEL) and Spn4A S – a bioengineered variant of Spn4A with a deletion of the HDEL sequence. Spn4A ER was expected to localize to the ER, whereas we predicted that Spn4A S would be secreted. We also assessed the ability of extracellularly applied recombinant Spn4A ER/S to inhibit gp160 processing. Although all the Spn4A variants were active as serpins of furin (with the exception of *E. coli*-expressed recombinant Spn4A S, whose activity was not tested) (Fig. 3.4 A, 3.5), our analyses of gp160 processing in the presence of the differentially targeted serpins demonstrated a complete block in processing by Spn4A S (Fig. 4.1, 4.3), a partial decrease induced by high levels of Spn4A ER expression (Fig. 4.1), and no effect generated by the extracellularly applied serpins (Table 4.1). We also showed that Spn4A S inhibits gp160 processing attributed to non-furin PCs (Fig. 4.5). Furthermore, we demonstrated that the serpin variant is an effective anti-viral agent, as its expression results in a nearly complete inhibition of productive HIV-1 infection (Fig. 4.2, 4.4).

5.1 Spn4A trafficking and anti-furin activity

Spn4A contains an HDEL sequence at its C-terminus, a variant of the well-known KDEL ER-retention motif. ER-retention motif-containing proteins are thought to be recognized by the KDEL or KDEL-like receptor, which resides in the *cis*-Golgi and is responsible for transporting ER-resident proteins back to the ER (150). Previously reported immunofluorescence studies indicated that Spn4A is localized to the ER when expressed in COS-7 cells (141), and that this localization is dependent on the HDEL motif, as its deletion results in the secretion of the serpin (140). Our studies of Spn4A ER and S expression in human cell lines largely agreed with these findings, as the serpins were intracellularly retained and secreted, respectively (Fig. 3.3). However, in infections with high titers of AdSpn4A ER or the RSL mutant AdSpn4A RRLL ER (MOI 8), we observed the secretion of the variants. Additionally, in Western blot analyses of Hsp47 in cells infected with high levels of the ER forms of AdSpn4A, we observed an extra band possibly corresponding to a differential glycosylation state, signifying a change in the

localization of Hsp47 (Fig. 4.1 A). Hsp47 is an ER-localized glycoprotein with a C-terminal RDEL sequence, another variant of the KDEL motif (149). The secretion of Spn4A ER and RRLL ER during high levels of expression, concurrently with a possible relocalization of another ER-resident protein, Hsp47, suggests these changes may be the result of a saturation of the KDEL receptor. This is supported by studies showing that overexpression of KDEL-containing proteins results in the partial secretion of both the overexpressed and uninduced ER-resident proteins (152, 153). Alternatively, the secretion of Spn4A ER and RRLL ER may be influenced by the presence of transfection reagent and gp160 expression, therefore further Spn4A ER expression studies in the absence of the two factors will be required to address this possibility. In summary, together with previous studies (142), our observations indicate that Spn4A ER is localized to the ER, however, its secretion in mammalian cells can be induced by deletion of the C-terminal HDEL motif and possibly, by high levels of expression.

Spn4A is a potent inhibitor of furin (K_i = 13 pM), forming an SDS-stable complex with furin *in vitro* (137, 141, 142) and in *Drosophila* S2 cells (137). We investigated the ability of Spn4A ER/S and Spn4A RRLL ER/S – variants with a two-residue substitution in the RSL at sites critical for furin recognition – to form an SDS-stable complex in human cells stably overexpressing furin. Our results indicated that both Spn4A ER and S were active as serpins of furin, while as predicted, the Spn4A RRLL variants did not form intracellular SDS-stable complexes with the protease (Fig. 3.4). The release of the inhibitory prodomain of furin in the *trans*-Golgi is a prerequisite for furin activity (20). Consequently, furin is predominantly active in the late secretory pathway – in the TGN, endosomal compartments, and the cell surface (1). Because protease activity is critical for the serpin mechanism of action, we had predicted that the ER-localized Spn4A ER would fail to form an EI* complex with furin, in contrast to Spn4A S which would route through sites of furin activity. Our observation of EI* complex formation between Spn4A ER and furin could be explained by several studies reporting furin activity in the early secretory pathway (53-55). Another possible explanation is that the activation and trafficking pathways of furin may be misregulated in cells stably overexpressing the protease. An analysis of EI* complex formation with endogenous furin would be useful in establishing to what extent active furin is represented in the ER.

5.2 Effect of Spn4A variants on gp160 processing

HIV-1 gp160 processing yielding active envelope glycoproteins gp120 and gp41, is a critical event in the viral life cycle. Cleavage is mediated by the PCs active in the late secretory pathway – furin and PC7, and possibly to a lesser extent, PACE4 and PC5/6B (103). The central role of the PCs in HIV-1 replication points to this group of proteases as a potential anti-viral target. Our analyses of gp160 processing in the presence of Spn4A delivered to different subcellular/extracellular sites yielded varied results. Spn4A S was the most effective variant in inhibiting gp160 processing, as its expression in MAGI-CCR5 cells generated a complete block in precursor cleavage (Fig. 4.1). Inhibition of gp160 processing by a furin-directed secretory pathway serpin has been previously demonstrated with the use of α_1-PDX. Like Spn4A S, α_1-PDX is secreted and inhibits gp160 processing when overexpressed in cell culture (114). However, the reported efficacy of inhibition ranges from a complete to a partial block in processing (102, 127, 133, 134). In contrast to α_1-PDX, whose anti-PC activity is limited to furin and PC5/6B as demonstrated by *in vitro* studies (114), Spn4A has been shown to inhibit *Drosophila* PCs – dPC2, furin1, and furin2 (137, 140). The full block in gp160 cleavage and evidence for broad-based PC inhibitory activity led us to hypothesize that in addition to furin, Spn4A S may target other PCs involved in the processing event. In line with this hypothesis, we observed full inhibition of gp160 processing in LoVo cells (Fig. 4.5), which are deficient in furin activity but retain their ability to correctly process gp160 (105).

Our observation of a complete block in gp160 processing in both MAGI-CCR5 and LoVo cells points to a previously unreported PC target for Spn4A. Vaccinia virus overexpression studies have implicated furin and PC7 as the main PCs involved in gp160 processing. PC5/6B and PACE4 are also active in the late secretory pathway, the site of gp160 cleavage (102, 106, 107, 109). However, evidence for their involvement is contentious, as several studies have shown that overexpression of PC5/6B and PACE4 either does not affect or only marginally increases gp160 processing efficiency (102, 106, 107). LoVo cells express PC7, PACE4, but not PC5/6B, or an active form of furin (106, 144). To our knowledge, a full PC expression profile of HeLa cells – the parental cell line of MAGI-CCR5 cells – has not been published. Northern blot analyses indicate that furin mRNA is present in HeLa cells, while PC5/6 is not (75, 154). A

recently published transcriptome of HeLa S3 cells, a HeLa-derived cell line adapted to grow in suspension, indicates that PC7 is transcribed (155). Consistent with the Northern blot reports in HeLa cells (75, 154), furin and PC5/6 transcripts were present and absent in HeLa S3 cells, respectively (155). Taking into account the available expression profiles for the PCs in MAGI-CCR5 and LoVo cells and evidence for their involvement in gp160 processing, it is likely that in addition to furin, Spn4A inhibits PC7 in the two cell lines.

We also investigated the effect of the naturally occurring form of the serpin, Spn4A ER, on gp160 processing. Inhibition of processing by Spn4A ER appeared to require AdSpn4A ER titers at levels at which secretion of the serpin was observed. While infection at an MOI of 0.5 resulted both in the intracellular retention of Spn4A ER and EI* complex formation in furin overexpressing cells, we did not observe inhibition of processing (Fig. 4.1). It is possible that the ER-localized serpin did not effectively deplete endogenous furin levels. However, evidence for furin activity in the ER (53-55), and the observation that Spn4A ER expression results in a partial block in HCMV pro-gB processing (unpublished observations, François Jean), suggests that Spn4A ER could be used to inhibit furin-directed processing. Unlike pro-gB, gp160 is not entirely dependent on furin for processing (105), and in our cell system PC7 likely contributes to gp160 cleavage. In contrast to furin, there are no reports of PC7 activity in the early secretory pathway. Therefore, an alternative interpretation for our results could be that Spn4A ER depletes furin levels in the early secretory pathway, but not those of PC7, which may not traffic through the ER/*cis*-Golgi in its active form. This would result in a scenario like that in LoVo cells where gp160 processing occurs in the absence of active furin. We were able to induce a partial block in gp160 processing when cells were infected with a considerably higher titer of AdSpn4A ER (MOI 8) (Fig. 4.1). However, at this level of expression we observed the secretion of the serpin, suggesting that the inhibitory effect could be largely attributed to Spn4A ER that had escaped to the late secretory compartments.

Finally, we tested the ability of Spn4A to inhibit gp160 processing when applied extracellularly. To avoid the loss of activity of the recombinant serpins as a result of possible degradation, we reapplied Spn4A to the media at several time points prior to, at the time of, and post-transfection. Incubation of MAGI-CCR5 cells in the presence of 3.8 to 350 μM of Spn4A

appeared to have no effect on gp160 processing (Table 4.1). This is in contrast to studies with recombinant α_1-PDX, which at a concentration of 8 μM fully inhibits pro-gB processing (131). α_1-PDX is 50 times less potent than Spn4A at inhibiting furin (114, 137), therefore it is unlikely that a higher concentration of Spn4A is required to observe an effect. Glycosylation state and the presence of the ER-retention motif is also unlikely to be a factor, as we tested Spn4A ER and S expressed in *E. coli* and Spn4A S expressed in MAGI-CCR5 cells. Studies with cells incubated with 8 μM of α_1-PDX showed that the serpin is internalized in a furin-dependent manner, resulting in an 80% reduction of intracellular furin levels (131). This suggests that Spn4A should be able to deplete furin by an analogous mechanism. Investigation of the effect of externally applied Spn4A on a furin-dependent processing event would be useful in demonstrating this mechanism of furin inhibition. Furthermore, the stability of recombinant Spn4A in the media should be evaluated in order to rule out the loss of activity due to degradation.

Given the existence of PC redundancy in gp160 processing, the inability of externally applied Spn4A to inhibit precursor cleavage implies a failure to deplete PC7 levels. Although our studies in LoVo cells suggest that PC7 is targeted by Spn4A, we have no evidence that inhibition occurs by the serpin mechanism rather than through the substrate pathway. Therefore, we can not rule out that the failure of externally applied Spn4A to deplete PC7 levels is due to its inability to form an EI* complex with the protease. An alternate explanation is that a PC7 targeted serpin applied at the cell surface cannot be used to effectively reduce intracellular PC7 stores. Although PC7 has been shown to be represented at the cell surface (131), it does not contain the same sorting motifs in its cytoplasmic tail as furin. PC7 contains a dileucine signal thought to act as an internalization motif, however, it lacks the tyrosine containing motif which has been shown to be both necessary and sufficient for retrieval of proteins from the cell surface to the TGN (28, 156, 157). This suggests that unlike furin, cell surface PC7 may not recycle to the TGN, the site of steady-state PC7 localization, and may instead sort to the lysosomes or recycle to the cell surface. The lack of gp160 processing inhibition observed in the presence of extracellularly applied Spn4A might be further evidence against the retrieval of cell surface PC7 to the TGN.

In Figure 5.1, we present a model for the anti-PC activity of differentially targeted Spn4A variants based on their effect on gp160 processing. The model is presented on the assumption

that MAGI-CCR5 cells express furin and PC7 as suggested by studies in HeLa and HeLa S3 cells (75, 154, 155), and in Fig. 5.1 C, that externally applied Spn4A inhibits furin by a mechanism analogous to that of externally applied α_1-PDX reported in (131). Confirmation of the PC expression profiles in MAGI-CCR5 cells and investigation into the potential parallels between Spn4A and α_1-PDX function will be required to validate the model.

5.3 Effect of Spn4A variants on HIV-1 production

The PCs occupy a central role in the HIV-1 life cycle, as the PC-mediated proteolytic maturation of the viral envelope glycoprotein is a requirement for the production of infectious virions. Cleavage of gp160 occurs during its trafficking to the cell surface, where the mature glycoproteins gp120 and gp41 are incorporated into the viral particle upon budding (103). Inhibition of gp160 processing results in the incorporation of immature glycoproteins into non-infectious virions (95, 158). These virions are incapable of entry, as gp160 is unable to mediate fusion following CD4 receptor recognition (91). Our HIV-1 production assays indicated that Spn4A S is an effective anti-viral agent, limiting productive HIV-1 infection to nearly background levels. The inhibitory effect was more pronounced in the secondary infection, indicating that replication detected during primary infection resulted largely in the production of non-infectious virions (Fig. 4.2 A, B). Furthermore, both the CCR5-tropic BaL strain and CXCR4-tropic IIIB strain of HIV-1 was inhibited, suggesting that Spn4A S inhibits processing at the highly conserved gp160 cleavage site (Fig. 4.2, 4.4). In our gp160 processing analyses, we observed a complete and partial block in cleavage upon expression of Spn4A S and Spn4A ER, respectively (Fig. 4.1). The incomplete inhibition of gp160 processing observed during Spn4A ER expression did not translate to inhibition of the virus, as productive HIV-1_{BaL} infection was unaffected by the serpin variant (Fig. 4.2). Therefore, inhibition of gp160 processing can serve as an effective means of limiting HIV-1 production but may require a complete block in the processing event, such as that generated by Spn4A S.

The PC-directed inhibitors, polyarginine and α_1-PDX have been reported to suppress productive HIV-1 infection (116, 133, 134). Like Spn4A S, polyarginine inhibits furin-independent processing and fully blocks HIV-1 production at a concentration of 1 μM (116). Although in our hands, polyarginine had only a modest impact on HIV-1_{IIIB} production (data not

shown), the published study suggests that broad-based PC inhibitors are effective anti-HIV-1 agents (116). By contrast, HIV-1 replication studies in cells stably expressing the furin-selective inhibitor, α_1-PDX, demonstrated that although the serpin is initially effective in limiting HIV-1 production, viral replication recovers 13 days post-infection. The recovery corresponded to an accumulation of cleaved α_1-PDX, which was suggested by the authors to be a product of PC7 cleavage (134). It would be of interest to investigate the effect of Spn4A S on HIV-1 production in a similar long-term study, as our results suggest that unlike α_1-PDX, Spn4A S effectively inhibits PC7.

In our gp160 processing experiments, the RSL variants Spn4A RRLL ER and Spn4A RRLL S served as negative controls, as they did not form intracellular EI* complexes with furin, and consequently, did not affect gp160 processing (Fig. 4.1, 4.3). We attributed the loss of anti-furin activity to the two-residue substitution at the P1 and P2 positions of the RSL (RRKR → RRLL). However, the resulting RSL sequence forms the consensus cleavage site of the S1P/Ski-1 protease, a more distantly related PC member. S1P/Ski-1 is a secretory pathway protease with a central role in cholesterol metabolism, as its cleavage of SREBPs leads to the induction of cholesterol synthesis (148). Interestingly, like furin, S1P/Ski-1 is involved in viral replication, including that of Old World arenaviruses that encode the S1P/Ski-1 cleavage site within their envelope glycoproteins (159). The ability of Spn4A RRLL to inhibit S1P/Ski-1 has not been directly investigated, however, studies with recombinant vesicular stomatitis virus (VSV) in which the Lassa virus glycoprotein is expressed in place of VSV G, showed that Spn4A RRLL S expression results in a two-log reduction in viral production (unpublished observations, Ute Ströher and Heinz Feldmann, National Microbiology Laboratory). This suggests that Spn4A RRLL S may be active as an inhibitor of S1P/Ski-1.

Cholesterol has been linked to the replication of a number of viruses, including HIV-1, as depletion of cholesterol results in an inhibition of HIV-1 infection and syncytia formation (160). Efficient HIV-1 entry is thought to require the clustering of CD4 and chemokine receptors to lipid rafts – sites that cholesterol plays a key role in maintaining (161). In our HIV-1 production experiments, we observed a decrease in productive HIV-1_{IIIB} infection in cells expressing Spn4A RRLL S (Fig. 4.4). Interestingly, we did not detect an effect on HIV-1_{BaL} infection (Fig. 4.2).

Thus, our studies suggest that Spn4A RRLL S has anti-viral activity against the CXCR4-tropic and not the CCR5-tropic virus. In our system, HIV-1_{IIIB} did not replicate as efficiently as HIV-1_{BaL} (Fig. 4.2, 4.4), therefore it is possible that infection with the latter strain was too robust to generate an inhibitory effect by Spn4A RRLL S. Alternatively, the observed discrepancy between the two viral strains may suggest underlying differences in their cholesterol dependency, possibly associated with co-receptor function and recruitment.

5.4 Conclusion

Our investigation into the trafficking, anti-PC, and anti-HIV activity of Spn4A and its bioengineered variants has resulted in the identification of Spn4A S as an effective inhibitor of productive HIV-1 infection. The anti-viral effect of Spn4A can be attributed to inhibition of PC-directed gp160 processing, indicating that PC inhibition can serve as a means of limiting HIV-1 production.

A major concern with inhibiting host-cell factors is the possibility of generating toxic effects associated with the loss of a critical cellular function. The apparent built-in redundancy existing for some PCs, as exemplified by the lack of observed abnormal phenotype in conditional furin knockout mice (80), suggests that PC inhibition may be a viable anti-viral strategy. However, the involvement of several PCs in HIV-1 gp160 maturation presents a further challenge in developing PC inhibitors to limit HIV-1 production (105). Conversely, the low efficiency of gp160 processing attributed to the highly conserved sub-optimal PC cleavage site (94), suggests that a partial knockdown of the PCs may be sufficient to effectively inhibit gp160 cleavage, while maintaining the processing of host cell-derived substrates.

Our results indicated that Spn4A S inhibits furin, and at least another PC involved in gp160 processing, likely PC7. We showed that actin levels of MAGI-CCR5 cells infected at AdSpn4A S titers required to generate the reported anti-HIV effect, were at over 85% compared to that of uninfected controls (Fig. 3.2 B). We also attempted to test for AdSpn4A S-induced apoptosis by Western blotting, probing for the zymogen and active form of caspase 3. Although we were unable to detect the active form, we observed the disappearance of inactive caspase 3 in staurosporine treated samples. By contrast, the inactive caspase band was present at equal levels

in the control and AdSpn4A S treated samples (Appendix 2). These preliminary analyses suggest that the expression of Spn4A S at levels that generated a robust inhibition of productive HIV-1 infection did not result in significant toxic effects.

Beyond their role in HIV-1 replication, the PCs participate in the replication and pathogenesis of numerous infectious agents and have links to many diseases including cancer and Alzheimer's. With the identification of Spn4A as an efficacious HIV inhibitor, we present a prospective broad-based agent for the inhibition of PC-related pathologies.

5.5 Future directions

The lack of abnormal phenotype reported in PC7 knockout mice, along with the observation that the tissue distribution and localization of PC7 and furin largely overlaps, suggests a redundant function for PC7 (79, 113). Evidence for a unique role for PC7 includes *in vitro* analysis of PC7 cleavage sequence requirements (34), and the modelled PC7 structure based on the furin crystal structure (19). These studies suggest that PC7 may have substrate specificity that is distinct from that of furin – namely, a greater and lesser requirement for a basic residue at the P2 position, and an arginine at the P4 position, respectively (34). Furthermore, PC7 and furin trafficking likely differs, as two of the three major domains that govern furin bi-cycling are not present in the cytoplasmic tail of PC7 (28). Studies of endogenous PC7 and furin localization in rat liver suggest that while furin is most abundant in the TGN, steady-state PC7 localization is shifted to the TGN-derived vesicles (162). While α_1-PDX has been useful in dissecting furin-dependent processing events, the lack of inhibitory activity against other PC members, including PC7, has limited its efficacy in inhibiting PC redundant processes. In our study of Spn4A and its variants, we provide evidence that Spn4A is a PC7 inhibitor. Spn4A therefore, represents a powerful tool for investigation of processing events with PC redundancy and may be used alone or in parallel with α_1-PDX to provide information on the trafficking and relative importance of the PCs in a given process. One of the hypotheses stemming from our studies of gp160 processing in the presence of externally applied Spn4A, is that PC7 may differ from furin in that it may not recycle to the TGN. This has important implications in the design of a therapeutic targeted at PC7. Support for this hypothesis could be provided by parallel studies of furin-dependent processing and gp160 processing in the presence of externally applied Spn4A.

In our gp160 processing studies in the presence of Spn4A, we observed that Spn4A did not affect processing when delivered to two sites (early secretory pathway and cell surface) at which there is evidence that furin could be inhibited (53, 131). Furthermore, furin-defective LoVo and RPE-40 cell lines are able to process gp160 as efficiently as cells expressing furin (102, 105). This brings into question the relative importance of furin in gp160 maturation. Most evidence for the involvement of individual PCs in gp160 processing has come from PC overexpression studies, which may not be indicative of their activity when expressed at endogenous levels. An alternative strategy towards identifying the PCs involved in gp160 processing is to employ RNAi directed at individual PCs. With information about the contribution of each PC towards gp160 maturation, a more focused anti-viral therapeutic strategy minimizing toxic effects can be devised.

Spn4A is a PC inhibitory serpin naturally occurring in *Drosophila*, however, little is known about its role. Our observation that Spn4A ER is secreted upon its overexpression, resulting in partial inhibition of a PC-dependent processing event, hints at a possible model for PC regulation in *Drosophila* cells. In a microarray study of the transcriptome of *Drosophila* larvae infected with the pathogenic bacterium *Pseudomonas entomophila*, Spn4 expression was found to be induced upon infection (163). Additionally, studies in mammalian cell lines have shown that the induction of ER stress, a hallmark of many diseases including those with links to the PCs (164), results in the upregulation of a number of ER-resident proteins (152, 165-167), but not of the KDEL receptor (152), leading to the partial secretion of KDEL containing proteins. If such a model is applied to *Drosophila*, a scenario could be envisioned in which a PC-related disease induces overexpression of specific ER-localized proteins, including Spn4A, causing the saturation of the KDEL-like receptor. This could result in the secretion of the potent PC inhibitor through the late secretory compartments – the site of PC activity (168, 169). Such a regulatory mechanism could allow for normal PC function in healthy cells while inhibiting the PCs when they contribute to disease. A study showing that Spn4A overexpression in a subset of cells of *Drosophila* larvae results in a disruption of neuropeptide processing lends support to the concept of Spn4A overexpression-induced PC inhibition (142). Moreover, several identified and predicted PC-directed secretory pathway serpins contain a C-terminal variant of an ER-retrieval

signal (136), suggesting the retention motif may be integral to a potential PC regulatory function of the serpins. Further investigation into the changes in expression levels and localization of Spn4A in *Drosophila* in response to immune challenge, ER stress, and particularly, infection with pathogens that may utilize the PCs, would be of interest towards defining a natural role for Spn4A.

Figure 5.1. A model for the effect of differentially localized PC inhibitors on gp160 processing in MAGI-CCR5 cells. **A)** Expression of Spn4A S results in the complete inhibition of gp160 processing. The Spn4A variant with a deletion of the ER-retention motif traffics through the secretory pathway, including to sites of PC activity. Inhibition of furin and PC7 by Spn4A S results in a complete block in gp160 processing, leading to the cell surface presentation of the immature envelope glycoproteins. In HIV-1 infection, in the absence of gp120/41, gp160 is incorporated into the viral envelope, forming non-infectious HIV-1 virions (95, 158) . **B)** Expression of Spn4A ER at levels at which secretion is not observed fails to inhibit gp160 processing. With the presence of an ER-retention motif at its C-terminus, the trafficking of the naturally occurring Spn4A variant is limited to the early secretory pathway (142). Furin and PC7 are predominantly active in the late secretory compartments where they are released from their inhibitory prodomain (1). Reports of furin activity in the early secretory pathway (53-55), in addition to our analyses presented in Fig. 3.4, suggest that inhibition of furin in the early secretory pathway may be feasible. The lack of inhibitory effect may therefore also be explained by the inability of Spn4A ER to inhibit PC7, as there is no evidence for PC7 activity in the early secretory pathway. **C)** Extracellularly applied Spn4A ER/S does not affect gp160 processing. Depletion of furin levels and inhibition of furin-mediated pro-gB processing in the presence of extracellularly applied α_1-PDX has been reported (131). Spn4A is predicted to act by a similar mechanism. Although PC7 is represented at the cell surface, it lacks the trafficking motifs within its cytoplasmic tail that are attributed to the ability of furin to recycle from the cell surface to the TGN (28, 156, 157). Therefore, although externally applied Spn4A may be capable of depleting furin stores, PC7 levels at the site of gp160 processing may remain largely intact, accounting for the retention of gp160 processing.

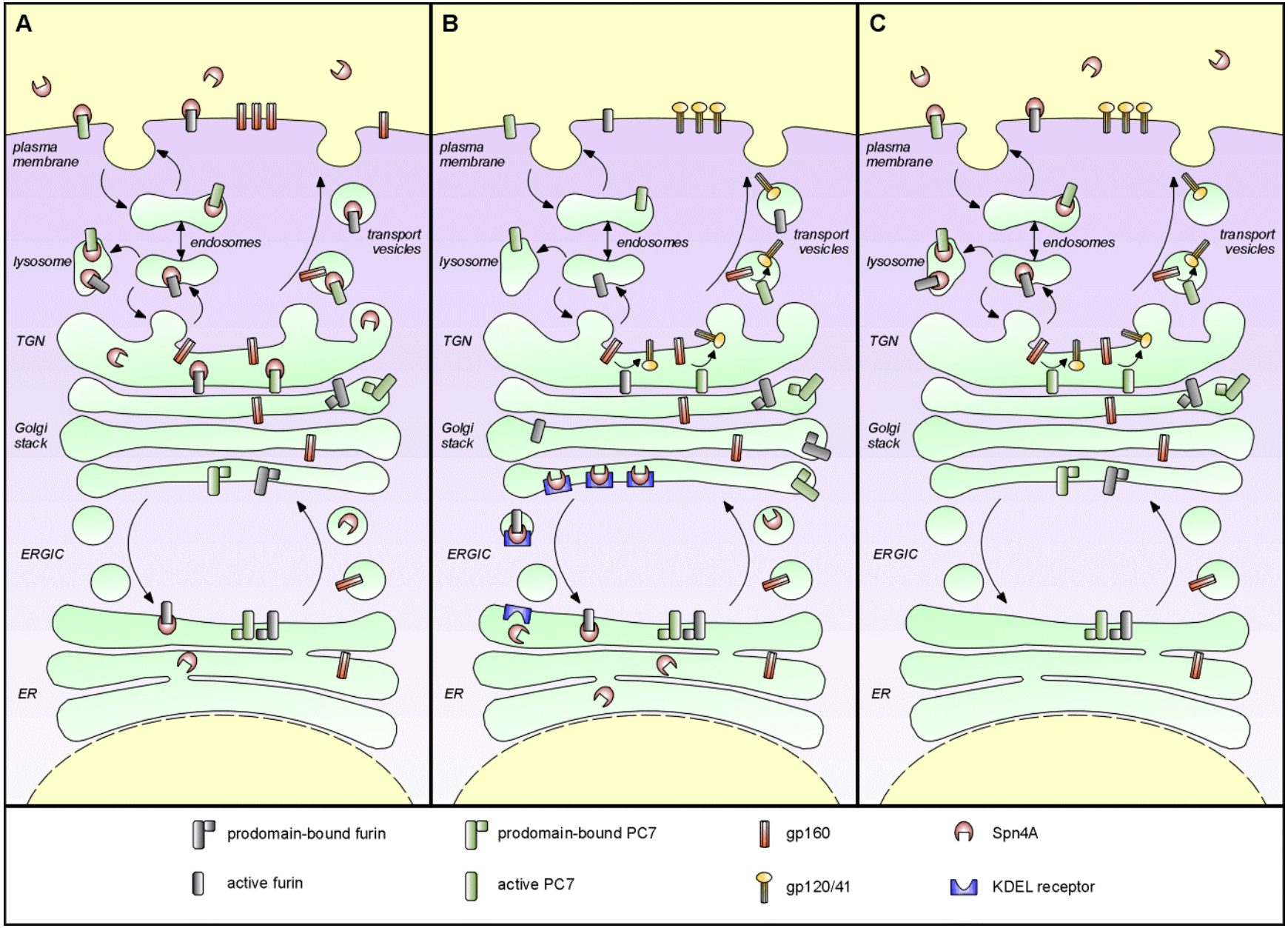
A
B
C
plasma membrane
endosomes
transport vesicles
lysosome
TGN
Golgi stack
ERGIC
ER
prodomain-bound furin
active furin
prodomain-bound PC7
active PC7
gp160
gp120/41
Spn4A
KDEL receptor

Bibliography

1. Thomas, G. (2002) Furin at the cutting edge: from protein traffic to embryogenesis and disease. *Nature Reviews Molecular Cell Biology* 3, 753-766.

2. Seidah, N. G., Mayer, G., Zaid, A., Rousselet, E., Nassoury, N., Poirier, S., Essalmani, R., and Prat, A. (2008) The activation and physiological functions of the proprotein convertases. *The International Journal of Biochemistry & Cell Biology* 40, 1111-1125.

3. Leduc, R., Molloy, S. S., Thorne, B. A., and Thomas, G. (1992) Activation of human furin precursor processing endoprotease occurs by an intramolecular autoproteolytic cleavage. *J Biol Chem* 267, 14304-14308.

4. Creemers, J. W., Siezen, R. J., Roebroek, A. J., Ayoubi, T. A., Huylebroeck, D., and Van de Ven, W. J. (1993) Modulation of furin-mediated proprotein processing activity by site-directed mutagenesis. *J Biol Chem* 268, 21826-21834.

5. Molloy, S. S., Thomas, L., VanSlyke, J. K., Stenberg, P. E., and Thomas, G. (1994) Intracellular trafficking and activation of the furin proprotein convertase: localization to the TGN and recycling from the cell surface. *Embo J* 13, 18-33.

6. Vey, M., Schafer, W., Berghofer, S., Klenk, H. D., and Garten, W. (1994) Maturation of the trans-Golgi network protease furin: compartmentalization of propeptide removal, substrate cleavage, and COOH-terminal truncation. *J Cell Biol* 127, 1829-1842.

7. Henrich, S., Cameron, A., Bourenkov, G. P., Kiefersauer, R., Huber, R., Lindberg, I., Bode, W., and Than, M. E. (2003) The crystal structure of the proprotein processing proteinase furin explains its stringent specificity. *Nat Struct Mol Biol* 10, 520-526.

8. Zhou, A., Martin, S., Lipkind, G., LaMendola, J., and Steiner, D. F. (1998) Regulatory roles of the P domain of the subtilisin-like prohormone convertases. *J Biol Chem* 273, 11107-11114.

9. Feliciangeli, S. F., Thomas, L., Scott, G. K., Subbian, E., Hung, C.-H., Molloy, S. S., Jean, F., Shinde, U., and Thomas, G. (2006) Identification of a pH Sensor in the Furin Propeptide That Regulates Enzyme Activation. *J Biol Chem* 281, 16108-16116.

10. Molloy, S. S., Anderson, E. D., Jean, F., and Thomas, G. (1999) Bi-cycling the furin pathway: from TGN localization to pathogen activation and embryogenesis. *Trends in Cell Biology* 9, 28-35.

11. Denault, J., Bissonnette, L., Longpre, J., Charest, G., Lavigne, P., and Leduc, R. (2002) Ectodomain shedding of furin: kinetics and role of the cysteine-rich region. *FEBS Lett* 527, 309-314.

12. Nour, N., Mayer, G., Mort, J. S., Salvas, A., Mbikay, M., Morrison, C. J., Overall, C. M., and Seidah, N. G. (2005) The Cysteine-rich Domain of the Secreted Proprotein Convertases PC5A and PACE4 Functions as a Cell Surface Anchor and Interacts with Tissue Inhibitors of Metalloproteinases. *Mol Biol Cell* 16, 5215-5226.

13. Molloy, S. S., Bresnahan, P. A., Leppla, S. H., Klimpel, K. R., and Thomas, G. (1992) Human furin is a calcium-dependent serine endoprotease that recognizes the sequence Arg-X-X-Arg and efficiently cleaves anthrax toxin protective antigen. *J Biol Chem* 267, 16396-16402.

14. Walker, J. A., Molloy, S. S., Thomas, G., Sakaguchi, T., Yoshida, T., Chambers, T. M., and Kawaoka, Y. (1994) Sequence specificity of furin, a proprotein-processing endoprotease, for the hemagglutinin of a virulent avian influenza virus. *J Virol* 68, 1213-1218.

15. Jean, F., Boudreault, A., Basak, A., Seidah, N. G., and Lazure, C. (1995) Fluorescent peptidyl substrates as an aid in studying the substrate specificity of human prohormone convertase PC1 and human furin and designing a potent irreversible inhibitor. *J Biol Chem* 270, 19225-19231.

16. Watanabe, T., Nakagawa, T., Ikemizu, J., Nagahama, M., Murakami, K., and Nakayama, K. (1992) Sequence requirements for precursor cleavage within the constitutive secretory pathway. *J Biol Chem* 267, 8270-8274.

17. Krysan, D. J., Rockwell, N. C., and Fuller, R. S. (1999) Quantitative characterization of furin specificity. Energetics of substrate discrimination using an internally consistent set of hexapeptidyl methylcoumarinamides. *J Biol Chem* 274, 23229-23234.

18. Chiron, M. F., Fryling, C. M., and FitzGerald, D. J. (1994) Cleavage of pseudomonas exotoxin and diphtheria toxin by a furin-like enzyme prepared from beef liver. *J Biol Chem* 269, 18167-18176.

19. Henrich, S., Lindberg, I., Bode, W., and Than, M. E. (2005) Proprotein Convertase Models based on the Crystal Structures of Furin and Kexin: Explanation of their Specificity. *Journal of Molecular Biology* 345, 211-227.

20. Anderson, E. D., Molloy, S. S., Jean, F., Fei, H., Shimamura, S., and Thomas, G. (2002) The ordered and compartment-specfific autoproteolytic removal of the furin intramolecular chaperone is required for enzyme activation. *J Biol Chem* 277, 12879-12890.

21. Creemers, J. W., Vey, M., Schafer, W., Ayoubi, T. A., Roebroek, A. J., Klenk, H. D., Garten, W., and Van de Ven, W. J. (1995) Endoproteolytic cleavage of its propeptide is a prerequisite for efficient transport of furin out of the endoplasmic reticulum. *J Biol Chem* 270, 2695-2702.

22. Anderson, E. D., VanSlyke, J. K., Thulin, C. D., Jean, F., and Thomas, G. (1997) Activation of the furin endoprotease is a multiple-step process: requirements for acidification and internal propeptide cleavage. *Embo J* 16, 1508-1518.

23. Siezen, R. J., Leunissen, J.A.M., Shinde, U. (1995) *in Intramolecular Chaperones and Protein Folding*, R.G. Landes Company, Austin, TX.

24. Zhou, A., Paquet, L., and Mains, R. E. (1995) Structural elements that direct specific processing of different mammalian subtilisin-like prohormone convertases. *J Biol Chem* 270, 21509-21516.

25. Muller, L., Cameron, A., Fortenberry, Y., Apletalina, E. V., and Lindberg, I. (2000) Processing and sorting of the prohormone convertase 2 propeptide. *J Biol Chem* 275, 39213-39222.

26. Boudreault, A., Gauthier, D., and Lazure, C. (1998) Proprotein Convertase PC1/3-related Peptides Are Potent Slow Tight-binding Inhibitors of Murine PC1/3 and Hfurin. *J Biol Chem* 273, 31574-31580.

27. Zhong, M., Munzer, J. S., Basak, A., Benjannet, S., Mowla, S. J., Decroly, E., Chretien, M., and Seidah, N. G. (1999) The prosegments of furin and PC7 as potent inhibitors of proprotein convertases. In vitro and ex vivo assessment of their efficacy and selectivity. *J Biol Chem* 274, 33913-33920.

28. De Bie, I., Marcinkiewicz, M., Malide, D., Lazure, C., Nakayama, K., Bendayan, M., and Seidah, N. G. (1996) The isoforms of proprotein convertase PC5 are sorted to different subcellular compartments. *J. Cell Biol.* 135, 1261-1275.

29. Smeekens, S. P., Montag, A. G., Thomas, G., Albiges-Rizo, C., Carroll, R., Benig, M., Phillips, L. A., Martin, S., Ohagi, S., Gardner, P., and et al. (1992) Proinsulin processing by the subtilisin-related proprotein convertases furin, PC2, and PC3. *Proc Natl Acad Sci U S A* 89, 8822-8826.

30. Malide, D., Seidah, N. G., Chretien, M., and Bendayan, M. (1995) Electron microscopic immunocytochemical evidence for the involvement of the convertases PC1 and PC2 in the processing of proinsulin in pancreatic beta-cells. *J Histochem Cytochem* 43, 11-19.

31. Tanaka, S., Kurabuchi, S., Mochida, H., Kato, T., Takahashi, S., Watanabe, T., and Nakayama, K. (1996) Immunocytochemical localization of prohormone convertases PC1/PC3 and PC2 in rat pancreatic islets. *Arch Histol Cytol* 59, 261-271.

32. Mains, R. E., Berard, C. A., Denault, J. B., Zhou, A., Johnson, R. C., and Leduc, R. (1997) PACE4: a subtilisin-like endoprotease with unique properties. *Biochem J* 321 (Pt 3), 587-593.

33. Schafer, W., Stroh, A., Berghofer, S., Seiler, J., Vey, M., Kruse, M. L., Kern, H. F., Klenk, H. D., and Garten, W. (1995) Two independent targeting signals in the cytoplasmic domain determine trans-Golgi network localization and endosomal trafficking of the proprotein convertase furin. *Embo J* 14, 2424-2435.

34. van de Loo, J.-W. H. P., Creemers, J. W. M., Bright, N. A., Young, B. D., Roebroek, A. J. M., and Van de Ven, W. J. M. (1997) Biosynthesis, Distinct Post-translational Modifications, and Functional Characterization of Lymphoma Proprotein Convertase. *J Biol Chem* 272, 27116-27123.

35. Bosshart, H., Humphrey, J., Deignan, E., Davidson, J., Drazba, J., Yuan, L., Oorschot, V., Peters, P. J., and Bonifacino, J. S. (1994) The cytoplasmic domain mediates localization of furin to the trans- Golgi network en route to the endosomal/lysosomal system. *J. Cell Biol.* 126, 1157-1172.

36. Jones, B. G., Thomas, L., Molloy, S. S., Thulin, C. D., Fry, M. D., Walsh, K. A., and Thomas, G. (1995) Intracellular trafficking of furin is modulated by the phosphorylation state of a casein kinase II site in its cytoplasmic tail. *Embo J* 14, 5869-5883.

37. Takahashi, S., Nakagawa, T., Banno, T., Watanabe, T., Murakami, K., and Nakayama, K. (1995) Localization of Furin to the trans-Golgi Network and Recycling from the Cell Surface Involves Ser and Tyr Residues within the Cytoplasmic Domain. *J Biol Chem* 270, 28397-28401.

38. Wan, L., Molloy, S. S., Thomas, L., Liu, G., Xiang, Y., Rybak, S. L., and Thomas, G. (1998) PACS-1 Defines a Novel Gene Family of Cytosolic Sorting Proteins Required for trans-Golgi Network Localization. *Cell* 94, 205-216.

39. Crump, C. M., Xiang, Y., Thomas, L., Gu, F., Austin, C., Tooze, S. A., and Thomas, G. (2001) PACS-1 binding to adaptors is required for acidic cluster motif-mediated protein traffic. *Embo J* 20, 2191-2201.

40. Molloy, S. S., Thomas, L., Kamibayashi, C., Mumby, M. C., and Thomas, G. (1998) Regulation of Endosome Sorting by a Specific PP2A Isoform. *J. Cell Biol.* 142, 1399-1411.

41. Bresnahan, P. A., Leduc, R., Thomas, L., Thorner, J., Gibson, H. L., Brake, A. J., Barr, P. J., and Thomas, G. (1990) Human fur gene encodes a yeast KEX2-like endoprotease that cleaves pro-beta-NGF in vivo. *J Cell Biol* 111, 2851-2859.

42. Cui, Y., Jean, F., Thomas, G., and Christian, J. L. (1998) BMP-4 is proteolytically activated by furin and/or PC6 during vertebrate embryonic development. *Embo J* 17, 4735-4743.

43. Bravo, D. A., Gleason, J. B., Sanchez, R. I., Roth, R. A., and Fuller, R. S. (1994) Accurate and efficient cleavage of the human insulin proreceptor by the human

proprotein-processing protease furin. Characterization and kinetic parameters using the purified, secreted soluble protease expressed by a recombinant baculovirus. *J Biol Chem* 269, 25830-25837.

44. Klimpel, K. R., Molloy, S. S., Thomas, G., and Leppla, S. H. (1992) Anthrax toxin protective antigen is activated by a cell surface protease with the sequence specificity and catalytic properties of furin. *Proc Natl Acad Sci U S A* 89, 10277-10281.

45. Abrami, L., Fivaz, M., Decroly, E., Seidah, N. G., Jean, F., Thomas, G., Leppla, S. H., Buckley, J. T., and van der Goot, F. G. (1998) The pore-forming toxin proaerolysin is activated by furin. *J Biol Chem* 273, 32656-32661.

46. Gordon, V. M., Benz, R., Fujii, K., Leppla, S. H., and Tweten, R. K. (1997) Clostridium septicum alpha-toxin is proteolytically activated by furin. *Infect Immun* 65, 4130-4134.

47. Molloy, S. S., and Thomas, G. (2001) *The Enzymes* Vol. 22, Academic Press, San Diego, CA.

48. Rehemtulla, A., and Kaufman, R. J. (1992) Preferred sequence requirements for cleavage of pro-von Willebrand factor by propeptide-processing enzymes. *Blood* 79, 2349-2355.

49. Vidricaire, G., Denault, J. B., and Leduc, R. (1993) Characterization of a secreted form of human furin endoprotease. *Biochem Biophys Res Commun* 195, 1011-1018.

50. Wise, R. J., Barr, P. J., Wong, P. A., Kiefer, M. C., Brake, A. J., and Kaufman, R. J. (1990) Expression of a human proprotein processing enzyme: correct cleavage of the von Willebrand factor precursor at a paired basic amino acid site. *Proc Natl Acad Sci U S A* 87, 9378-9382.

51. Ashworth, J. L., Kelly, V., Rock, M. J., Shuttleworth, C. A., and Kielty, C. M. (1999) Regulation of fibrillin carboxy-terminal furin processing by N-glycosylation, and association of amino- and carboxy-terminal sequences. *J Cell Sci* 112 (Pt 22), 4163-4171.

52. Leitlein, J., Aulwurm, S., Waltereit, R., Naumann, U., Wagenknecht, B., Garten, W., Weller, M., and Platten, M. (2001) Processing of immunosuppressive pro-TGF-beta 1,2 by human glioblastoma cells involves cytoplasmic and secreted furin-like proteases. *J Immunol* 166, 7238-7243.

53. Bass, J., Turck, C., Rouard, M., and Steiner, D. F. (2000) Furin-mediated processing in the early secretory pathway: Sequential cleavage and degradation of misfolded insulin receptors. *Proceedings of the National Academy of Sciences* 97, 11905-11909.

54. Salvas, A., Benjannet, S., Reudelhuber, T. L., Chrétien, M., and Seidah, N. G. (2005) Evidence for proprotein convertase activity in the endoplasmic reticulum/early Golgi. *FEBS Letters* 579, 5621-5625.

55. Bissonnette, L., Charest, G., Longpre, J. M., Lavigne, P., and Leduc, R. (2004) Identification of furin pro-region determinants involved in folding and activation. *Biochem J* 379, 757-763.

56. Cole, N. B., Ellenberg, J., Song, J., DiEuliis, D., and Lippincott-Schwartz, J. (1998) Retrograde Transport of Golgi-localized Proteins to the ER. *J. Cell Biol.* 140, 1-15.

57. Nagamune, H., Muramatsu, K., Akamatsu, T., Tamai, Y., Izumi, K., Tsuji, A., and Matsuda, Y. (1995) Distribution of the Kexin family proteases in pancreatic islets: PACE4C is specifically expressed in B cells of pancreatic islets [published erratum appears in Endocrinology 1995 Jun;136(6):2586]. *Endocrinology* 136, 357-360.

58. Zheng, M., Streck, R. D., Scott, R. E., Seidah, N. G., and Pintar, J. E. (1994) The developmental expression in rat of proteases furin, PC1, PC2, and carboxypeptidase E: implications for early maturation of proteolytic processing capacity. *J. Neurosci.* 14, 4656-4673.

59. Schafer, M. K., Day, R., Cullinan, W. E., Chretien, M., Seidah, N. G., and Watson, S. J. (1993) Gene expression of prohormone and proprotein convertases in the rat CNS: a comparative in situ hybridization analysis. *J. Neurosci.* 13, 1258-1279.

60. Nakayama, K., Kim, W. S., Torii, S., Hosaka, M., Nakagawa, T., Ikemizu, J., Baba, T., and Murakami, K. (1992) Identification of the fourth member of the mammalian endoprotease family homologous to the yeast Kex2 protease. Its testis-specific expression. *J Biol Chem* 267, 5897-5900.

61. Seidah, N. G., Day, R., Hamelin, J., Gaspar, A., Collard, M. W., and Chretien, M. (1992) Testicular expression of PC4 in the rat: molecular diversity of a novel germ cell-specific Kex2/subtilisin-like proprotein convertase. *Mol Endocrinol* 6, 1559-1570.

62. Lusson, J., Vieau, D., Hamelin, J., Day, R., ChrÃ©tien, M., and Seidah, N. G. (1993) cDNA structure of the mouse and rat subtilisin/kexin-like PC5: a candidate proprotein convertase expressed in endocrine and nonendocrine cells. *Proceedings of the National Academy of Sciences of the United States of America* 90, 6691-6695.

63. Zheng, M., Seidah, N.G., Pintar, J.E. (1997) The Developmental Expression in the Rat CNS and Peripheral Tissues of Proteases PC5 and PACE4 mRNAs: Comparison with Other Proprotein Processing Enzymes. *Developmental Biology* 181, 268-283.

64. Hatsuzawa, K., Hosaka, M., Nakagawa, T., Nagase, M., Shoda, A., Murakami, K., and Nakayama, K. (1990) Structure and expression of mouse furin, a yeast Kex2-related protease. Lack of processing of coexpressed prorenin in GH4C1 cells. *J Biol Chem* 265, 22075-22078.

65. Day, R., Schafer, M.K.-H., Cullinan, W.E., Watson, S.J., Chrétien, M., Seidah, N.G. (1993) Region specific expression of furin mRNA in the rat brain. *Neuroscience Letters* 149, 27-30.

66. Meerabux, J., Yaspo, M.-L., Roebroek, A. J., Van de Ven, W. J. M., Andrew Lister, T., and Young, B. D. (1996) A New Member of the Proprotein Convertase Gene Family (LPC) Is Located at a Chromosome Translocation Breakpoint in Lymphomas. *Cancer Res* 56, 448-451.

67. Bruzzaniti, A., Goodge, K., Jay, P., Taviaux, S. A., Lam, M. H., Berta, P., Martin, T. J., Moseley, J. M., and Gillespie, M. T. (1996) PC8 [corrected], a new member of the convertase family. *Biochem. J.* 314, 727-731.

68. Seidah, N. G., Hamelin, J., Mamarbachi, M., Dong, W., Tardos, H., Mbikay, M., Chretien, M., and Day, R. (1996) cDNA structure, tissue distribution, and chromosomal localization of rat PC7, a novel mammalian proprotein convertase closest to yeast kexin-like proteinases. *Proceedings of the National Academy of Sciences of the United States of America* 93, 3388-3393.

69. Seidah, N. G., and Chretien, M. (1999) Proprotein and prohormone convertases: a family of subtilases generating diverse bioactive polypeptides. *Brain Res* 848, 45-62.

70. Taylor, N. A., Van De Ven, W. J. M., and Creemers, J. W. M. (2003) Curbing activation: proprotein convertases in homeostasis and pathology. *FASEB J.* 17, 1215-1227.

71. Zhu, X., Zhou, A., Dey, A., Norrbom, C., Carroll, R., Zhang, C., Laurent, V., Lindberg, I., Ugleholdt, R., Holst, J. J., and Steiner, D. F. (2002) Disruption of PC1/3 expression in mice causes dwarfism and multiple neuroendocrine peptide processing defects. *Proc Natl Acad Sci U S A* 99, 10293-10298.

72. Furuta, M., Yano, H., Zhou, A., Rouille, Y., Holst, J. J., Carroll, R., Ravazzola, M., Orci, L., Furuta, H., and Steiner, D. F. (1997) Defective prohormone processing and altered pancreatic islet morphology in mice lacking active SPC2. *Proc Natl Acad Sci U S A* 94, 6646-6651.

73. Mbikay, M., Tadros, H., Ishida, N., Lerner, C. P., De Lamirande, E., Chen, A., El-Alfy, M., Clermont, Y., Seidah, N. G., Chretien, M., Gagnon, C., and Simpson, E. M. (1997) Impaired fertility in mice deficient for the testicular germ-cell protease PC4. *Proc Natl Acad Sci U S A* 94, 6842-6846.

74. Constam, D. B., and Robertson, E. J. (2000) SPC4/PACE4 regulates a TGFbeta signaling network during axis formation. *Genes Dev* 14, 1146-1155.

75. Essalmani, R., Hamelin, J., Marcinkiewicz, J., Chamberland, A., Mbikay, M., Chretien, M., Seidah, N. G., and Prat, A. (2006) Deletion of the gene encoding proprotein convertase 5/6 causes early embryonic lethality in the mouse. *Mol Cell Biol* 26, 354-361.

76. Roebroek, A. J., Umans, L., Pauli, I. G., Robertson, E. J., van Leuven, F., Van de Ven, W. J., and Constam, D. B. (1998) Failure of ventral closure and axial rotation in embryos lacking the proprotein convertase Furin. *Development* 125, 4863-4876.

77. Dunker, N., and Krieglstein, K. (2000) Targeted mutations of transforming growth factor-beta genes reveal important roles in mouse development and adult homeostasis. *Eur J Biochem* 267, 6982-6988.

78. Cross, J. C., Simmons, D. G., and Watson, E. D. (2003) Chorioallantoic morphogenesis and formation of the placental villous tree. *Ann N Y Acad Sci* 995, 84-93.

79. Constam, D. B., Calfon, M., and Robertson, E. J. (1996) SPC4, SPC6, and the novel protease SPC7 are coexpressed with bone morphogenetic proteins at distinct sites during embryogenesis. *J Cell Biol* 134, 181-191.

80. Roebroek, A. J. M., Taylor, N. A., Louagie, E., Pauli, I., Smeijers, L., Snellinx, A., Lauwers, A., Van de Ven, W. J. M., Hartmann, D., and Creemers, J. W. M. (2004) Limited Redundancy of the Proprotein Convertase Furin in Mouse Liver. *J Biol Chem* 279, 53442-53450.

81. Khatib, A.-M., Siegfried, G., Chretien, M., Metrakos, P., and Seidah, N. G. (2002) Proprotein Convertases in Tumor Progression and Malignancy : Novel Targets in Cancer Therapy. *Am J Pathol* 160, 1921-1935.

82. Creemers, J. W., Ines Dominguez, D., Plets, E., Serneels, L., Taylor, N. A., Multhaup, G., Craessaerts, K., Annaert, W., and De Strooper, B. (2001) Processing of beta-secretase by furin and other members of the proprotein convertase family. *J Biol Chem* 276, 4211-4217.

83. Benjannet, S., Elagoz, A., Wickham, L., Mamarbachi, M., Munzer, J. S., Basak, A., Lazure, C., Cromlish, J. A., Sisodia, S., Checler, F., Chretien, M., and Seidah, N. G. (2001) Post-translational processing of beta-secretase (beta-amyloid-converting enzyme) and its ectodomain shedding. The pro- and transmembrane/cytosolic domains affect its cellular activity and amyloid-beta production. *J Biol Chem* 276, 10879-10887.

84. Zambon, M. C. (2001) The pathogenesis of influenza in humans. *Rev Med Virol* 11, 227-241.

85. UN AIDS (2008) 2008 Report on the global AIDS epidemic.

86. Public Health Agency of Canada (2007) HIV/AIDS Epi Updates, November 2007. Surveillance and Risk Assessment Division, Centre for Infectious Disease Prevention and Control, Public Health Agency of Canada.

87. Miedema, F. (2008) A brief history of HIV vaccine research: stepping back to the drawing board? *Aids* 22, 1699-1703.

88. Temesgen, Z., Warnke, D., and Kasten, M. J. (2006) Current status of antiretroviral therapy. *Expert Opinion on Pharmacotherapy* 7, 1541-1554.

89. Cheung, P. K., Wynhoven, B., and Harrigan, P. R. (2004) 2004: which HIV-1 drug resistance mutations are common in clinical practice? *AIDS Rev* 6, 107-116.

90. Freed, E. O., and Martin, M.A. (2007) HIVs and their replication. *Fields Virology, 5th Ed.*, Lippincott, Williams, and Wilkins.

91. Bolmstedt, A., Hemming, A., Flodby, P., Berntsson, P., Travis, B., Lin, J. P., Ledbetter, J., Tsu, T., Wigzell, H., Hu, S. L., and et al. (1991) Effects of mutations in glycosylation sites and disulphide bonds on processing, CD4-binding and fusion activity of human immunodeficiency virus envelope glycoproteins. *J Gen Virol* 72 (Pt 6), 1269-1277.

92. Zhu, P., Liu, J., Bess, J., Chertova, E., Lifson, J. D., Grisac, H., Ofek, G. A., Taylor, K. A., and Roux, K. H. (2006) Distribution and three-dimensional structure of AIDS virus envelope spikes. *Nature* 441, 847-852.

93. Ugolini, S., Mondor, I., and Sattentau, Q. J. (1999) HIV-1 attachment: another look. *Trends in Microbiology* 7, 144-149.

94. Willey, R. L., Klimkait, T., Frucht, D. M., Bonifacino, J. S., and Martin, M. A. (1991) Mutations within the human immunodeficiency virus type 1 gp160 envelope glycoprotein alter its intracellular transport and processing. *Virology* 184, 319-329.

95. Moulard, M., Montagnier, L., and Bahraoui, E. (1994) Effects of calcium ions on proteolytic processing of HIV-1 gp160 precursor and on cell fusion. *FEBS Lett* 338, 281-284.

96. Willey, R. L., Bonifacino, J. S., Potts, B. J., Martin, M. A., and Klausner, R. D. (1988) Biosynthesis, cleavage, and degradation of the human immunodeficiency virus 1 envelope glycoprotein gp160. *Proc Natl Acad Sci U S A* 85, 9580-9584.

97. Pinter, A., Honnen, W. J., Tilley, S. A., Bona, C., Zaghouani, H., Gorny, M. K., and Zolla-Pazner, S. (1989) Oligomeric structure of gp41, the transmembrane protein of human immunodeficiency virus type 1. *J Virol* 63, 2674-2679.

98. Earl, P. L., Doms, R. W., and Moss, B. (1990) Oligomeric structure of the human immunodeficiency virus type 1 envelope glycoprotein. *Proc Natl Acad Sci U S A* 87, 648-652.

99. Earl, P. L., Koenig, S., and Moss, B. (1991) Biological and immunological properties of human immunodeficiency virus type 1 envelope glycoprotein: analysis of proteins with truncations and deletions expressed by recombinant vaccinia viruses. *J Virol* 65, 31-41.

100. Pal, R., Hoke, G. M., and Sarngadharan, M. G. (1989) Role of oligosaccharides in the processing and maturation of envelope glycoproteins of human immunodeficiency virus type 1. *Proc Natl Acad Sci U S A* 86, 3384-3388.

101. Dewar, R. L., Vasudevachari, M. B., Natarajan, V., and Salzman, N. P. (1989) Biosynthesis and processing of human immunodeficiency virus type 1 envelope glycoproteins: effects of monensin on glycosylation and transport. *J Virol* 63, 2452-2456.

102. Vollenweider, F., Benjannet, S., Decroly, E., Savaria, D., Lazure, C., Thomas, G., Chretien, M., and Seidah, N. G. (1996) Comparative cellular processing of the human immunodeficiency virus (HIV-1) envelope glycoprotein gp160 by the mammalian subtilisin/kexin-like convertases. *Biochem. J.* 314, 521-532.

103. Moulard, M., and Decroly, E. (2000) Maturation of HIV envelope glycoprotein precursors by cellular endoproteases. *Biochimica et Biophysica Acta (BBA) - Reviews on Biomembranes* 1469, 121-132.

104. Hallenberger S, B. V., Angliker H, Shaw E, Klenk HD, Garten W. (1992) Inhibition of furin-mediated cleavage activation of HIV-1 glycoprotein gp160. *Nature* 360, 358-361.

105. Ohnishi, Y., Shioda, T., Nakayama, K., Iwata, S., Gotoh, B., Hamaguchi, M. (1994) A furin-defective cell line is able to process correctly the gp160 of human immunodeficiency virus type 1. *J Virol* 68, 4075-4079.

106. Hallenberger, S., Moulard, M., Sordel, M., Klenk, H. D., and Garten, W. (1997) The role of eukaryotic subtilisin-like endoproteases for the activation of human immunodeficiency virus glycoproteins in natural host cells. *J Virol* 71, 1036-1045.

107. Moulard, M., Hallenberger, S., Garten, W., and Klenk, H. D. (1999) Processing and routage of HIV glycoproteins by furin to the cell surface. *Virus Res* 60, 55-65.

108. Decroly, E., Wouters, S., Di Bello, C., Lazure, C., Ruysschaert, J. M., and Seidah, N. G. (1996) Identification of the paired basic convertases implicated in HIV gp160 processing based on in vitro assays and expression in CD4(+) cell lines. *J Biol Chem* 271, 30442-30450.

109. Decroly, E., Benjannet, S., Savaria, D., and Seidah, N. G. (1997) Comparative functional role of PC7 and furin in the processing of the HIV envelope glycoprotein gp160. *FEBS Letters* 405, 68-72.

110. Binley, J. M., Sanders, R. W., Master, A., Cayanan, C. S., Wiley, C. L., Schiffner, L., Travis, B., Kuhmann, S., Burton, D. R., Hu, S. L., Olson, W. C., and Moore, J. P. (2002) Enhancing the proteolytic maturation of human immunodeficiency virus type 1 envelope glycoproteins. *J Virol* 76, 2606-2616.

111. Stieneke-Grober, A., Vey, M., Angliker, H., Shaw, E., Thomas, G., Roberts, C., Klenk, H. D., and Garten, W. (1992) Influenza virus hemagglutinin with multibasic cleavage site is activated by furin, a subtilisin-like endoprotease. *Embo J* 11, 2407-2414.

112. Vey, M., Schafer, W., Reis, B., Ohuchi, R., Britt, W., Garten, W., Klenk, H. D., and Radsak, K. (1995) Proteolytic processing of human cytomegalovirus glycoprotein B (gpUL55) is mediated by the human endoprotease furin. *Virology* 206, 746-749.

113. Nakayama, K. (1997) Furin: a mammalian subtilisin/Kex2p-like endoprotease involved in processing of a wide variety of precursor proteins. *Biochem J* 327 (Pt 3), 625-635.

114. Jean, F., Stella, K., Thomas, L., Liu, G., Xiang, Y., Reason, A. J., and Thomas, G. (1998) alpha1-Antitrypsin Portland, a bioengineered serpin highly selective for furin: application as an antipathogenic agent. *Proc Natl Acad Sci U S A* 95, 7293-7298.

115. Cameron, A., Appel, J., Houghten, R. A., and Lindberg, I. (2000) Polyarginines are potent furin inhibitors. *J Biol Chem* 275, 36741-36749.

116. Kibler, K. V., Miyazato, A., Yedavalli, V. S., Dayton, A. I., Jacobs, B. L., Dapolito, G., Kim, S. J., and Jeang, K. T. (2004) Polyarginine inhibits gp160 processing by furin and suppresses productive human immunodeficiency virus type 1 infection. *J Biol Chem* 279, 49055-49063.

117. Sarac, M. S., Cameron, A., and Lindberg, I. (2002) The furin inhibitor hexa-D-arginine blocks the activation of Pseudomonas aeruginosa exotoxin A in vivo. *Infect Immun* 70, 7136-7139.

118. Coppola, J. M., Hamilton, C. A., Bhojani, M. S., Larsen, M. J., Ross, B. D., and Rehemtulla, A. (2007) Identification of inhibitors using a cell-based assay for monitoring Golgi-resident protease activity. *Analytical Biochemistry* 364, 19-29.

119. Jiao, G.-S., Cregar, L., Wang, J., Millis, S. Z., Tang, C., O'Malley, S., Johnson, A. T., Sareth, S., Larson, J., and Thomas, G. (2006) Synthetic small molecule furin inhibitors derived from 2,5-dideoxystreptamine. *Proceedings of the National Academy of Sciences* 103, 19707-19712.

120. Coppola, J. M., M.S. Bhojani, B.D. Ross, and A. Rehemtulla (2008) A small-molecule furin inhibitor inhibits cancer cell motility and invasiveness. *Neoplasia* 10, 363-370.

121. Sato, H., Kinoshita, T., Takino, T., Nakayama, K., and Seiki, M. (1996) Activation of a recombinant membrane type 1-matrix metalloproteinase (MT1-MMP) by furin and its interaction with tissue inhibitor of metalloproteinases (TIMP)-2. *FEBS Lett* 393, 101-104.

122. Basak, A., Cooper, S., Roberge, A. G., Banik, U. K., Chretien, M., and Seidah, N. G. (1999) Inhibition of proprotein convertases-1, -7 and furin by diterpines of Andrographis paniculata and their succinoyl esters. *Biochem J* 338 (Pt 1), 107-113.

123. Podsiadlo, P., Komiyama, T., Fuller, R. S., and Blum, O. (2004) Furin inhibition by compounds of copper and zinc. *J Biol Chem* 279, 36219-36227.

124. Huntington, J. A. (2006) Shape-shifting serpins--advantages of a mobile mechanism. *Trends Biochem Sci* 31, 427-435.

125. Huntington, J. A., Read, R. J., and Carrell, R. W. (2000) Structure of a serpin-protease complex shows inhibition by deformation. *Nature* 407, 923-926.

126. Wright, H. T. (1996) The structural puzzle of how serpin serine proteinase inhibitors work. *Bioessays* 18, 453-464.

127. Anderson, E. D., Thomas, L., Hayflick, J. S., and Thomas, G. (1993) Inhibition of HIV-1 gp160-dependent membrane fusion by a furin-directed alpha 1-antitrypsin variant. *J Biol Chem* 268, 24887-24891.

128. Perlmutter, D. H., and Pierce, J. A. (1989) The alpha 1-antitrypsin gene and emphysema. *Am J Physiol* 257, L147-162.

129. Matheson, N. R., van Halbeek, H., and Travis, J. (1991) Evidence for a tetrahedral intermediate complex during serpin-proteinase interactions. *J Biol Chem* 266, 13489-13491.

130. Benjannet, S., Savaria, D., Laslop, A., Munzer, J. S., Chretien, M., Marcinkiewicz, M., and Seidah, N. G. (1997) Alpha1-antitrypsin Portland inhibits processing of precursors mediated by proprotein convertases primarily within the constitutive secretory pathway. *J Biol Chem* 272, 26210-26218.

131. Jean, F., Thomas, L., Molloy, S. S., Liu, G., Jarvis, M. A., Nelson, J. A., and Thomas, G. (2000) A protein-based therapeutic for human cytomegalovirus infection. *Proc Natl Acad Sci U S A* 97, 2864-2869.

132. Scamuffa, N., Siegfried, G., Bontemps, Y., Ma, L., Basak, A., Cherel, G., Calvo, F., Seidah, N. G., and Khatib, A. M. (2008) Selective inhibition of proprotein convertases represses the metastatic potential of human colorectal tumor cells. *J Clin Invest* 118, 352-363.

133. Bahbouhi, B., Bendjennat, M., Guetard, D., Seidah, N. G., and Bahraoui, E. (2000) Effect of alpha-1 antitrypsin Portland variant (alpha 1-PDX) on HIV-1 replication. *Biochem J* 352 (Pt 1), 91-98.

134. Bahbouhi, B., Seidah, N. G., and Bahraoui, E. (2001) Replication of HIV-1 viruses in the presence of the Portland alpha1-antitrypsin variant (alpha1-PDX) inhibitor. *Biochem J* 360, 127-134.

135. Bentele, C., Kruger, O., Todtmann, U., Oley, M., and Ragg, H. (2006) A proprotein convertase-inhibiting serpin with an endoplasmic reticulum targeting signal from Branchiostoma lanceolatum, a close relative of vertebrates. *Biochem J* 395, 449-456.

136. Ragg, H. (2007) The role of serpins in the surveillance of the secretory pathway. *Cell Mol Life Sci* 64, 2763-2770.

137. Richer, M. J., Keays, C. A., Waterhouse, J., Minhas, J., Hashimoto, C., and Jean, F. (2004) The Spn4 gene of Drosophila encodes a potent furin-directed secretory pathway serpin. *Proc Natl Acad Sci U S A* 101, 10560-10565.

138. Dahlen, J. R., Jean, F., Thomas, G., Foster, D. C., and Kisiel, W. (1998) Inhibition of soluble recombinant furin by human proteinase inhibitor 8. *J Biol Chem* 273, 1851-1854.

139. Kruger, O., Ladewig, J., Koster, K., and Ragg, H. (2002) Widespread occurrence of serpin genes with multiple reactive centre-containing exon cassettes in insects and nematodes. *Gene* 293, 97-105.

140. Bruning, M., Lummer, M., Bentele, C., Smolenaars, M. M., Rodenburg, K. W., and Ragg, H. (2007) The Spn4 gene from Drosophila melanogaster is a multipurpose defence tool directed against proteases from three different peptidase families. *Biochem J* 401, 325-331.

141. Oley, M., Letzel, M. C., and Ragg, H. (2004) Inhibition of furin by serpin Spn4A from Drosophila melanogaster. *FEBS Letters* 577, 165-169.

142. Osterwalder, T., Kuhnen, A., Leiserson, W. M., Kim, Y.-S., and Keshishian, H. (2004) Drosophila Serpin 4 Functions as a Neuroserpin-Like Inhibitor of Subtilisin-Like Proprotein Convertases. *J. Neurosci.* 24, 5482-5491.

143. Chackerian, B., Long, E. M., Luciw, P. A., and Overbaugh, J. (1997) Human immunodeficiency virus type 1 coreceptors participate in postentry stages in the virus replication cycle and function in simian immunodeficiency virus infection. *J Virol* 71, 3932-3939.

144. Takahashi, S., Kasai, K., Hatsuzawa, K., Kitamura, N., Misumi, Y., Ikehara, Y., Murakami, K., and Nakayama, K. (1993) A mutation of furin causes the lack of precursor-processing activity in human colon carcinoma LoVo cells. *Biochem Biophys Res Commun* 195, 1019-1026.

145. Schutz-Geschwender, A. Z., Y.;Holt, T.;McDermitt, D.;Olive, D.M. (2004) Quantitative, two-color Western blot detection with infrared fluorescence. In, Li-Cor Biosciences, Lincoln, Nebraska.

146. Waheed, A. A., Ablan, S. D., Roser, J. D., Sowder, R. C., Schaffner, C. P., Chertova, E., and Freed, E. O. (2007) HIV-1 escape from the entry-inhibiting effects of a cholesterol-

binding compound via cleavage of gp41 by the viral protease. *Proceedings of the National Academy of Sciences* 104, 8467-8471.

147. Brown, M. S., and Goldstein, J. L. (1999) A proteolytic pathway that controls the cholesterol content of membranes, cells, and blood. *Proceedings of the National Academy of Sciences* 96, 11041-11048.

148. DeBose-Boyd, R. A., Brown, M. S., Li, W.-P., Nohturfft, A., Goldstein, J. L., and Espenshade, P. J. (1999) Transport-Dependent Proteolysis of SREBP: Relocation of Site-1 Protease from Golgi to ER Obviates the Need for SREBP Transport to Golgi. *Cell* 99, 703-712.

149. Nagata, K. (1998) Expression and function of heat shock protein 47: A collagen-specific molecular chaperone in the endoplasmic reticulum. *Matrix Biology* 16, 379-386.

150. Pelham, H. R. (1996) The dynamic organisation of the secretory pathway. *Cell Struct Funct* 21, 413-419.

151. Kimpton, J., and Emerman, M. (1992) Detection of Replication-Competent and Pseudotyped Human Immunodeficiency Virus with a Sensitive Cell Line on the Basis of Activation of an Integrated β-Galactosidase Gene. *J Virol* 66, 2232-2239.

152. Llewellyn, D. H., Roderick, H. L., and Rose, S. (1997) KDEL Receptor Expression Is Not Coordinatedly Up-regulated with ER Stress-Induced Reticuloplasmin Expression in HeLa Cells. *Biochemical and Biophysical Research Communications* 240, 36-40.

153. Yamamoto, K., Fujii, R., Toyofuku, Y., Saito, T., Koseki, H., Hsu, V. W., and Aoe, T. (2001) The KDEL receptor mediates a retrieval mechanism that contributes to quality control at the endoplasmic reticulum. *Embo J* 20, 3082-3091.

154. McColl, B. K., Paavonen, K., Karnezis, T., Harris, N. C., Davydova, N., Rothacker, J., Nice, E. C., Harder, K. W., Roufail, S., Hibbs, M. L., Rogers, P. A. W., Alitalo, K., Stacker, S. A., and Achen, M. G. (2007) Proprotein convertases promote processing of VEGF-D, a critical step for binding the angiogenic receptor VEGFR-2. *FASEB J.* 21, 1088-1098.

155. Morin, R., Bainbridge, M., Fejes, A., Hirst, M., Krzywinski, M., Pugh, T., McDonald, H., Varhol, R., Jones, S., and Marra, M. (2008) Profiling the HeLa S3 transcriptome using randomly primed cDNA and massively parallel short-read sequencing. *Biotechniques* 45, 81-94.

156. Johnson, K. F., and Kornfeld, S. (1992) The cytoplasmic tail of the mannose 6-phosphate/insulin-like growth factor-II receptor has two signals for lysosomal enzyme sorting in the Golgi. *J Cell Biol* 119, 249-257.

157. Trowbridge, I. S., Collawn, J. F., and Hopkins, C. R. (1993) Signal-dependent membrane protein trafficking in the endocytic pathway. *Annu Rev Cell Biol* 9, 129-161.

158. Freed, E. O., and Martin, M. A. (1995) The role of human immunodeficiency virus type 1 envelope glycoproteins in virus infection. *J Biol Chem* 270, 23883-23886.

159. Lenz, O., ter Meulen, J., Klenk, H. D., Seidah, N. G., and Garten, W. (2001) The Lassa virus glycoprotein precursor GP-C is proteolytically processed by subtilase SKI-1/S1P. *Proc Natl Acad Sci U S A* 98, 12701-12705.

160. Liao, Z., Cimakasky, L. M., Hampton, R., Nguyen, D. H., and Hildreth, J. E. (2001) Lipid rafts and HIV pathogenesis: host membrane cholesterol is required for infection by HIV type 1. *AIDS Res Hum Retroviruses* 17, 1009-1019.

161. Nguyen, D. H., Giri, B., Collins, G., and Taub, D. D. (2005) Dynamic reorganization of chemokine receptors, cholesterol, lipid rafts, and adhesion molecules to sites of CD4 engagement. *Experimental Cell Research* 304, 559-569.

162. Wouters, S., Leruth, M., Decroly, E., Vandenbranden, M., Creemers, J. W., van de Loo, J. W., Ruysschaert, J. M., and Courtoy, P. J. (1998) Furin and proprotein convertase 7 (PC7)/lymphoma PC endogenously expressed in rat liver can be resolved into distinct post-Golgi compartments. *Biochem J* 336 (Pt 2), 311-316.

163. Vodovar, N., Vinals, M., Liehl, P., Basset, A., Degrouard, J., Spellman, P., Boccard, F., and Lemaitre, B. (2005) Drosophila host defense after oral infection by an entomopathogenic Pseudomonas species. *Proc Natl Acad Sci U S A* 102, 11414-11419.

164. Lin, J. H., Walter, P., and Yen, T. S. B. (2008) Endoplasmic Reticulum Stress in Disease Pathogenesis. *Annual Review of Pathology: Mechanisms of Disease* 3, 399-425.

165. Dorner, A. J., Wasley, L. C., Raney, P., Haugejorden, S., Green, M., and Kaufman, R. J. (1990) The stress response in Chinese hamster ovary cells. Regulation of ERp72 and protein disulfide isomerase expression and secretion. *J Biol Chem* 265, 22029-22034.

166. Llewellyn, D. H., Kendall, J. M., Sheikh, F. N., and Campbell, A. K. (1996) Induction of calreticulin expression in HeLa cells by depletion of the endoplasmic reticulum Ca2+ store and inhibition of N-linked glycosylation. *Biochem J* 318 (Pt 2), 555-560.

167. Macer, D. R., and Koch, G. L. (1988) Identification of a set of calcium-binding proteins in reticuloplasm, the luminal content of the endoplasmic reticulum. *J Cell Sci* 91 (Pt 1), 61-70.

168. De Bie, I., Savaria, D., Roebroek, A. J. M., Day, R., Lazure, C., Van de Ven, W. J. M., and Seidah, N. G. (1995) Processing Specificity and Biosynthesis of the Drosophila melanogaster Convertases dfurin1, dfurin1-CRR, dfurin1-X, and dfurin2. *J Biol Chem* 270, 1020-1028.

169. Hwang, J. R., Siekhaus, D. E., Fuller, R. S., Taghert, P. H., and Lindberg, I. (2000) Interaction of Drosophila melanogaster Prohormone Convertase 2 and 7B2. Insect Cell-Specific Processing and Secretion. *J Biol Chem* 275, 17886-17893.

Appendix 1. Supporting recombinant Spn4A data.

Table A1.1. Determination of concentration of purified *E. coli*-expressed His-FLAG-Spn4A ER based on pmol amounts of selected residues determined by Amino Acid Analysis (AAA). Total volume analyzed was 20 µl. Residues used to calculate Spn4A concentration are highlighted in yellow and were chosen based on the criteria of relatively high % composition within the Spn4A molecule and agreement between AAA % composition and actual % composition.

residue	number of residues	pmol amount	actual % composition	AAA % composition	nmol of Spn4A	concentration of Spn4A (mM)
Asp	37	10737	9.1	9.75	290.19	14.51
Glu	56	15294	13.8	13.89	273.11	13.66
Ser		6632	6.9			
Gly		4961	3.7			
His		4556	4.4			
Arg		5511	4.4			
Thr		4418	4.7			
Ala		11156	10.1			
NH3		672				
Pro		4846	4.2			
Tyr		2620	2			
Val	24	6882	5.9	6.25	286.75	14.34
Met		3014	3			
Cys		38	0.2			
Ile		4617	4.2			
Leu	45	12605	11.1	11.44	280.11	14.01
Phe		6067	5.9			
Lys		5518	5.7			
Sum		110144				
Average						14

Figure A1.1. Western blot images of **A)** concentrated media of MAGI-CCR5 cells expressing Spn4A S and flowthrough resulting from concentration; **B)** unbound and eluted fraction of *E. coli*-expressed Spn4A S purified with a magnetic nickel bead His tag protein purification kit. See section 2.2 for details. Blots were probed with mouse monoclonal anti-FLAG Ab and secondary infrared 800CW anti-mouse Ab. Molecular weight (kDa) is shown on the left.

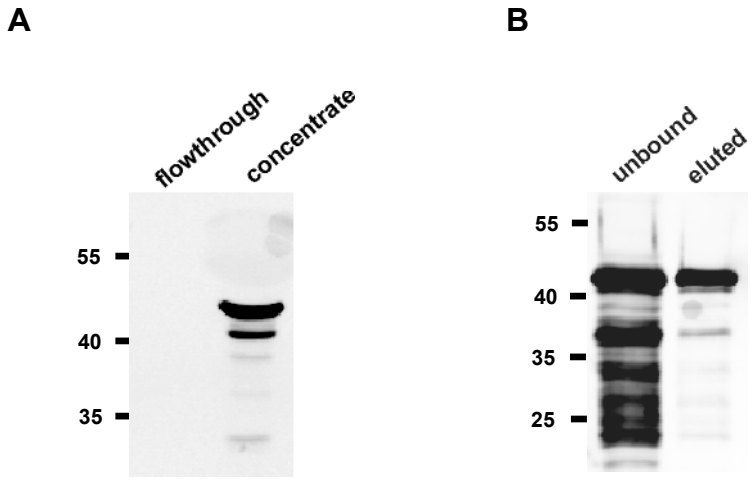

Figure A1.2. Determination of concentration of **A)** Spn4A S in concentrated MAGI-CCR5 media and **B)** *E. coli*-expressed Spn4A S purified with a magnetic nickel bead His tag protein purification kit. Spn4A samples were run on SDS-PAGE alongside a dilution series of known amounts of *E. coli* Spn4A ER (based on AAA, Table A1.1). Integrated intensity of bands was determined using Li-Cor Odyssey Software 2.0 and graphed versus pmol amount or concentration of Spn4A ER (black circles). The concentration of Spn4A samples was determined by plotting integrated band intensities (grey circles) on the best fit line. Average of two independent experiments is shown.

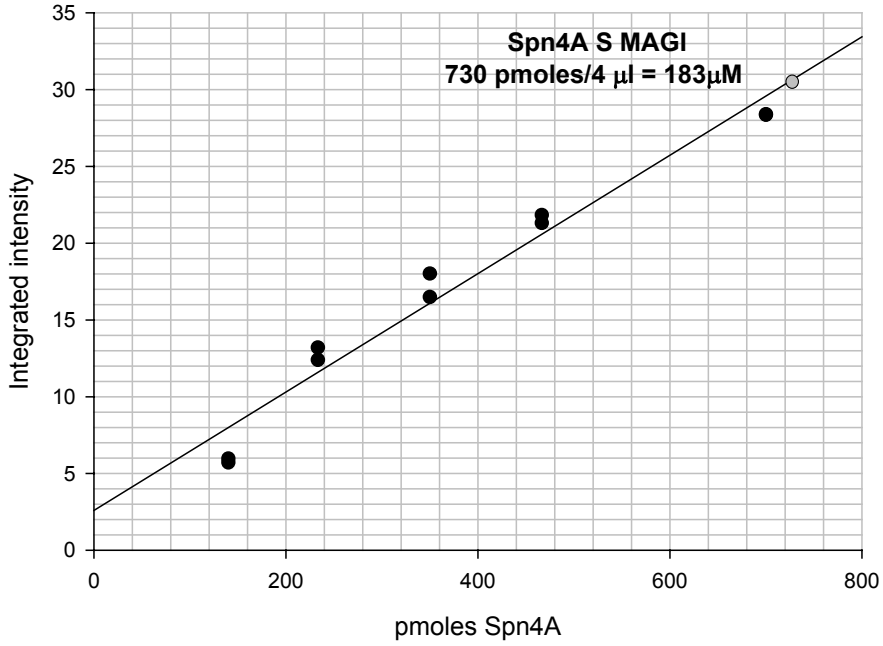

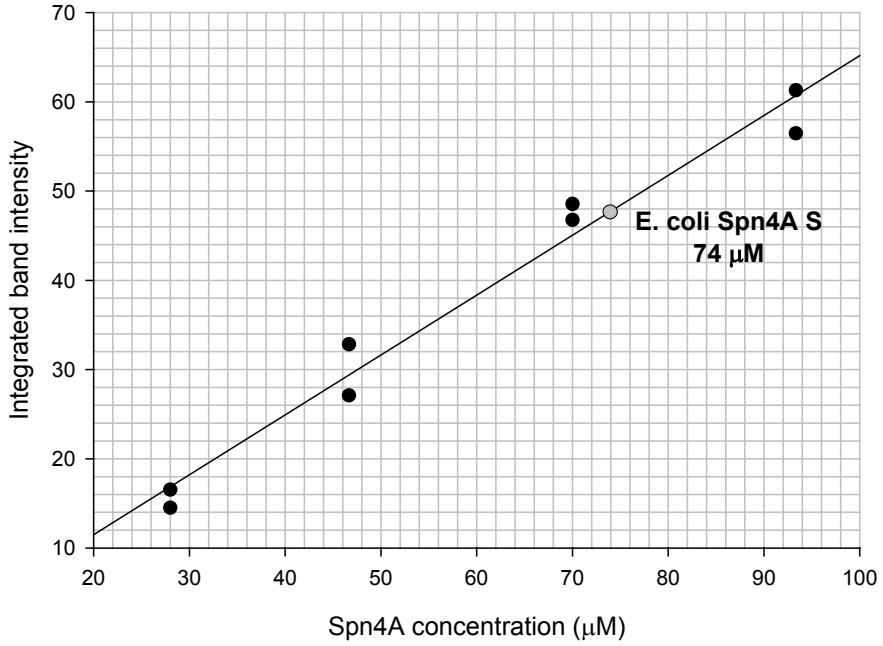

Appendix 2. Caspase activation analysis in the presence of AdSpn4A variants

Figure A2.1. Detection of inactive caspase 3 in MAGI-CCR5 cells infected with AdSpn4A variants. MAGI-CCR5 cells (2×10^5 cells per well) were seeded in 6 well plates and incubated overnight. AdSpn4A variants were added to cell media at the MOI indicated in the image label and incubated for 48 hours. Six hours prior to cell harvesting, 0.75 μM staurosporine (ST.) was added to corresponding cells. Whole cell lysates were prepared as described in section 2.5 and run on SDS-PAGE. Western blot analysis was performed as described in section 2.6 probing with 1:500 rabbit anti-caspase 3 Ab (9665, Cell Signalling Technology) and 1:1000 mouse anti-tubulin Ab (MS-1226-P1 Lab Vision) and secondary infrared 700CW anti-rabbit (red) and 800CW anti-mouse (green) Abs. Con. denotes untreated control cells. A representative image of one experiment performed in duplicate is shown; molecular weight (kDa) is shown on the left.